Universität Bremen

Enteroviral infection as a cause for β-cell failure and diabetes

Dissertation

Zur Erlangung des Grades eines Doktors der Naturwissenschaften
Im Fachbereich Biologie/Chemie der Universität Bremen

Vorgelegt von
Niels Busse, M.Sc.

Bremen, Januar 2017

1. Gutachter: Prof. Dr. Kathrin Mädler
2. Gutachter: Prof. Dr. Urs Christen

Versicherung an Eides Statt

Ich, _____ (Vorname, Name, Anschrift, Matr.-Nr.)

versichere an Eides Statt durch meine Unterschrift, dass ich die vorstehende Arbeit selbständig und ohne fremde Hilfe angefertigt und alle Stellen, die ich wörtlich dem Sinne nach aus Veröffentlichungen entnommen habe, als solche kenntlich gemacht habe, mich auch keiner anderen als der angegebenen Literatur oder sonstiger Hilfsmittel bedient habe.
Ich versichere an Eides Statt, dass ich die vorgenannten Angaben nach bestem Wissen und Gewissen gemacht habe und dass die Angaben der Wahrheit entsprechen und ich nichts verschwiegen habe.
Die Strafbarkeit einer falschen eidesstattlichen Versicherung ist mir bekannt, namentlich die Strafandrohung gemäß § 156 StGB bis zu drei Jahren Freiheitsstrafe oder Geldstrafe bei vorsätzlicher Begehung der Tat bzw. gemäß § 161 Abs. 1 StGB bis zu einem Jahr Freiheitsstrafe oder Geldstrafe bei fahrlässiger Begehung.

_____
Ort, Datum Unterschrift

Table of contents

1 Abstract 1
1 Zusammenfassung 2
2 **Introduction** 4
2.1 Diabetes, a global health problem 4
2.1.1 Type 1 Diabetes 5
2.2 Pancreas: structure and function 6
2.2.1 Pancreatic islets 7
2.3 Risk factors 10
2.3.1 Genetic Predisposition to T1D 10
2.3.1.1 HLA 10
2.3.1.2 Non-HLA 11
2.3.2 Environmental Factors 12
2.3.2.1 Sunlight/Vitamin D 12
2.3.2.2 Diet/ Nutrition 13
2.3.2.3 Microorganisms 13
2.4 Coxsackieviruses infection as cause for T1D 15
2.4.1 Enteroviral lifecycle in infected cells 15
2.4.2 CVBs utilize host cell survival pathways 17
2.4.3 Viral recognition in the host cell and immune response 18
2.4.4 Actions of the Immune system in response to β-cell "SOS" signals 19
2.4.4.1 Immune cell mediated β-cell destruction. 20
2.4.5 Virus induced autoimmunity 21
2.5 CVB detection in human T1D donor tissues 22
2.5.1 Immunohistochemistry 22
2.5.2 PCR 23
2.5.3 Fluorescence in situ hybridization 24
2.6 Aim of the thesis 26
3 **Results** 39
3.1 TLR3 activates coxsackievirus-induced chemokine secretion and apoptosis in pancreatic β-cells 39
3.2 Detection and localization of viral infection in the pancreas of patients with type 1 diabetes using short fluorescently-labelled oligonucleotide probes 84
4 **Discussion** 125
4.1 Outlook 132
4.2 Conclusion 133

Abbreviation

APC	APC Antigen presenting cells
ATP	Adenosine triphosphate
CAR	coxsackie- and adenovirus receptor
CMV	Cytomegalovirus
CTLA-4	Cytotoxic T-lymphocyte-associated protein 4
CVB	Coxsackievirus B
CXCL10	C-X-C motif chemokine ligand 10
CXCR3	C-X-C motif chemokine receptor 3
DAF	Decay accelerating factor
DNA	Deoxyribonucleic acid
eIF2α	Eukaryotic translation initiation factor 2a
ER	Endoplasmic reticulum
ERK	Extracellular-signal-regulated kinases
EV	Enterovirus
FFPE	formalin-fixed paraffin-embedded
FISH	Fluorescence in situ hybridization
GAD65	glutamic decarboxylase 65
GLUT	glucose transporter
HLA	Human leukocyte antigen
IA-2	insulinoma-associated antigen-2
ICA	islet cell autoantibodies
ICI	insulin-containing islet
IFIH1	Interferon induced with helicase D domain 1
IFN	Interferon
IHC	immunohistochemistry
ILR2A	Interleukin-2 receptor alpha chain
JNK	c-Jun N-terminal kinase
MAPK	mitogen-activated protein kinase
MDA5	Melanoma differentiation-associated protein 5
MHC	Major Histocompatibility Complex
mRNA	messenger Ribonucleic acid
mTORC	mammalian Target of Rapamycin Complex
MyD88	Myeloid differentiation factor 88
NF-κB	nuclear factor ‘kappa-light-chain-enhancer’ of activated B-cells
NLR	(NOD)-like receptors
PAMP	pathogen associated molecular patterns
PBMC	Peripheral Blood Mononuclear Cell
PCR	Polymerase Chain Reaction
PI3K	phosphatidylinositol 3-kinase
PKR	protein kinase R
poly(I:C)	Polyinosinic-polycytidylic acid
PP	Pancreatic Polypeptide

PRR	pattern recognition receptors
PTPN22	Protein tyrosine phosphatase non-receptor type 22
RIG1	Retinoic acid inducible gene 1
RLR	RIG-I-like receptor
ROS	reactive oxygen species
RT-PCR	real-time PCR
ssRNA	single-stranded Ribonucleic acid
T1D	Type 1 Diabetes
T2D	Type 2 Diabetes
TBK1	tank-binding kinase 1
TCR	T-cell Receptor
TIR	Toll/Interleukin-1 receptor
TLR	Toll-like receptors
TNF	tumor necrosis factor
TRIF	TIR domain-containing adaptor inducing INF-β
UTR	Untranslated region
VDR	Vitamin D receptor
VNTR	variable number of tandem repeats
VP1	viral protein 1
VPg	viral protein genome-linked
ZnT8	Zinc transporter 8

1 Abstract

Autoreactive T-cell mediated destruction of insulin-containing β-cells is the hallmark of Type 1 Diabetes (T1D). Although the disease is known for centuries, neither is the cause of onset clearly identified, nor has the worldwide raise of incidences been stopped. To provide a cure, it is mandatory to uncover the causes triggering the disease such as environmental and/ or genetic factors that induce the activation of the immune system. Based on epidemiological studies, previous virus infections, especially by Coxsackieviruses B (CVB) of the Picornaviridae family, are highly associated with the onset of T1D. However, the proof of causality between CVB infection and T1D onset is still missing in humans and evidences of β-cell infection in human pancreata remain controversial.

In this work, I aimed to identify the initial pathways to enterovirus-mediated β-cell destruction and to develop a highly sensitive and specific method to characterize expression and localization of viral RNA in pancreatic tissue sections.

Cultured human islets and β-cell lines were used to analyze the first cellular mechanism during viral infection. From the tested viruses, only the enteroviruses (CVB3 and CVB4) induced apoptosis in infected β-cells. Both CVBs also infiltrated, but with different ratios, α-cells that remained unaffected by the virus. The Pathogen-recognition receptors (PRRs) TLR3 and PKR were the first receptors that recognized the virus in β-cells and TLR7 in α-cells, whereas MDA5 and RIG-I bound the genome at a much later time point. TLR3 and PKR had a dual role in β-cells, as they triggered the first immune response and cytokine release, but also activated the survival pathways AKT and ERK, upon virus recognition. Both activated kinases promoted viral replication and counter-balanced the absence of each other.

While through this work, it became clear, that enterovirus infection is causative for β-cell destruction and dysfunction in human islets *in vitro*. But the question, whether virus infection indeed coincide with diabetes *in vivo* remained elusive.

With a newly developed method I could detect enteroviral genomes in human T1D donor tissues. I adapted single molecular fluorescence in situ hybridization (smFISH) to screen for viral RNA molecules in formalin-fixed paraffin-embedded (FFPE) pancreatic tissue sections. Specifically designed oligonucleotide probes to detect a wide range of Coxsackieviruses were successfully tested in an array of cell lines and pathological tissues. Oligonucleotide probes show a specificity and sensitivity that exceed classical immunohistochemistry (IHC) assays and was comparable in its sensitivity to PCR. With the combination of smFISH and IHC I could detect and locate viral RNA in T1D donor tissues in a blinded concordance study. I confirmed

former VP1 staining and showed that enteroviral genomes are located in the pancreas of patients with T1D, but not exclusively within insulin-containing cells. The results of this thesis strongly point towards viral induced T1D onset in humans. They represent a central step for diabetes care and provide groundwork for future preventive strategies.

1 Zusammenfassung

Die Zerstörung von Insulin-haltigen β-Zellen, durch autoreaktive T-Zellen, charakterisiert Typ 1 Diabetes (T1D). Obwohl die Krankheit seit Jahrhunderten bekannt ist, konnte weder der genaue Grund für ihren Ausbruch aufgeklärt, noch der weltweite Anstieg an Neuerkrankungen gestoppt werden. Um eine zukünftige Heilung zu ermöglichen, ist es zwingend erforderlich die krankheitsauslösenden Ursachen, wie etwa Umwelt- und/ oder genetische Faktoren, die die Aktivierung des Immunsystems auslösen, aufzudecken. Anhand von epidemiologischen Studien vermutet man, dass frühere Virusinfektionen, insbesondere durch Coxsackieviren B (CVB) die zur Familie der Picornaviridae gehören, am wahrscheinlichsten mit dem Ausbruch von T1D in Verbindung stehen. Dennoch konnte ein kausaler Zusammenhang zwischen CVB Infektionen und dem Ausbruch von T1D bisher nicht eindeutig in Menschen bewiesen werden, zudem bleibt der Nachweis von β-Zell Infektionen in humanen Pankreata weiterhin umstritten. In dieser Arbeit beabsichtigte ich, die ersten Schritte innerhalb einer Virus-vermittelten β-Zell Zerstörung zu identifizieren sowie eine hochsensible und spezifische Methode, um virale RNA Expression und Lokalisation in pankreatischen Gewebeschnitten zu charakterisieren, zu entwickeln.

Kultivierte humane Inselzellen und β-Zelllinien wurden verwendet, um die zellulären Mechanismen während einer viralen Infektion zu studieren. Von allen getesteten Viren, induzierten nur die Enteroviren (CVB3 und CVB4) Apoptose in infizierten β-Zellen. Beide CVBs infiltrierten, wenn auch im unterschiedlichen Verhältnis, α-Zellen, die aber unbeeinflusst vom Virus blieben. Die „Pathogen-recognition receptors“ (PRRs) TLR3 und PKR waren die ersten Rezeptoren, die den Virus in β-Zellen und TLR7 in α-Zellen erkannten, wohingegen MDA5 und RIG1 erst zu einem viel späteren Zeitpunkt das Genom banden. TLR3 und PKR haben eine doppelte Rolle in β-Zellen, da sie nach Erkennen einer viralen Infektion sowohl die erste Immunantwort sowie Zytokinfreisetzung auslösten, als auch die zellulären Überlebenssignalwege AKT und ERK aktivierten. Beide aktivierte Kinasen fördern die virale Replikation und kompensieren ihre gegenseitige Abwesenheit.

Durch diese Arbeit wurde klar, dass eine Enterovirus-Infektion ursächlich für β-Zellzerstörung und Dysfunktion in menschlichen Inselzellen *in vitro* ist. Aber die Frage, ob eine Virusinfektion tatsächlich *in vivo* mit Diabetes koinzidiert verbleibt unbeantwortet.

Mit einer neu entwickelten Methode konnte ich enterovirale Genome in humanen T1D Spendergeweben nachweisen. „Single molecule fluorescence in situ hybridization" (smFISH) wurde von uns erfolgreich adaptiert, um mit dieser Technik nach viralen Molekülen in FFPE pankreatischen Gewebeschnitten zu suchen. Um ein breites Spektrum an Coxsackieviren nachzuweisen, wurden spezifische Oligonukleotid-Sonden entworfen und erfolgreich in einer Reihe von Zelllinien und pathologischen Schnitten getestet. Die hier verwendeten Oligonukleotid-Sonden, zeigen eine höhere Spezifizität und Sensitivität als übliche IHC Techniken und sind in ihrer der Sensitivität mit PCR vergleichbar. In einer Blindstudie war es mir möglich, durch die Kombination von smFISH und IHC, virale RNA in T1D Spendergewebe nachzuweisen und zu lokalisieren. Vorherige VP1-Färbungen wurden von mir bestätigt und ich zeige, dass enterovirale Genome im Pankreas von Patienten mit T1D, aber nicht ausschließlich in insulin-haltigen Zellen, vorhanden sind. Die Ergebnisse dieser Thesis deuten stark auf viral-induzierten T1D in Menschen hin. Sie stellen einen zentralen Schritt für die Diabetesbehandlung da und bilden einen Grundstein für zukünftige Präventionsmaßnahmen.

2 Introduction

At the time when patients are diagnosed with Type 1 Diabetes (T1D), most of insulin-containing β-cells are irreversibly destroyed by autoreactive T-cells. To prevent the continuous rise of new T1D incidences worldwide, the stimuli that induce autoimmune attacks in genetic predisposed individuals need to be identified **(1)**. Among the multitude of potential environmental factors **(2-6)** viruses are considered as the highest risk for T1D induction **(7-10)**. However, the initiation of viral-related β-cell death is not completely understood. Even though several hypotheses are established how the pathogen could draw the attention of immune-cells towards islets **(11)**, little is known about the cellular events during an early time point of infection.

The results of the following doctoral thesis strongly support the theory of viruses as causative environmental agents and contribute to the understanding of T1D pathogenesis upon viral infection.

2.1 Diabetes, a global health problem

People are suffering from diabetes (Greek, 'syphon') mellitus (Latin, 'sweet like honey') since centuries and respective symptoms were first documented by the ancient Egyptians (12). Starting with the isolation of insulin and its commercial manufacturing in the early 20th century patient's treatment and survival improved significantly over the last decades (13, 14). However, little is known about the factors that trigger the disease while its epidemic is still on the rise. The World Health Organization (WHO) reports that the number of people suffering from diabetes almost doubled in the last 30 years. An increase from 4,7% of the world population in 1980 to 8,5%, a total of 422 million adults, in 2014. Especially in low- and middle-income countries the numbers of patients are increasing. Even nowadays the course of the disease can be fatal. In 2012 around 3,7 million patients died due to consequences of increased blood glucose levels and almost half of them (43%) before the age of 70. An early diagnosis is crucial to manage a life with the disease and to reduce the chances of further complications. Highly elevated blood-sugar levels can lead to diabetic ketoacidosis and vastly low levels to seizures, loss of consciousness and rapid death. Long-term complications include damage of kidney, heart, eyes, blood-vessels and nerves. Untreated diabetes in pregnant women can have severe effects on the mother and the child (15). Diabetes is commonly classified as type 1 (T1D) and type 2 diabetes (T2D), other often occurring forms are gestational diabetes mellitus (GDM) and maturity-onset diabetes of the young (MODY) (16). Symptoms of type 1 and 2 are similar,

which sometimes makes these types difficult to distinguish without laboratory testing. Initially diagnosed with type 2 some patients have eventually T1D (1). 10% of the patients are diagnosed with T1D and depend on insulin injection to survive. Their immune system destroys insulin-containing β-cells, the own insulin production is mostly lost over the course of disease. The majority (90%) of patients is diagnosed with T2D, which is usually triggered by obesity and lifestyle (16). Islet β-cells can not compensate for the increasing insulin demand of the body in the long-term, leading to loss of β-cell mass and insufficient insulin secretion (16-18), to maintain normoglycemia. Premature death can be caused by both types. Whereas T2D can be prevented by strict life style intervention, a causative therapy of T1D could not be achieved yet, with our current knowledge (15). GDM is detected in pregnant women during prenatal screening and affects 7% women during pregnancy. MODY is caused by autosomal inherited genetic defects (e.g. hepatocyte nuclear factor (HNF)-1α, HNF-4α, glucokinase) that affect β-cell function and induce onset of hyperglycemia at an early age (<25 years) (16).

2.1.1 Type 1 Diabetes

T1D is characterized by an auto-immune mediated destruction of insulin secreting β-cells in genetically predisposed individuals. The onset of diabetes appears in two waves with the first in young children and the second close to puberty (19). However, the disease usually remains undiscovered until the majority (80%-90%) of insulin-positive cells has been destroyed. According to Eisenbarth (1986) (20), genetically predisposed individuals encounter an environmental factor that initiates a linear decline in β-cell mass over time (Fig. 1).

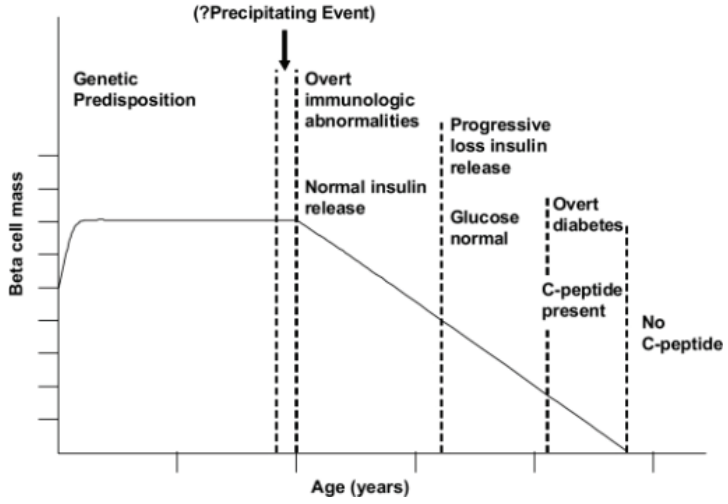

Figure 1: Progression of T1D (Eisenbarth model). Graphical depiction of β-cell decay in genetic risk-individuals, upon contact to an environmental factor. (Adapted from **(20)**)

Several adaptations have been made to this model since its original publication. For instance, the course of the disease is probably not linear, rather appears in small waves and varies among individuals and the break of autoimmune tolerance could start years before β-cell demise **(21)**. In order to better understand the destructive effect of environmental triggered autoimmunity as well as viral localization in infected pancreatic tissues, structure and function of the human pancreas need to be described.

2.2 Pancreas: structure and function

Human pancreata are about 12-15 cm in length and located in the abdomen behind the stomach. The digestive gland weights about 45g-120g and can be visually divided in head, body and tail (**Fig. 2)**. The head is connected to the duodenum from where the main pancreatic duct runs through the whole pancreas down to the tail, which ends next to the spleen. The pancreas has two main functions, controlling food intake and control of the blood sugar level: Around 98% of the organ has an exocrine function and encloses a network of ductal and acinar cells. The latter secrete inactive digestive enzymes into small ducts, which drain into the main pancreatic duct and finally flow into the duodenum, where the enzymes become activated. Less than 2% of the pancreatic cells have an endocrine function. They are organized in small, highly vascularized networks and are named after Paul Langerhans (1847-1888) -islets of Langerhans- who first described them back in 1869. Up to one million islets are dispersed throughout the pancreas with increasing numbers towards the tail-region and all are involved in glucose homeostasis regulation. After fasting or exercise the decrease of blood glucose stimulates glucagon secretion to adjust the imbalance. Glucose concentration raises after food-intake and promotes insulin release to trigger cellular glucose uptake and restore glucose homeostasis **(22-24)**.

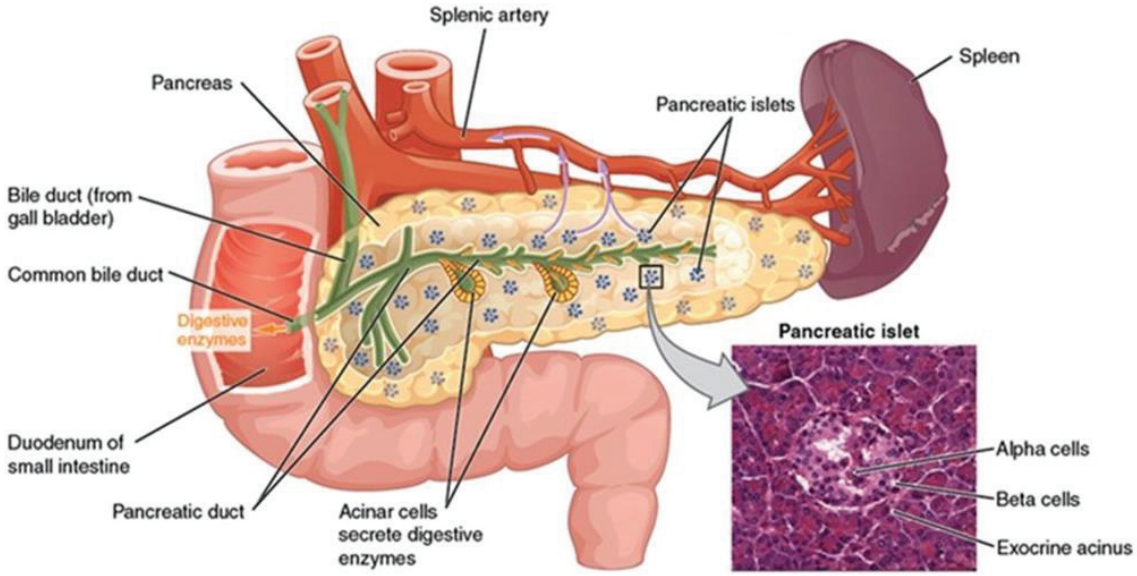

Figure 2: Anatomical structure of the human pancreas. The pancreas is located in the abdomen, between the duodenum of small intestines and the spleen. Acinar cells secrete digestive enzymes and are connected to the pancreatic duct. Blood glucose level is regulated by islets, which are embedded in the exocrine tissue throughout the pancreas. (Adapted from (24))

2.2.1 Pancreatic islets

The mini-organ consists of five different cell types that each secrete a characteristic hormone. β-cells are the prevalent cell type within human islets (~55%), followed by α-cells (~35%), δ-cells (~11%), PP (3-5%) and rarely ghrelin cells (<1%) **(24, 25)**. The proportion of endocrine cells varies among islets; however, the non-β cells determine the cytoarchitecture, but cellular organization of human islets is still under debate. In the classical perception, endocrine cells are intermingled, whereas a "mantle-core" like arrangement, where β-cells are surrounded by non-β-cells, is found in rodent islets (**Fig. 3) (25, 26)**. A recent study suggests that the cytoarchitecture is size-dependent, smaller human islets resemble that of rodents while larger islets show a more random organization **(27)**.

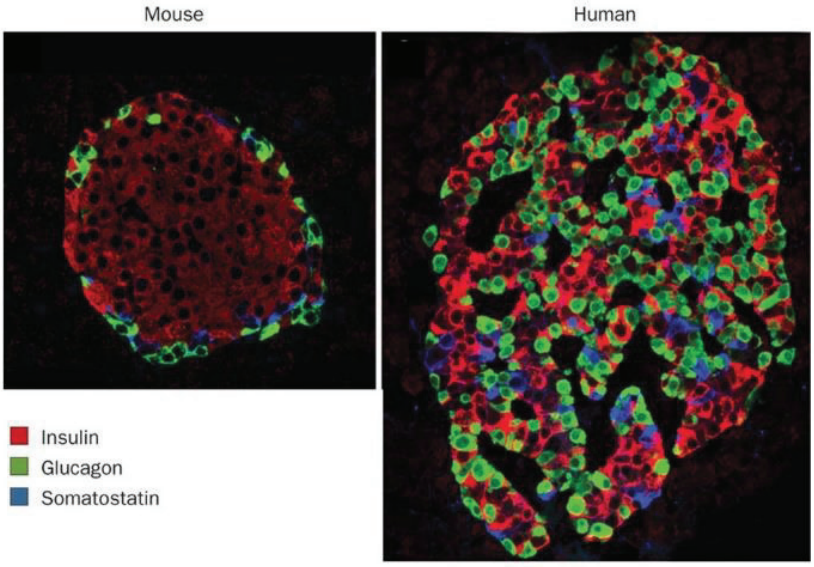

Figure 3: Cell composition of mouse and human islets. Representative images of a mouse islet, with centered insulin containing cells, and a human islet with a diffused arrangement of endocrine cells. (Adapted from **(28)**)

β-cells secrete the hormone insulin in response to high blood glucose levels to prevent hyperglycemia **(22)**. The small dipeptide consists of an A-chain (21 amino acids) and a B-chain (30 amino acids) connected via two disulfide bonds. Insulin is produced as proinsulin (A- and B-chain joined by C-chain) at the rough endoplasmic reticulum (ER) and packed in small vesicles. Endoproteases PC2 and PC1/3 cleave the inactive precursor at the trans-golgi-network (TGN), where equal amounts of mature insulin and C-peptide are stored in secretory granules **(29, 30)**. Various stimuli such as fatty acids, monosaccharides, amino acids and glucose initiate the release of the peptides into the bloodstream, with glucose as the main trigger. Plasma glucose enters β-cells via glucose transporter Glut2 and is phosphorylate by glucokinase in a rate-limiting step. Glucose-6-phosphate is oxidized to Pyruvate in glycolysis and further metabolized in the mitochondrial tricarboxylic acid cycle (also known as Krebs cycle) and subsequent oxidative phosphorylation. The following increase in cellular ATP/ADP ratio leads to closure of ATP-sensitive potassium channels (K_{ATP}), β-cell membrane depolarization and opening of voltage-dependent calcium (Ca^{2+}) channels (VDCC). Elevated intracellular Ca^{2+} concentration activates exocytosis of insulin-containing secretory granules (**Fig. 4**). Released insulin regulates glucose homeostasis and acts on insulin sensitive tissue, i.e. skeletal muscle tissue, adipose tissue and the liver. Here, specific binding of the insulin receptor (IRS) triggers

several downstream pathways such as glucose uptake, glycogen and protein synthesis, as well as inhibition of lipolysis to decrease blood-sugar concentration **(31-33).**

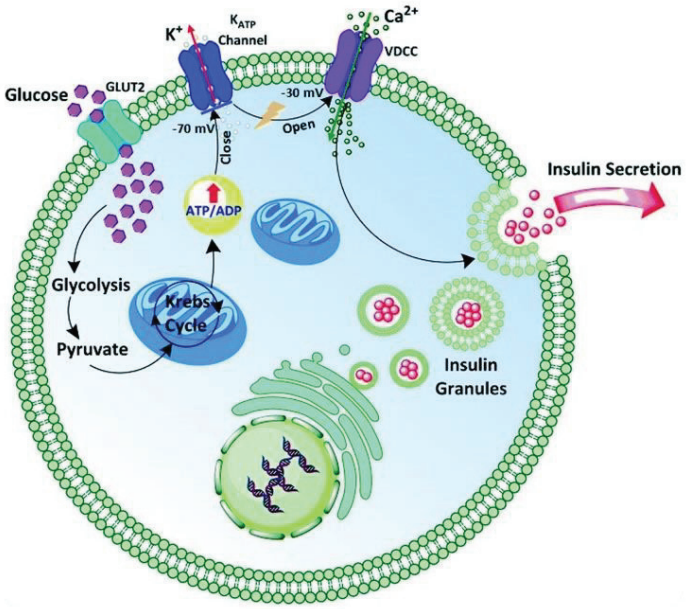

Figure 4: Insulin secretion by β-cells. Glucose metabolism results in an elevated ATPD/ADP ratio, which triggers potassium channel closure, membrane depolarization and subsequent VDCC opening. The following increase of cellular Ca^{2+} concentration promotes insulin release. (Adapted from **(34)**)

α-cells in the islets secrete the glucose promoting hormone glucagon to prevent hypoglycemia. Glucagon is produced as proglucagon and processed by the enzyme prohormone convertase 2 (PC2) into its mature forms glucagon or to the incretin glucagon-like peptide 1 (GLP-1) or GLP-2 by PC1/3 **(35, 36)**. The main target of glucagon is the liver where it controls glucose metabolism. Activation of the highly specific glucagon-receptor triggers gluconeogenesis and glycogenolysis, while inhibiting glycogenesis and glycolysis, to increase the blood-sugar concentration. Release of glucagon is regulated and inhibited by glucose **(37)**. Whether this is a direct effect of glucose or a paracrine effect from adjacent endocrine cells is still not solved. Insulin, ɣ-Aminobutyric acid (GABA) and Zn^{2+} released by β-cells as well as somatostatin secreted by δ-cells are among the potential candidates **(38-41)**.

δ-cells transcribe two somatostatin isoforms: SST-28 (28 amino acid) and SST-14 (14 amino acid). Pancreatic δ-cells express mainly the small peptide upon glucose stimulation and are a major regulator of neighboring endocrine cells. Binding of SST-14 to somatostatin receptor 2 (SSTR2) inhibits exocytosis of insulin and glucagon in human β- and α-cells **(41, 42)**.

Pancreatic polypeptide secreting PP-cells (also known as F-cells) are more abundant in the head region of the pancreas. Food intake stimulates exocytosis of PP (36 amino acids) and it mainly controls appetite, gastric emptying and energy metabolism **(22, 43).** Recent studies suggest further an involvement in islet regulated glucose homeostasis **(44, 45)**.

Ghrelin (28 amino acids) increases plasma glucose level, however, the exact effect of pancreatic ghrelin-cells on glucose homeostasis is still under debate **(46-48)**.

Communication of neighboring cells is crucial to control glucose homeostasis of the body. Any disturbances that either disrupt these mini-organs or interferes with the proper regulation of hyperglycemia can lead to the severe disease diabetes. In the following chapters, I will highlight the potential risk factors that might be involved in autoimmune mediated β-cell death and clinical onset of T1D.

2.3 Risk factors

The frequency of new T1D cases is increasing worldwide, although its quantity differs between individual countries. Finland and Sweden are highly affected, whereas it is rarely detected in India and China **(1)** but incidences can also vary among neighboring countries **(49, 50)**. Children of immigrants from low risk-countries, have higher chances to develop diabetes when born in high-risk countries than in their native country **(51)**. Genetic inheritance seems to be an additional risk factor besides the place of residence. Individuals with first-degree diabetic relatives have higher chances to develop T1D than with unaffected family members. Similar for monogenetic twins (50%) compared to dizygotic twins (10%) **(1)**. These observations point toward a fatal combination of genetic predisposition and environmental factors that trigger T1D onset.

2.3.1 Genetic Predisposition to T1D

2.3.1.1 HLA

Human leucocyte antigen (HLA) is one of >50 genes that are associated with an increased T1D susceptibility. The loci is located on chromosome 6p21 and probably responsible for around half of familiar inherited T1D. This highly polymorphic region is divided in three classes: HLA class II shows the strongest association with a genetic risk and class I just to a minor extent. Genes encode for extracellular antigen presenting protein complexes involved in immune reactions, one gene for the single-chain of HLA class I and two for the α and β chain of HLA class II heterodimers. MHC class I is expressed by all nucleated cells and present cellular antigens to $CD8^+$ T-cells, whereas MHC class II is expressed on immune APCs (Antigen

presenting cells) such as macrophages, dendritic cells, B-cells and present extracellular antigens to $CD4^+$ T-cells. Classical HLA class I genes are HLA-A, -B and –C, and HLA- class II genes are DR, DQ and DP. A genetic susceptibility to diabetes is strongly related to the DR- and DQ encoding loci **(52, 53)**. Children with the HLA haplotype HLA DRB1*03,*04;DQB1*0302 have the highest risk to develop diabetes in future life. Individuals who inherited this genotype have a 6,8% risk for T1D, which raises to 25% when born in families with one and even up to 50% with two or more family members with diabetes **(54)**. The most common DR-DQ haplotype in Caucasians DRB1*15:01-DQA1*01:02-DQB1*06:02 shows protection from T1D and is found rarely (<1%) in T1D patients **(52, 55)**.

HLA class I has been linked to inherited T1D as well. For instance, HLA-A*24 is associated with complete destruction of β-cells **(56)** and HLA-A*02 increases the risk of disease onset in patients who are class II DR3/4-DQ8 haplotype **(57)**. Within the HLA-class I B genes HLA-B*57:01 show protective and HLA-B*39:06 a predisposing function **(58)**.

2.3.1.2 Non-HLA

The group of non-HLA T1D-associated genes includes both immune and β-cell dependent genes. Insulin is one of the highest non-HLA T1D risk gene and is divided in various classes. The amount of variable number of tandem repeats (VNTR) in the promoter region upstream of the *INS* gene is crucial **(59, 60)**. Individuals with short class I VNTR have 26 to 63 repeats and a high predisposition for T1D. Whereas long class III VNTR have 140 up to 210 repeats and show low risk for T1D. VNTRS with an intermediate length (class II) are hardly observed **(59, 61)**. Insulin production in pancreatic islets is just slightly affected by VNTRs. Their length is important in the thymus where *INS* with class III VNTRs is significantly more expressed than *INS* with class I. Higher amount of insulin in the thymus reduces the chance of autoreactive T-cells towards insulin and T1D development **(62)**.

Protein tyrosine phosphatase non-receptor type 22 (PTPN22) gene encodes for the lymphoid tyrosine phosphatase (LYP), which negatively regulates the T-cell receptor (TCR) signaling cascade and T-cell activation. The risk of T1D is associated with a single nucleotide polymorphism (SNP) within the catalytic domain **(63)**. The SNP impairs the interaction of LYP with carboxy-terminale SRC kinase (CSK) and alters T-cell response **(64)**. Another T1D risk gene encodes Cytotoxic T-lymphocyte-associated protein 4 (CTLA-4) **(65)**. As a negative regulator of T-cell activation, it is expressed on the surface of activated $CD4^+$ and $CD8^+$ T-cells. A SNP has been related to T1D and presumably influences processing and intracellular trafficking, as well as functional surface expression of the protein. Individuals with a nucleotide

polymorphism in the ILR2A gene are at genetic risk for T1D. IL2RA encodes for the alpha subunit of the Interleukin 2 receptor (IL2Rα /CD25) that is required for high affinity Interleukin-2 (IL-2) binding. The receptor is expressed on activated T-cells and constantly on T_{reg}-cells. The latter can suppress inflammatory responses by competing for IL2 with $CD4^+$ T-cells and prevent autoimmunity **(66, 67)**.

Genes of the innate immune system, which connect a potential environmental trigger to interferon based immune response, are among the potential T1D risk alleles as well. Interferon induced with helicase D domain 1 (*IFIH1*) gene encodes for the cytoplasmic double stranded RNA-receptor Melanoma differentiation-associated protein 5 (MDA5) **(68)**. SNPs in the IFIH1 gene that decrease the expression or function of MDA5 should reduce antiviral immune response and potentially lower the risk of T1D. Whereas normal to elevated expression and function of MDA5 could lead to high-risk of T1D development upon viral infection **(69, 70)**. Several mutations in genes encoding for the mammalian homologues of Drosophila toll proteins were documented. Toll-like receptors (TLRs) 3 and 7 are located within endosomes and recognize viral pathogens upon cell entering. Nucleotide polymorphisms in the dsRNA binding TLR3 and ssRNA binding TLR7 genes have been associated with T1D **(71, 72)** or affected the response to viral infections **(73-76)**. Considering the potential combination of environmental factors, such as viruses, and genetic predisposition in T1D onset, TLR3/7 represent a highly interesting target group among the non-HLA risk genes. Therefore, this thesis addresses the role of these receptors in early viral recognition and cellular response in infected human pancreatic islets.

2.3.2 Environmental Factors

2.3.2.1 Sunlight/Vitamin D

Regional differences in T1D incidences among countries like Finland and India, as well as the seasonal pattern of disease onset, suggested sunlight and especially lack of Vitamin D as environmental trigger. Almost all Vitamin D synthesized by the human body is induced by sunlight. Provitamin D_3 is transformed upon UV-B exposure to Vitamin D and further metabolized along with dietary in taken Vitamin D. *VDRs (*Vitamin D receptor) are expressed on activated T-cells as well as on APCs and ligand binding can affect the immune responses **(77, 78)**. Human β-cells express VDRs too **(77)**, however, studies about the beneficial effect of Vitamin D supplementation on T1D risk reduction remain controversial **(79-81);** likewise, a connection of Vitamin D metabolites serum levels in pregnant women and the risk of T1D onset in offspring has not been fully confirmed **(82, 83)**.

2.3.2.2 Diet/ Nutrition

Infant's diet is linked to T1D onset, but one sole candidate has not been identified so far. Shortening of breastfeeding and nursing with dietary supplements have been proposed as risk-factors. Only few studies could show a connection **(3, 4)** of short breastfeeding and diabetes but most did not observe a protective effect **(84, 85)**. Also data about early cow's milk feeding as risk factor **(5)** or the protective effect of casein hydrolysate instead of cow's milk formula **(6)** could not be completely supported **(84, 86)**. The discrepancy of these studies might be explained by Lempainen et al., **(87)**. The authors suggest that the risk of cow's milk induced autoimmunity only applies for young children with a C1858T polymorphism in the *PTPN22* gene. Also, an early gluten-containing diet has been associated with T1D onset since a report of children with T1D and celiac disease in the late 1960s **(88)**. However, neither gluten-containing food itself nor the time point of its introduction **(85, 89, 90)** could be fully confirmed as potential trigger of T1D **(91)**. Additional studies did not show any rescuing effect of a gluten-free diet at early life **(92, 93)**. Other candidates that have been linked to T1D are root vegetables and eggs **(91)**, as well as the percentage of vegetables in the mothers' diet **(94)**. Ingested N-nitroso compounds from food or drinking water have been considered as risk-factor too **(95)**, since high concentrations can be toxic to β-cells **(96)**, but also this theory could not be confirmed **(97)**.

2.3.2.3 Microorganisms

A potential explanation for the increasing rates of T1D is provided by the 'hygiene hypothesis', which has been originally postulated back in 1989 **(98)**. Although the study focused on increasing cases of allergies, such as hay fever in the "western-world", it also applies for autoimmune diseases such as T1D. The immune system of children growing up in an almost germ-free environment, with less siblings and late introduction to daycare encounters insufficient numbers of pathogens during early maturation **(98-100)**. Lack of exposure to foreign antigens might result in future reaction to self-antigens. This hypothesis could explain the regional differences of T1D cases and their increasing numbers described earlier. A correlation of sterile environment and increased chances of T1D as well as a protective effect of HEV infections has been shown in rodent experiments **(101).** In line with this hypothesis, cellular pathogen recognition receptors detect harmful invaders are among the non-HLA risk genes. Although the hygiene hypothesis has not been fully proven in humans so far **(102-105)**, it strongly points towards a relationship between microorganisms and T1D pathogenesis.

2.3.2.3.1 Bacteria

T1D patients are at great risk of bacterial infection **(106, 107)** and a preproinsulin reactive $CD8^+$ T cell clone showed potential cross-reactivity to a peptide sequence within the proteomes of *Bacteroides fragilis/thetaiotaomicron* and *Clostridium asparagiforme* **(108)**. Still, bacterial pathogen driven T1D onset has not been reported so far. Bacteria are rather implied in development of autoimmune diseases as part of the gut intestinal microbiota, which consists of up to 10^{14} microorganisms and numerous different species **(109)**. Colonization of the new born babies' gut starts directly after birth **(110)** and future diet furthermore affects the composition of the microbiota **(111)**. Most data linking microbiota and development of diabetes are based on rodent experiments **(112-115)**, but some studies could show a reduction in microbiome diversity among young high-risk T1D individuals from Finland **(116, 117)** and Estonia **(118)**. However, a direct correlation of human gut microbiota and development of diabetes is still missing.

2.3.2.3.2 Viruses associated with T1D

Regular T1D outbreaks during the cold time of the year points toward viral pathogens as environmental trigger **(7, 119).** A multitude of viruses have been linked to T1D onset in the past:

The first theoretical connection of a disease with T1D was made in 1898, when a patient showed signs of diabetes one month after mumps attack **(120)**. About 100 years later it became clear, that mumps virus can infect cultured human β-cells **(121)** and might induce an autoimmune-response **(122)**. Islet autoantibodies have even been found in mumps infected children **(123)**, but a Finnish vaccination program just resulted in a plateau of new T1D incidences in the following years **(124)**. Rubella virus has been associated with T1D **(125, 126)** and sequence similarities between the viral agent and islet proteins supported this theory **(127, 128)**. The virus can also infect and impair cultured β-cells, but does not show any cytopathic effect **(129, 130)**. Recent studies suggest therefore that diabetes in congenital rubella syndrome patients is not auto-immune mediated, but based on pancreatic development deficiencies **(131, 132)**. Rotaviruses that commonly infect young children and cause gastrointestinal disturbance have been linked to diabetes induction as well. Infected T1D-risk children showed an increased level of islet autoantibodies and sequence similarities of β-cell and rotaviral autoantigens are documented **(133)**. However, a rotavirus induced β-cell autoimmunity in T1D susceptible children could not be confirmed **(134)**. Also, human Cytomegalovirus (CMV) has been suggested to cause T1D; an infant suffering from a CMV infection developed T1D within one

year and a correlation of islet autoantibodies and the identification of the viral genome in PBMCs of patients with T1D has been detected **(135, 136)**. An infection could break self-tolerance to induce autoimmunity **(137)** and *in vitro* experiments further support the risk-potential of CMV infection **(138)**. However, these observations were not confirmed among Finnish children **(139, 140)**.

The most prominent candidates for viral-induced T1D are enteroviruses, especially Coxsackieviruses. Infections are very common and most (80%) induce just mild diseases as rash, upper respiratory symptoms or myalgia, but also severe and chronic diseases such as myocarditis are possible **(141)**. Gamble and Taylor **(7)** found a correlation of Coxsackievirus B4 (CVB4) infections and diabetes onset among young T1D patients, as well as an increased level of enterovirus antibodies. The same virus was isolated from the pancreas of one ten-year-old boy with diabetic ketoacidosis, who has just suffered from a flu-like illness **(8)**. Isolated enteroviruses from patients with T1D could even induce diabetes in mice **(142)** and impaired function and survival of cultured human islets **(143)**. Of special interest are two recent studies that strongly support the hypothesis of coxsackievirus-induced T1D. The first one re-evaluated 24 individual studies, including 4448 participants. The authors clearly show a significant association of molecular markers of enterovirus infection and autoimmunity with T1D in humans **(9)**. The second one analyzed biopsy samples from the pancreatic tail-region of living human patients, collected within few weeks after T1D diagnosis. The endocrine pancreas of all six patients with T1D was positive for enteroviral protein (VP1) and enteroviral RNA was detected in four cases **(10)**. Among the presented environmental factors, enteroviruses (coxsackieviruses) are the most likely candidates that could trigger T1D onset in genetic predisposed individuals. Taking this into consideration, this thesis addresses the role of coxsackieviruses in β-cell destruction as well as the presence of enteroviral genomes in the pancreas of patients with diabetes.

2.4 Coxsackieviruses infection as cause for T1D

2.4.1 Enteroviral lifecycle in infected cells

Enteroviruses belong to the family of Picornaviridae and are based on their phylogenetic relations subdivided in the four species Enterovirus A-D. Among the various serotypes, the most prominent are within group A Enterovirus 71 and Coxsackievirus A16 and Coxsackievirus B1-6 of group B **(144)**. Picornaviridae are small (30 nm diameter) non-enveloped viruses. One particle is a symmetric icosahedral capsid made of 60 copies of each of the four structural viral

proteins VP1-4. VP1-3 (240-290 residues) shape the outer shelf whereas the smaller (70 residue) VP4 is located inside **(145)**. The viral genome (7,5kb) is enclosed in the capsid and consists of a linear positive-sense single-stranded RNA (+(ssRNA)). Each genome is composed of one single open reading frame (ORF) flanked by untranslated regions (UTRs) at 5' (800 bases) and a smaller at 3' (100 bases). The 5'-terminus is covalently linked to VPg (viral protein genome-linked) and the 3'-terminal end contains a poly-A-tail **(146, 147)**.

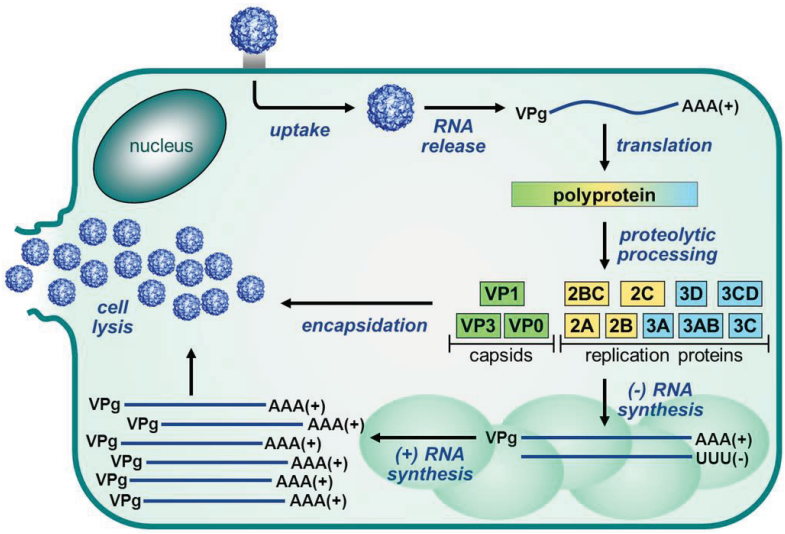

Figure 5: Enteroviral replication cycle in infected cells. Enteroviruses infiltrate the host and release the +(ssRNA) genome into the cell. The +(ssRNA) is directly translated into one single polyprotein, which is processed to structural and non-structural proteins. Viral –(ssRNA) intermediates serve as template for further +(ssRNA) genome amplification, which are subsequently encapsidated. Viral capsids leave the host via cell-lysis at the end of the replication cycle **(146)**.

Coxsackieviruses are commonly transmitted between humans via the fecal-oral-route and attach to the host cells through the cell-surface receptors CAR (coxsackie and adenovirus receptor) and DAF (Decay accelerating factor), also known as CD55 **(Fig. 5)**. Human α- and β-cells only express CAR **(148, 149)** and its expression level is increased in islets of T1D patients **(150)**. Interaction of virion and receptor induces a capsid reorganization and genome transfer into the cell, but also clathrin-mediated endocytosis is possible. The following initiation of translation starts with binding of host ribosomes at the internal ribosome-entry site (IRES) located within the 5' UTR, where VPg acts as primer for the RNA-polymerase. Viral +(ssRNA) serves as messenger RNA and can directly be translated in a cap-independent fashion to one large polyprotein (2300 amino acids), which is subsequently cleaved in structural and non-

structural proteins. The +(ssRNA) is transcribed into complementary –(ssRNA) intermediate that act as template for further genome production. This process occurs in replication complexes on reorganized cellular membranes. To enforce its own IRES-dependent translation, viral 2A protein shuts-off host cap-dependent translation by cleavage of eIF-4G. Viral genome transcription is the driving-force for capsid production and RNA encapsidation, the newly formed virions finally exit their hosts via cell-lysis during an acute phase of infection **(146, 147, 151)**. In addition, Coxsackievirus can promote a non-lytic persistent infection in β-cells **(148)** with reduced genome replication and diminished protein production **(152)**. Non-lethal truncation of the 5'-UTR **(153, 154)**, as well as formation of dsRNA complexes **(155)** that allow persistent infections are possible.

To complete the viral replication cycle, pathogens are dependent on the host survival, whereas infected cells need to detect the foreign invader and recruit immune cells to stop further infections.

2.4.2 CVBs utilize host cell survival pathways

Infected cells can directly undergo apoptosis **(156)** to prevent pathogen spreading among neighboring cells **(157)**. To circumvent this self-defense mechanism, viruses adapted several ways to stop or delay cellular apoptosis with the aim to utilize components of the cellular survival pathways for their own replication.

The phosphatidylinositol 3-kinase (PI3K)/AKT signaling pathway is involved in several regulatory processes and commonly used by viruses. The serine/threonine kinase AKT, also known as protein kinase b (PKB), consists of a N-terminal PH domain, a catalytic domain and a C-terminal hydrophobic domain. PI3K generates phosphatitdylinositol-3,4,5-triphosphates (PIP_3) upon activation, which serves as binding platform at the cellular membrane for the PH domains of AKT and phosphoinositide-dependent kinase 1 (PDK1). PDK1 phosphorylates AKT in the catalytic domain at Threonine 308 and becomes fully activated by phosphorylation in the hydrophobic domain at Serine 473 by mammalian target of rapamycin complex 2 (mTORC2). Activated AKT has several downstream targets and functions as a pro-survival regulator **(158, 159)**. CVB3 replication has been shown to be dependent on PI3K induced AKT activation in HeLa cells, which is probably mediated by AKT induced NF-$_k$B activation **(160, 161),** and the kinase is further involved in β-cell survival **(162, 163)**. Therefore, the role of AKT in CVB infected human β-cells was studied in this thesis.

Another important group of protein kinases involved in viral replication are the Extracellular-signal-regulated kinases (ERKs, also known as p42/ p44 MAPK). ERKs belong to the family

of mitogen-activated protein kinases (MAPKs) and regulate proliferation, survival and apoptosis. MAPKS are activated by extracellular stimuli such as external growth factors, integrins or G-proteins, which induces a signaling cascade. RAFs are activated by RAS-GTP at the cellular membrane and phosphorylate downstream target MEK1/2. The latter finally activates the serine/threonine kinase ERK. Upon dimerization, Erk1/2 controls several downstream targets to regulate, among other things, cellular survival and apoptosis. **(164, 165)**. Furthermore, CVB3 infection induces ERK1/2 activation and EV71 replication is dependent on both, ERK1/2, and MEK1 but not MEK2 **(166-168)**. However, the role of ERK1/2 in CVB infected β-cell lines remains elusive and was investigated in this thesis.

AKT and ERK signaling pathways can also interact and share downstream targets. ERK phosphorylates TSC2 and induce mTORC1 activation **(169)** and Ras can directly interact and activate PI3K **(170)**. On the other side, AKT can phosphorylate and inhibit the ERK regulator RAF **(171)**. A dual involvement of these kinases seems also to apply for enteroviral infection, where AKT and ERK1/2 are both activated **(172)**. Based on these findings it was investigated, whether both survival pathways can compensate for each other during viral replication in β-cell lines.

2.4.3 Viral recognition in the host cell and immune response

The cellular host needs to recognize infiltrating pathogens to initiate an immune response. Macrophages and dendritic cell are the center of the innate immune system but also non-professional cells such as endothelial cells, fibroblasts and β-cells can be involved. The innate immune system recognizes pathogen associated molecular patterns (PAMPs) of foreign intruders. These conserved structures are bound by germline-encoded pattern recognition receptors (PRRs) and induce an intracellular signaling-cascade that activates gene transcription for pro-inflammatory cytokines and chemokines. Involved in an antiviral response are four families of PRRs: Toll-like receptors (TLRs) on cellular membranes and endosomes, cytosolic RIG-I-like receptor (RLR) family, cytosolic dsRNA-dependent protein kinase R (PKR) and cytosolic the nucleotide-binding oligomerization domain (NOD)-like receptors (NLR) **(149, 173-175)**. Around ten different TLRs are known in humans and recognize mainly bacterial and viral derived ligands. TLRs consist of an extracellular N-terminal leucine-rich repeat domain that binds PAMPs, a transmembrane domain and a cytosolic Toll/IL-1 (TIR) domain that activates the signaling cascade. TIR domains of two adjacent TLRs dimerize upon ligand binding and enable docking of intracellular adaptor proteins. Two distinct proteins can bind to the TLR C-terminus and determine the cellular response. Myeloid differentiation factor 88

(MyD88) activates the transcription factors NF-$_k$B and IRF7 and mitogen-activated protein kinases (MAPK) p38 and JNK. The TIR domain-containing adaptor inducing INF-β (TRIF) also activates NF-$_k$B and further IRF3. The activated transcription factors translocate to the nucleus and stimulate cytokine (NF-$_k$B) and type I interferon (IRF3/ IRF7) expression **(176, 177)**. Endosomal TLR3 recognizes viral dsRNA and exclusively uses TRIF as adaptor protein. TRIF can activate two different downstream pathways via TRAF-6 and TRAF-3 activation. The former activates TAK1 and induces finally NF-$_k$B translocation and inflammatory cytokine upregulation. The latter activates tank-binding kinase 1 (TBK1) that triggers IRF-7 and IRF-3 translocation and Type 1 interferon upregulation **(178)**. Viral ssRNA is detected by endosomal TLR7 that activates the MyD88 and TRIF signaling-pathways **(177)**.

Cytosolic viral dsRNA is bound by the two RLRs RIG-I and MDA5. Both contain a N-terminal caspase recruitment domain (CARD), DExD/H-box-containing RNA helicases and a regulatory domain at the C-terminus. RIG-I recognizes rather short dsRNA (up to 1kb) and MDA5 long dsRNA (more than 2kb). Ligand binding induces a signaling cascade that requires CARD and the adaptor molecule MAVS located at mitochondrial membrane. Downstream TBK1 activation triggers IRF3, IRF7 and NF-$_k$B signaling pathways and type 1 interferon and cytokine upregulation **(175, 177, 179)**. Interestingly, CVB3 can directly abolish these response mechanisms as non-structural protein 3C^{pro} can cleave MAVS and TRIF **(180)**.

PKR has a N-terminal dsRNA binding domain and a C-terminal serine/threonine kinase domain. Ligand binding induces autophosphorylation and dimerization, followed by inactivation of eukaryotic initiation factor 2α (eIF2α). Phosphorylated eIF2α cannot interact with Met-tRNA and inhibits initiation of translation, which globally stops cellular and pathogen protein syntheses. PKR further activates the MAPK kinases JNK and p38, modifies insulin response via insulin receptor IRS, as well as activates the NF-$_k$B signaling pathway **(181)**.

2.4.4 Actions of the Immune system in response to β-cell "SOS" signals

Anti-islet T-cells, CD4 and CD8, have been found in animal models, as well as in T1D positive humans and seem to be the driven force of autoimmune mediated β-cell destruction **(182-184)**. The invaders are joined by B-cells (CD 20) and Macrophages (CD 68) and islet inflammation is accompanied by MHC class 1 upregulation **(185, 186)**. Lymphocytes, as well as neutrophils also reside in the exocrine tissue **(187, 188)**.

2.4.4.1 Immune cell mediated β-cell destruction.

T-cell Receptors (TCRs) of autoreactive $CD8^+$ T-cells recognize antigens displayed by MHC class I molecules on the surface of β-cells **(189)**. This event triggers T-cell secretion of cytotoxic granules, including perforin and granzyme, which initiates β-cell death **(Fig.6)**. Perforin targets cellular membranes and facilitate granzyme entering and induction of apoptosis. Interaction of T-cell FasL with β-cell Fas receptor activates a caspase signaling cascade and mitochondria mediated apoptosis, although to a lesser extent than granzymes. Further proinflammatory cytokine secretion (TNF-α and INF-ɣ) triggers free radical production and ER-stress induced cell-death **(190)**. Surrounding antigen presenting cells (APCs) pick up cellular debris of dying cells and display processed self-antigens via MHC class II molecules. Those are recognized by $CD4^+$ T-cells, which secrete cytokines (INF-ɣ and IL-2) to recruit more Macrophages, CD8-cells and B-cells to the inflamed islet and enhance the immune response. INF-ɣ stimulate Macrophages to release further cytokines (IL1-β and TNF-α), free radicals and upregulate MHC class II expression. Recruited B-cells present self-antigen via MHC class II and secrete islet cell autoantibodies (ICAs) **(191)**. Most prominent ICAs recognize insulinoma-associated antigen-2 (IA-2), Zinc transporter 8 (ZnT8), glutamic decarboxylase 65 (GAD65) and mIAA (Insulin) **(54)**. This seroconversion to ICAs represents a valid indicator for future disease's onset and is a crucial characteristic to distinguish T1D from T2D patients **(192, 193)**.

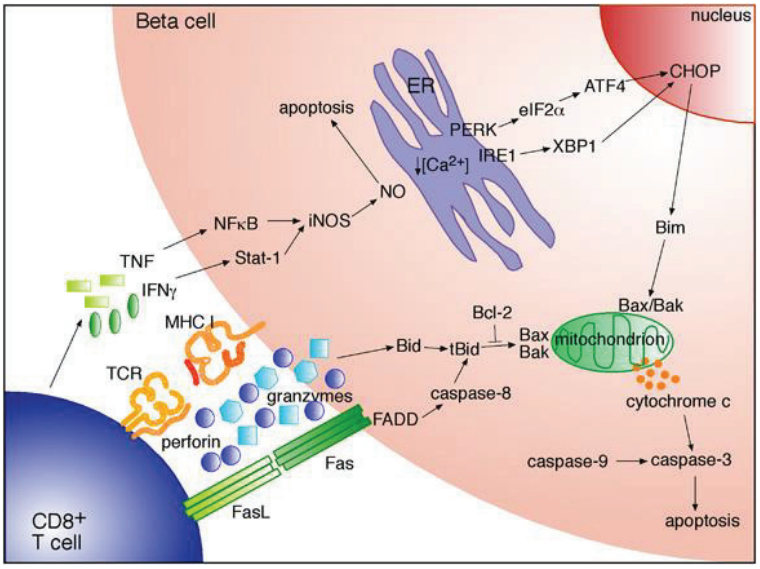

Figure 6: $CD8^+$ T-cell induced β-cell death. Autoreactive $CD8^+$ T-cells recognize antigens displayed by MHC-1 molecules on the β-cell surface via TCRs. Following interaction induces perforin and granzyme secretion, as well as FasL and Fas interaction, which trigger mitochondrial apoptosis pathways. In addition, inflammatory cytokines (TNF and INFɣ) provoke free radical production and ER-stress in β-cells **(190)**.

2.4.5 Virus induced autoimmunity

Coxsackieviruses were found in pancreata of T1D donors and show islet tropisms **(148, 149, 194, 195)**. However, if and how a viral infection causes β-cell demise is still under debate.

Peptide fragments of infiltrating pathogens and host proteins can share sequence homologies. This molecular mimicry of epitopes can trigger auto-aggressive T-cells to cross-attack non-pathogen proteins and induce autoimmunity **(196)**. Sequence similarity of an anti-islet T-cell target (GAD65) and CVB4 non-structural protein P2-C could supposedly induce cross-reactivity **(197)**. However, further data remain controversial and do not fully support this hypothesis **(196, 198-200)**. Hence, molecular mimicry of epitopes probably does not trigger autoimmunity, but rather promotes diseases development **(201)**.

Pathogens might induce autoimmunity indirectly by bystander-activation or -killing. Viral infiltration creates an area of inflammation that attracts virus-specific T-cells along with non-selected auto-aggressive T-cells, that might be activated irrespective of the presented antigen. Within the center of inflammation can uninfected cells be killed by released cytokines and chemokines of apoptotic cells, infiltrating virus-specific $CD8^+$ T-cells and macrophages. Sequestered peptide fragments of β-cells are subsequently presented by APCs and might trigger autoreactive T-cells to attack neighboring β-cells **(11, 196, 202)**.

Molecular mimicry and bystander activation are united in the fertile field hypotheses. An initial acute viral infection is cleared by the immune system, but triggers the production of auto-aggressive T-cells, primed for self-antigens via molecular mimicry and/or bystander activation. Every future, single, viral encounter will enlarge this pool of pancreatic resident autoimmune cells indefinitely. The final activation and induction of autoimmunity occurs at a much later time point as the initial priming. This event can be induced by a non-related viral infection or other mechanism that cause self-antigen presentation **(203)**.

In another model do β-cells expose themselves to the adaptive immune system and recruit auto-aggressive T-cells. This could be a long-lasting effect of persistent viral infections. Viral RNA, but not protein, has been detected in gut mucosa biopsies samples and was confirmed in a one year later follow-up **(204)**. Hyperexpression of HLA1 in long-term T1D patients **(205)** and low amounts of VP1 positive human islets **(206)** further indicate chances of persistent infection in humans. Finally, the hypothesis of low-replicating and long-standing viral infection in pancreata was confirmed in mouse and *in vitro* studies **(153)**. Acute and persistent CVB infection trigger β-cell secretion of pro-inflammatory cytokines and chemokines that orchestrate T-cell migration **(207)**. Among those is interferon-ɣ induced chemokine (C-X-C

motif) ligand 10 (CXCL10) **(208)**. The corresponding receptor CXCR3 is located on NK cells, activated T-cells and memory T-cells and CXCL10 induces T-cell migration towards β-cells **(209, 210)**. CXCL10 has been found in elevated concentrations in serum of T1D patients **(211)** and along with CXCR3 in autopsy pancreatic islets sections **(212)**. Pathogens might therefore induce an inflammatory amplification loop in fulminant T1D. Infected β-cells secrete CXCL10 and recruit auto-aggressive T-cells and macrophages to the site of inflammation. Infiltrating T-cells attack β-cells and secrete INF-ɣ and TNF-α that triggers further CXCL10 release and T-cell recruitment **(213, 214)**.

2.5 CVB detection in human T1D donor tissues

From the presented environmental factors that could trigger an autoimmune response in genetically predisposed individuals, enteroviruses are the most likely candidates. Yet, the puzzle is still not solved. Viral presence in human pancreata and causality between infection and T1D onset has not been fully proven so far. In line with the hygiene hypothesis enteroviral infection has even been connected with a protective function **(101)**. Most of the data generated in humans is based on autopsy samples from T1D donors and molecular approaches are generally applied **(9)**. Hence, three of the most common techniques to show presence of viruses in the pancreas of patients with T1D, together with their advantages and disadvantages, are described below.

2.5.1 Immunohistochemistry

One established tool to screen for enteroviral infections in human tissues is immunohistochemistry (IHC). A commercial monoclonal antibody (Clone 5-D8/1, Dako Denmark) that detects a highly-conserved epitope on the VP1 peptide (35kDa) of CVB5, but also of other Enterovirus species as Echo- Coxsackie- and Polioviruses, is widely used for this purpose **(215, 216)**. Viral proteins have been found in pancreata of three out of six recent-onset T1D organ donors and in none of the tested controls. The resident pathogen was identified as CVB4 via whole-genome sequencing in one infected section **(195)**. In another extensive analysis of formalin-fixed paraffin embedded (FFPE) pancreas sections from a UK cohort, 61% of recent-onset T1D patients were VP1 positive. Interestingly, also 40% of T2D patients showed VP1 staining in islets, but just few (7.7%) non-diabetic controls **(194)**. However, the specificity of this antibody is under debate. Hansson et al. **(217)** showed that clone 5-D8/1 could cross-react with the mitochondrial enzymes creatin kinase B-type (CKBB) and ATP-synthase subunit beta (ATP5B). This study does not exclude the high affinity of clone 5-D8/1 to EV71,

it rather suggests to use increased dilutions to avoid any potential cross-reactivity. Lack of specificity was further confirmed in *in vitro* assays **(218)** and on various tissue samples of human and mice **(219)**. However, under "carefully designed optimal conditions" no cross-reactivity was observed **(220)**. Other antibodies for viral protein 1 **(219)**, as well as dsRNA **(152)** were tested and proposed for future IHC studies as potential remedies. Still, usage of antibodies without further verification is under debate and their reliability questioned. Aside from cross-reactivity, variations in commercial antibodies among different batches or wrong application by the operator are possible and could inhibit reproducibility **(221, 222)**. In addition, this technique is just suitable for an early phase of acute infection. Since in a persistent infection, with low viral replication rates, the protein level is below the detection limit of IHC **(223)**.

2.5.2 PCR

A valid tool to screen for enteroviral genomes is polymerase-chain-reaction (PCR). Primers are generally chosen to bind within the highly conserved 5'-terminus or the capsid encoding region such as VP1. PCR is a highly specific and sensitive method **(224)** with the advantage to theoretically detect acute viral infections before or at the onset of the disease and material from living donors is available. More than half (64%) of PCR analyzed serum samples from young children with recent-onset T1D were positive for enteroviral RNA and some sequences showed even homology to CVB3 and CVB4 **(225)**. Further PCR-based studies of serum and stool samples showed an association of enteroviral RNA and T1D **(9)**. Enteroviral genome within serum appears to be a valid indicator for T1D, whereas stool samples can be neglected. However, in the case of an acute infection, viral RNA remains just for a short period within serum and during a persistent infection, if any, in numbers below the detection limit **(226)**. Detected viral genomes in the serum cannot be linked to a pancreatic infiltration, especially for common Coxsackievirus-infections **(141)**. A Finnish study found more enteroviral RNA in small-bowel mucosal biopsies samples of T1D patients (19%) than in controls (10%) and affirmed this observation in a follow-up study **(204)**. Yet, these data were challenged by an Italian group **(227)**. When PCR is used to confirm IHC staining in autopsy FFPE sections several obstacles arise. Extraction of high-quality RNA from pancreatic samples is challenging due to high amounts of endogenous RNases, DNases and proteases that start autolysis of the tissue shortly after organ removal **(228)**, leading to short fragments of extracted RNA **(229)**. Formalin-fixation further induces cross-linking of RNA and proteins, which aggravates extraction, and can modify RNA by addition of methyl groups ($-CH_2OH$) as well as formation of methylene bridges among amino groups **(230)**. RNA identification by PCR reactions can be

inhibited by these chemical modifications as well as by genomic mutations that affect the common primer annealing sites **(231)**. Although PCR has the potential for higher specificity and sensitivity than IHC **(232)**, viral localization within tissue sections cannot be identified by PCR.

2.5.3 Fluorescence *in situ* hybridization

The advantages of IHC and PCR are combined by fluorescence *in situ* hybridization (FISH) and allows to bypass their respective limitations. Oligonucleotide probes hybridize with their complementary sequence via Watson-Crick base-pairing and do not disturb tissue or cell morphology. Direct or subsequent indirect visualization of probes allows genome recognition within the respective cell. ISH as screening for nucleic acids was first introduced by Gall and Pardue (1969) **(233)** who used radiolabeled ribosomal RNA and autoradiography to detected DNA. Another significant step in the single molecule FISH (smFISH) assay development was performed by the Singer lab in 1998 **(234)**. Their probes were respectively labeled with five fluorochromes and five of each DNA probes (50mer) were used per target, creating a single distinguishable diffraction limited spot per mRNA molecule. Unfortunately, this method showed low coupling efficiency and problematic probe generation. Verification of IHC staining requires an assay that provides high sensitivity and specificity to detect even single viral genomes in persistent infected tissue samples. Three, now, commercially available FISH techniques are commonly used to detect single RNA molecules with high efficiency. Two of them, RNascope and ViewRNA, are based on paired probes and a branched DNA amplification system with indirect visualization (**Fig. 7A) (235)**. Two probes, each one resembles the letter "Z" with a 18-25 base region, a linker and 14 bases tail region, need to bind adjacent to their target region (around 50 bases). The combined tail region (28 bases) of the two individual probes provide a platform for the complementary pre-amplifier. Each preamplifier binds up to 20 amplifiers that provide 20 binding sites for multiple fluorescent molecules. Up to 20 probe pairs per target RNA bind to around 8000 fluorescent molecules **(236)**. Enteroviral RNA detection within FFPE sections has just recently been demonstrated via this technique **(237)**. The third method is based on a large pool (up to 48 probes) of rather short probes (17-22 nucleotides) (**Fig. 7B)**. Oligonucleotides bind individually to their target and can directly be visualized. Each single RNA probe is fluorescently labeled on the 3' terminus and does not require any further amplification. Most oligonucleotides must anneal in proximity but not adjacent on their complementary target to be fluorescently visible. Single false-binding probes

can therefore be neglected as their faint fluorescent signals are not detectable **(238, 239)**. This technique has only been used for viral cell culture experiments so far **(240, 241)**.

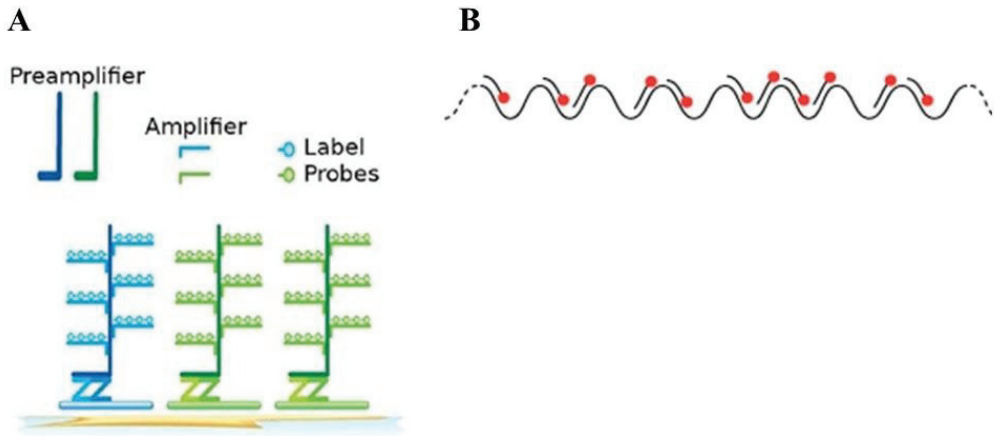

Figure 7: Principle of commercial available FISH techniques. (**A**) Scheme of branched amplification system, showing target probe hybridization with indirect signal amplifier and fluorescent labeling **(236)**. (**B**) Schematic model of single-labeled probes binding individually to their target, without signal amplification. (Adapted from **(242)**)

Both systems allow specific and sensitive single RNA detection. The branched tree assay provides in total a higher signal amplification compared to the single-labeled probes. However, the latter provides a better tool to screen even for degraded or fragmented RNA within FFPE tissue sections. smFISH probes require a smaller target region (20 bases vs. 50 bases) and can bind independently from another, which allows a higher-degree of freedom. The size and the independence further increase the chances to penetrate and bind their target within RNA-protein complexes **(243)**. FISH represents in general a powerful tool to screen for enteroviruses. It allows to detect the genome with high sensitivity and specificity and provides further information of localization.

Thus, I proposed the use of single-labeled probes in T1D pancreata to identify viral pathogens. With this new technique, I will overcome the presented limitations of IHC and PCR and provide solid-proof of enteroviral infections in pancreas of T1D patients.

2.6 Aim of the thesis

A fully convincing prove of enteroviral infections and induction of T1D in humans is still missing. Material from living diabetic donors is rare and common detection approaches showed limitations in autopsy recovered pancreata **(10, 217)**.

The aim of this study was to analyze, whether coxsackieviruses are located within pancreata of patients with diabetes and to identify the first cellular mechanisms during β-cell infiltration. With the help of *in vitro* assays, I identified cellular targets that are involved in the early viral life cycle and β-cell death. To support the hypothesis of viral-driven diabetes onset, I introduced short molecule FISH for the detection of up to single viral RNA molecules to the armory of enteroviral screening techniques. Establishment of this tool enabled me to detect even low amounts of viral genomes in commonly used FFPE human donor sections and validate previous results. This finally proved that enteroviral genomes are present in pancreata of patients with diabetes and suggests, based on the results of the *in vitro* study, that these infections are contributing to T1D onset in humans.

References

1. Atkinson MA. The pathogenesis and natural history of type 1 diabetes. Cold Spring Harb Perspect Med. 2012;2(11).
2. Wolden-Kirk H, Overbergh L, Christesen HT, Brusgaard K, Mathieu C. Vitamin D and diabetes: its importance for beta cell and immune function. Mol Cell Endocrinol. 2011;347(1-2):106-20.
3. Kimpimaki T, Erkkola M, Korhonen S, Kupila A, Virtanen SM, Ilonen J, et al. Short-term exclusive breastfeeding predisposes young children with increased genetic risk of Type I diabetes to progressive beta-cell autoimmunity. Diabetologia. 2001;44(1):63-9.
4. Holmberg H, Wahlberg J, Vaarala O, Ludvigsson J, Group AS. Short duration of breast-feeding as a risk-factor for beta-cell autoantibodies in 5-year-old children from the general population. Br J Nutr. 2007;97(1):111-6.
5. Gerstein HC. Cow's milk exposure and type I diabetes mellitus. A critical overview of the clinical literature. Diabetes Care. 1994;17(1):13-9.
6. Knip M, Virtanen SM, Seppa K, Ilonen J, Savilahti E, Vaarala O, et al. Dietary intervention in infancy and later signs of beta-cell autoimmunity. N Engl J Med. 2010;363(20):1900-8.
7. Gamble DR, Taylor KW. Seasonal incidence of diabetes mellitus. Br Med J. 1969;3(5671):631-3.
8. Yoon JW, Austin M, Onodera T, Notkins AL. Isolation of a virus from the pancreas of a child with diabetic ketoacidosis. N Engl J Med. 1979;300(21):1173-9.
9. Yeung WC, Rawlinson WD, Craig ME. Enterovirus infection and type 1 diabetes mellitus: systematic review and meta-analysis of observational molecular studies. BMJ. 2011;342:d35.
10. Krogvold L, Edwin B, Buanes T, Frisk G, Skog O, Anagandula M, et al. Detection of a low-grade enteroviral infection in the islets of langerhans of living patients newly diagnosed with type 1 diabetes. Diabetes. 2015;64(5):1682-7.
11. Coppieters KT, Boettler T, von Herrath M. Virus infections in type 1 diabetes. Cold Spring Harb Perspect Med. 2012;2(1):a007682.
12. Lakhtakia R. The history of diabetes mellitus. Sultan Qaboos Univ Med J. 2013;13(3):368-70.
13. Karamanou M, Protogerou A, Tsoucalas G, Androutsos G, Poulakou-Rebelakou E. Milestones in the history of diabetes mellitus: The main contributors. World J Diabetes. 2016;7(1):1-7.
14. Karamitsos DT. The story of insulin discovery. Diabetes Res Clin Pract. 2011;93 Suppl 1:S2-8.
15. Roglic G, World Health Organization. Global report on diabetes. Geneva, Switzerland: World Health Organization; 2016. 86 pages p.
16. American Diabetes A. Diagnosis and classification of diabetes mellitus. Diabetes Care. 2014;37 Suppl 1:S81-90.
17. Rhodes CJ. Type 2 diabetes-a matter of beta-cell life and death? Science. 2005;307(5708):380-4.
18. Kahn SE. Clinical review 135: The importance of beta-cell failure in the development and progression of type 2 diabetes. J Clin Endocrinol Metab. 2001;86(9):4047-58.
19. Harjutsalo V, Sjoberg L, Tuomilehto J. Time trends in the incidence of type 1 diabetes in Finnish children: a cohort study. Lancet. 2008;371(9626):1777-82.
20. Eisenbarth GS. Type I diabetes mellitus. A chronic autoimmune disease. N Engl J Med. 1986;314(21):1360-8.
21. Simmons KM, Michels AW. Type 1 diabetes: A predictable disease. World J Diabetes. 2015;6(3):380-90.
22. In't Veld P, Marichal M. Microscopic anatomy of the human islet of Langerhans. Adv Exp Med Biol. 2010;654:1-19.
23. Standring S. Gray's anatomy : the anatomical basis of clinical practice. Forty-first edition. ed. New York: Elsevier Limited; 2016. xviii, 1562 pages p.

24. Roder PV, Wu B, Liu Y, Han W. Pancreatic regulation of glucose homeostasis. Exp Mol Med. 2016;48:e219.
25. Seino S, Bell GI. Pancreatic beta cell in health and disease. Tokyo: Springer; 2008. xv, 474 p. p.
26. Brereton MF, Vergari E, Zhang Q, Clark A. Alpha-, Delta- and PP-cells: Are They the Architectural Cornerstones of Islet Structure and Co-ordination? J Histochem Cytochem. 2015;63(8):575-91.
27. Bonner-Weir S, Sullivan BA, Weir GC. Human Islet Morphology Revisited: Human and Rodent Islets Are Not So Different After All. J Histochem Cytochem. 2015;63(8):604-12.
28. Wang P, Fiaschi-Taesch NM, Vasavada RC, Scott DK, Garcia-Ocana A, Stewart AF. Diabetes mellitus--advances and challenges in human beta-cell proliferation. Nat Rev Endocrinol. 2015;11(4):201-12.
29. Dodson G, Steiner D. The role of assembly in insulin's biosynthesis. Curr Opin Struct Biol. 1998;8(2):189-94.
30. Steiner DF. The proinsulin C-peptide--a multirole model. Exp Diabesity Res. 2004;5(1):7-14.
31. Newgard CB, McGarry JD. Metabolic coupling factors in pancreatic beta-cell signal transduction. Annu Rev Biochem. 1995;64:689-719.
32. Fu Z, Gilbert ER, Liu D. Regulation of insulin synthesis and secretion and pancreatic Beta-cell dysfunction in diabetes. Curr Diabetes Rev. 2013;9(1):25-53.
33. Wilcox G. Insulin and insulin resistance. Clin Biochem Rev. 2005;26(2):19-39.
34. Castiello FR, Heileman K, Tabrizian M. Microfluidic perfusion systems for secretion fingerprint analysis of pancreatic islets: applications, challenges and opportunities. Lab Chip. 2016;16(3):409-31.
35. Mojsov S, Heinrich G, Wilson IB, Ravazzola M, Orci L, Habener JF. Preproglucagon gene expression in pancreas and intestine diversifies at the level of post-translational processing. J Biol Chem. 1986;261(25):11880-9.
36. Rouille Y, Westermark G, Martin SK, Steiner DF. Proglucagon is processed to glucagon by prohormone convertase PC2 in alpha TC1-6 cells. Proc Natl Acad Sci U S A. 1994;91(8):3242-6.
37. Quesada I, Tuduri E, Ripoll C, Nadal A. Physiology of the pancreatic alpha-cell and glucagon secretion: role in glucose homeostasis and diabetes. J Endocrinol. 2008;199(1):5-19.
38. Ostenson CG. Regulation of glucagon release: effects of insulin on the pancreatic A2-cell of the guinea pig. Diabetologia. 1979;17(5):325-30.
39. Rorsman P, Berggren PO, Bokvist K, Ericson H, Mohler H, Ostenson CG, et al. Glucose-inhibition of glucagon secretion involves activation of GABAA-receptor chloride channels. Nature. 1989;341(6239):233-6.
40. Zhou H, Zhang T, Harmon JS, Bryan J, Robertson RP. Zinc, not insulin, regulates the rat alpha-cell response to hypoglycemia in vivo. Diabetes. 2007;56(4):1107-12.
41. Kailey B, van de Bunt M, Cheley S, Johnson PR, MacDonald PE, Gloyn AL, et al. SSTR2 is the functionally dominant somatostatin receptor in human pancreatic beta- and alpha-cells. Am J Physiol Endocrinol Metab. 2012;303(9):E1107-16.
42. Francis BH, Baskin DG, Saunders DR, Ensinck JW. Distribution of somatostatin-14 and somatostatin-28 gastrointestinal-pancreatic cells of rats and humans. Gastroenterology. 1990;99(5):1283-91.
43. Asakawa A, Inui A, Yuzuriha H, Ueno N, Katsuura G, Fujimiya M, et al. Characterization of the effects of pancreatic polypeptide in the regulation of energy balance. Gastroenterology. 2003;124(5):1325-36.
44. Kim W, Fiori JL, Shin YK, Okun E, Kim JS, Rapp PR, et al. Pancreatic polypeptide inhibits somatostatin secretion. FEBS Lett. 2014;588(17):3233-9.
45. Aragon F, Karaca M, Novials A, Maldonado R, Maechler P, Rubi B. Pancreatic polypeptide regulates glucagon release through PPYR1 receptors expressed in mouse and human alpha-cells. Biochim Biophys Acta. 2015;1850(2):343-51.

46. Dezaki K, Kakei M, Yada T. Ghrelin uses Galphai2 and activates voltage-dependent K+ channels to attenuate glucose-induced Ca2+ signaling and insulin release in islet beta-cells: novel signal transduction of ghrelin. Diabetes. 2007;56(9):2319-27.
47. Chuang JC, Sakata I, Kohno D, Perello M, Osborne-Lawrence S, Repa JJ, et al. Ghrelin directly stimulates glucagon secretion from pancreatic alpha-cells. Mol Endocrinol. 2011;25(9):1600-11.
48. DiGruccio MR, Mawla AM, Donaldson CJ, Noguchi GM, Vaughan J, Cowing-Zitron C, et al. Comprehensive alpha, beta and delta cell transcriptomes reveal that ghrelin selectively activates delta cells and promotes somatostatin release from pancreatic islets. Mol Metab. 2016;5(7):449-58.
49. Kondrashova A, Reunanen A, Romanov A, Karvonen A, Viskari H, Vesikari T, et al. A six-fold gradient in the incidence of type 1 diabetes at the eastern border of Finland. Ann Med. 2005;37(1):67-72.
50. Podar T, Solntsev A, Karvonen M, Padaiga Z, Brigis G, Urbonaite B, et al. Increasing incidence of childhood-onset type I diabetes in 3 Baltic countries and Finland 1983-1998. Diabetologia. 2001;44 Suppl 3:B17-20.
51. Soderstrom U, Aman J, Hjern A. Being born in Sweden increases the risk for type 1 diabetes - a study of migration of children to Sweden as a natural experiment. Acta Paediatr. 2012;101(1):73-7.
52. Noble JA, Valdes AM. Genetics of the HLA region in the prediction of type 1 diabetes. Curr Diab Rep. 2011;11(6):533-42.
53. Noble JA. Immunogenetics of type 1 diabetes: A comprehensive review. J Autoimmun. 2015;64:101-12.
54. Ziegler AG, Nepom GT. Prediction and pathogenesis in type 1 diabetes. Immunity. 2010;32(4):468-78.
55. Redondo MJ, Fain PR, Eisenbarth GS. Genetics of type 1A diabetes. Recent Prog Horm Res. 2001;56:69-89.
56. Nakanishi K, Kobayashi T, Murase T, Nakatsuji T, Inoko H, Tsuji K, et al. Association of HLA-A24 with complete beta-cell destruction in IDDM. Diabetes. 1993;42(7):1086-93.
57. Robles DT, Eisenbarth GS, Wang T, Erlich HA, Bugawan TL, Babu SR, et al. Millennium award recipient contribution. Identification of children with early onset and high incidence of anti-islet autoantibodies. Clin Immunol. 2002;102(3):217-24.
58. Noble JA, Valdes AM, Varney MD, Carlson JA, Moonsamy P, Fear AL, et al. HLA class I and genetic susceptibility to type 1 diabetes: results from the Type 1 Diabetes Genetics Consortium. Diabetes. 2010;59(11):2972-9.
59. Bell GI, Horita S, Karam JH. A polymorphic locus near the human insulin gene is associated with insulin-dependent diabetes mellitus. Diabetes. 1984;33(2):176-83.
60. Lucassen AM, Julier C, Beressi JP, Boitard C, Froguel P, Lathrop M, et al. Susceptibility to insulin dependent diabetes mellitus maps to a 4.1 kb segment of DNA spanning the insulin gene and associated VNTR. Nat Genet. 1993;4(3):305-10.
61. Stead JD, Hurles ME, Jeffreys AJ. Global haplotype diversity in the human insulin gene region. Genome Res. 2003;13(9):2101-11.
62. Pugliese A, Zeller M, Fernandez A, Jr., Zalcberg LJ, Bartlett RJ, Ricordi C, et al. The insulin gene is transcribed in the human thymus and transcription levels correlated with allelic variation at the INS VNTR-IDDM2 susceptibility locus for type 1 diabetes. Nat Genet. 1997;15(3):293-7.
63. Bottini N, Musumeci L, Alonso A, Rahmouni S, Nika K, Rostamkhani M, et al. A functional variant of lymphoid tyrosine phosphatase is associated with type I diabetes. Nat Genet. 2004;36(4):337-8.
64. Vang T, Liu WH, Delacroix L, Wu S, Vasile S, Dahl R, et al. LYP inhibits T-cell activation when dissociated from CSK. Nat Chem Biol. 2012;8(5):437-46.
65. Nistico L, Buzzetti R, Pritchard LE, Van der Auwera B, Giovannini C, Bosi E, et al. The CTLA-4 gene region of chromosome 2q33 is linked to, and associated with, type 1 diabetes. Belgian Diabetes Registry. Hum Mol Genet. 1996;5(7):1075-80.

66. Liao W, Lin JX, Leonard WJ. Interleukin-2 at the crossroads of effector responses, tolerance, and immunotherapy. Immunity. 2013;38(1):13-25.
67. Yu A, Snowhite I, Vendrame F, Rosenzwajg M, Klatzmann D, Pugliese A, et al. Selective IL-2 responsiveness of regulatory T cells through multiple intrinsic mechanisms supports the use of low-dose IL-2 therapy in type 1 diabetes. Diabetes. 2015;64(6):2172-83.
68. Meylan E, Tschopp J, Karin M. Intracellular pattern recognition receptors in the host response. Nature. 2006;442(7098):39-44.
69. Shigemoto T, Kageyama M, Hirai R, Zheng J, Yoneyama M, Fujita T. Identification of loss of function mutations in human genes encoding RIG-I and MDA5: implications for resistance to type I diabetes. J Biol Chem. 2009;284(20):13348-54.
70. Nejentsev S, Walker N, Riches D, Egholm M, Todd JA. Rare variants of IFIH1, a gene implicated in antiviral responses, protect against type 1 diabetes. Science. 2009;324(5925):387-9.
71. Assmann TS, Brondani Lde A, Bauer AC, Canani LH, Crispim D. Polymorphisms in the TLR3 gene are associated with risk for type 1 diabetes mellitus. Eur J Endocrinol. 2014;170(4):519-27.
72. Cooper JD, Walker NM, Smyth DJ, Downes K, Healy BC, Todd JA, et al. Follow-up of 1715 SNPs from the Wellcome Trust Case Control Consortium genome-wide association study in type I diabetes families. Genes Immun. 2009;10 Suppl 1:S85-94.
73. Esposito S, Molteni CG, Giliani S, Mazza C, Scala A, Tagliaferri L, et al. Toll-like receptor 3 gene polymorphisms and severity of pandemic A/H1N1/2009 influenza in otherwise healthy children. Virol J. 2012;9:270.
74. Sironi M, Biasin M, Cagliani R, Forni D, De Luca M, Saulle I, et al. A common polymorphism in TLR3 confers natural resistance to HIV-1 infection. J Immunol. 2012;188(2):818-23.
75. Schott E, Witt H, Neumann K, Taube S, Oh DY, Schreier E, et al. A Toll-like receptor 7 single nucleotide polymorphism protects from advanced inflammation and fibrosis in male patients with chronic HCV-infection. J Hepatol. 2007;47(2):203-11.
76. Wei XS, Wei CD, Tong YQ, Zhu CL, Zhang PA. Single nucleotide polymorphisms of toll-like receptor 7 and toll-like receptor 9 in hepatitis C virus infection patients from central China. Yonsei Med J. 2014;55(2):428-34.
77. Holick MF. Vitamin D: the underappreciated D-lightful hormone that is important for skeletal and cellular health. Current Opinion in Endocrinology, Diabetes and Obesity. 2002;9(1):87-98.
78. Mathieu C, Waer M, Laureys J, Rutgeerts O, Bouillon R. Prevention of autoimmune diabetes in NOD mice by 1,25 dihydroxyvitamin D3. Diabetologia. 1994;37(6):552-8.
79. Zipitis CS, Akobeng AK. Vitamin D supplementation in early childhood and risk of type 1 diabetes: a systematic review and meta-analysis. Arch Dis Child. 2008;93(6):512-7.
80. Bizzarri C, Pitocco D, Napoli N, Di Stasio E, Maggi D, Manfrini S, et al. No protective effect of calcitriol on beta-cell function in recent-onset type 1 diabetes: the IMDIAB XIII trial. Diabetes Care. 2010;33(9):1962-3.
81. Walter M, Kaupper T, Adler K, Foersch J, Bonifacio E, Ziegler AG. No effect of the 1alpha,25-dihydroxyvitamin D3 on beta-cell residual function and insulin requirement in adults with new-onset type 1 diabetes. Diabetes Care. 2010;33(7):1443-8.
82. Sorensen IM, Joner G, Jenum PA, Eskild A, Torjesen PA, Stene LC. Maternal serum levels of 25-hydroxy-vitamin D during pregnancy and risk of type 1 diabetes in the offspring. Diabetes. 2012;61(1):175-8.
83. Miettinen ME, Reinert L, Kinnunen L, Harjutsalo V, Koskela P, Surcel HM, et al. Serum 25-hydroxyvitamin D level during early pregnancy and type 1 diabetes risk in the offspring. Diabetologia. 2012;55(5):1291-4.
84. Couper JJ, Steele C, Beresford S, Powell T, McCaul K, Pollard A, et al. Lack of association between duration of breast-feeding or introduction of cow's milk and development of islet autoimmunity. Diabetes. 1999;48(11):2145-9.
85. Ziegler AG, Schmid S, Huber D, Hummel M, Bonifacio E. Early infant feeding and risk of developing type 1 diabetes-associated autoantibodies. JAMA. 2003;290(13):1721-8.

86. Knip M, Akerblom HK, Becker D, Dosch HM, Dupre J, Fraser W, et al. Hydrolyzed infant formula and early beta-cell autoimmunity: a randomized clinical trial. JAMA. 2014;311(22):2279-87.
87. Lempainen J, Vaarala O, Makela M, Veijola R, Simell O, Knip M, et al. Interplay between PTPN22 C1858T polymorphism and cow's milk formula exposure in type 1 diabetes. J Autoimmun. 2009;33(2):155-64.
88. Walker-Smith JA, Vines R, Grigor W. Coeliac disease and diabetes. Lancet. 1969;2(7621):650.
89. Norris JM, Barriga K, Klingensmith G, Hoffman M, Eisenbarth GS, Erlich HA, et al. Timing of initial cereal exposure in infancy and risk of islet autoimmunity. JAMA. 2003;290(13):1713-20.
90. Wahlberg J, Vaarala O, Ludvigsson J, group AB-s. Dietary risk factors for the emergence of type 1 diabetes-related autoantibodies in 21/2 year-old Swedish children. Br J Nutr. 2006;95(3):603-8.
91. Virtanen SM, Takkinen HM, Nevalainen J, Kronberg-Kippila C, Salmenhaara M, Uusitalo L, et al. Early introduction of root vegetables in infancy associated with advanced ss-cell autoimmunity in young children with human leukocyte antigen-conferred susceptibility to Type 1 diabetes. Diabet Med. 2011;28(8):965-71.
92. Hummel M, Bonifacio E, Naserke HE, Ziegler AG. Elimination of dietary gluten does not reduce titers of type 1 diabetes-associated autoantibodies in high-risk subjects. Diabetes Care. 2002;25(7):1111-6.
93. Hummel S, Pfluger M, Hummel M, Bonifacio E, Ziegler AG. Primary dietary intervention study to reduce the risk of islet autoimmunity in children at increased risk for type 1 diabetes: the BABYDIET study. Diabetes Care. 2011;34(6):1301-5.
94. Brekke HK, Ludvigsson J. Daily vegetable intake during pregnancy negatively associated to islet autoimmunity in the offspring--the ABIS study. Pediatr Diabetes. 2010;11(4):244-50.
95. Dahlquist GG, Blom LG, Persson LA, Sandstrom AI, Wall SG. Dietary factors and the risk of developing insulin dependent diabetes in childhood. BMJ. 1990;300(6735):1302-6.
96. Wilson GL, Mossman BT, Craighead JE. Use of pancreatic beta cells in culture to identify diabetogenic N-nitroso compounds. In Vitro. 1983;19(1):25-30.
97. Winkler C, Mollenhauer U, Hummel S, Bonifacio E, Ziegler AG. Exposure to environmental factors in drinking water: risk of islet autoimmunity and type 1 diabetes--the BABYDIAB study. Horm Metab Res. 2008;40(8):566-71.
98. Strachan DP. Hay fever, hygiene, and household size. BMJ. 1989;299(6710):1259-60.
99. Cardwell CR, Carson DJ, Yarnell J, Shields MD, Patterson CC. Atopy, home environment and the risk of childhood-onset type 1 diabetes: a population-based case-control study. Pediatr Diabetes. 2008;9(3 Pt 1):191-6.
100. Ball TM, Castro-Rodriguez JA, Griffith KA, Holberg CJ, Martinez FD, Wright AL. Siblings, day-care attendance, and the risk of asthma and wheezing during childhood. N Engl J Med. 2000;343(8):538-43.
101. Tracy S, Drescher KM, Chapman NM, Kim KS, Carson SD, Pirruccello S, et al. Toward testing the hypothesis that group B coxsackieviruses (CVB) trigger insulin-dependent diabetes: inoculating nonobese diabetic mice with CVB markedly lowers diabetes incidence. J Virol. 2002;76(23):12097-111.
102. Tracy S, Drescher KM, Jackson JD, Kim K, Kono K. Enteroviruses, type 1 diabetes and hygiene: a complex relationship. Rev Med Virol. 2010;20(2):106-16.
103. Kondrashova A, Seiskari T, Ilonen J, Knip M, Hyoty H. The 'Hygiene hypothesis' and the sharp gradient in the incidence of autoimmune and allergic diseases between Russian Karelia and Finland. APMIS. 2013;121(6):478-93.
104. Chatenoud L, You S, Okada H, Kuhn C, Michaud B, Bach JF. 99th Dahlem conference on infection, inflammation and chronic inflammatory disorders: immune therapies of type 1 diabetes: new opportunities based on the hygiene hypothesis. Clin Exp Immunol. 2010;160(1):106-12.
105. Bach JF, Chatenoud L. The hygiene hypothesis: an explanation for the increased frequency of insulin-dependent diabetes. Cold Spring Harb Perspect Med. 2012;2(2):a007799.

106. Simonsen JR, Harjutsalo V, Jarvinen A, Kirveskari J, Forsblom C, Groop PH, et al. Bacterial infections in patients with type 1 diabetes: a 14-year follow-up study. BMJ Open Diabetes Res Care. 2015;3(1):e000067.
107. Casqueiro J, Casqueiro J, Alves C. Infections in patients with diabetes mellitus: A review of pathogenesis. Indian J Endocrinol Metab. 2012;16 Suppl 1:S27-36.
108. Cole DK, Bulek AM, Dolton G, Schauenberg AJ, Szomolay B, Rittase W, et al. Hotspot autoimmune T cell receptor binding underlies pathogen and insulin peptide cross-reactivity. J Clin Invest. 2016;126(6):2191-204.
109. Gill SR, Pop M, Deboy RT, Eckburg PB, Turnbaugh PJ, Samuel BS, et al. Metagenomic analysis of the human distal gut microbiome. Science. 2006;312(5778):1355-9.
110. Dominguez-Bello MG, Costello EK, Contreras M, Magris M, Hidalgo G, Fierer N, et al. Delivery mode shapes the acquisition and structure of the initial microbiota across multiple body habitats in newborns. Proc Natl Acad Sci U S A. 2010;107(26):11971-5.
111. Guaraldi F, Salvatori G. Effect of breast and formula feeding on gut microbiota shaping in newborns. Front Cell Infect Microbiol. 2012;2:94.
112. Brugman S, Klatter FA, Visser JT, Wildeboer-Veloo AC, Harmsen HJ, Rozing J, et al. Antibiotic treatment partially protects against type 1 diabetes in the Bio-Breeding diabetes-prone rat. Is the gut flora involved in the development of type 1 diabetes? Diabetologia. 2006;49(9):2105-8.
113. Wen L, Ley RE, Volchkov PY, Stranges PB, Avanesyan L, Stonebraker AC, et al. Innate immunity and intestinal microbiota in the development of Type 1 diabetes. Nature. 2008;455(7216):1109-13.
114. Candon S, Perez-Arroyo A, Marquet C, Valette F, Foray AP, Pelletier B, et al. Antibiotics in early life alter the gut microbiome and increase disease incidence in a spontaneous mouse model of autoimmune insulin-dependent diabetes. PLoS One. 2015;10(5):e0125448.
115. Brown K, Godovannyi A, Ma C, Zhang Y, Ahmadi-Vand Z, Dai C, et al. Prolonged antibiotic treatment induces a diabetogenic intestinal microbiome that accelerates diabetes in NOD mice. ISME J. 2016;10(2):321-32.
116. Davis-Richardson AG, Ardissone AN, Dias R, Simell V, Leonard MT, Kemppainen KM, et al. Bacteroides dorei dominates gut microbiome prior to autoimmunity in Finnish children at high risk for type 1 diabetes. Front Microbiol. 2014;5:678.
117. de Goffau MC, Luopajarvi K, Knip M, Ilonen J, Ruohtula T, Harkonen T, et al. Fecal microbiota composition differs between children with beta-cell autoimmunity and those without. Diabetes. 2013;62(4):1238-44.
118. Kostic AD, Gevers D, Siljander H, Vatanen T, Hyotylainen T, Hamalainen AM, et al. The dynamics of the human infant gut microbiome in development and in progression toward type 1 diabetes. Cell Host Microbe. 2015;17(2):260-73.
119. Adams S. The seasonal variation in the onset of acute diabetes: The age and sex factors in 1,000 diabetic patients. Archives of Internal Medicine. 1926;37(6):861-4.
120. HARRIS HF. A Case of Diabetes Mellitus Quickly Following Mumps. The Boston Medical and Surgical Journal. 1899;140(20):465-9.
121. Parkkonen P, Hyoty H, Koskinen L, Leinikki P. Mumps virus infects beta cells in human fetal islet cell cultures upregulating the expression of HLA class I molecules. Diabetologia. 1992;35(1):63-9.
122. Hyoty H, Parkkonen P, Rode M, Bakke O, Leinikki P. Common peptide epitope in mumps virus nucleocapsid protein and MHC class II-associated invariant chain. Scand J Immunol. 1993;37(5):550-8.
123. Helmke K, Otten A, Willems W. Islet cell antibodies in children with mumps infection. Lancet. 1980;2(8187):211-2.
124. Hyoty H, Hiltunen M, Reunanen A, Leinikki P, Vesikari T, Lounamaa R, et al. Decline of mumps antibodies in type 1 (insulin-dependent) diabetic children and a plateau in the rising incidence of type 1 diabetes after introduction of the mumps-measles-rubella vaccine in Finland. Childhood Diabetes in Finland Study Group. Diabetologia. 1993;36(12):1303-8.
125. Menser MA, Forrest JM, Bransby RD. Rubella infection and diabetes mellitus. Lancet. 1978;1(8055):57-60.

126. Ramondetti F, Sacco S, Comelli M, Bruno G, Falorni A, Iannilli A, et al. Type 1 diabetes and measles, mumps and rubella childhood infections within the Italian Insulin-dependent Diabetes Registry. Diabet Med. 2012;29(6):761-6.
127. Karounos DG, Wolinsky JS, Thomas JW. Monoclonal antibody to rubella virus capsid protein recognizes a beta-cell antigen. J Immunol. 1993;150(7):3080-5.
128. Ou D, Mitchell LA, Metzger DL, Gillam S, Tingle AJ. Cross-reactive rubella virus and glutamic acid decarboxylase (65 and 67) protein determinants recognised by T cells of patients with type I diabetes mellitus. Diabetologia. 2000;43(6):750-62.
129. Numazaki K, Goldman H, Wong I, Wainberg MA. Infection of cultured human fetal pancreatic islet cells by rubella virus. Am J Clin Pathol. 1989;91(4):446-51.
130. Numazaki K, Goldman H, Seemayer TA, Wong I, Wainberg MA. Infection by human cytomegalovirus and rubella virus of cultured human fetal islets of Langerhans. In Vivo. 1990;4(1):49-54.
131. Viskari H, Paronen J, Keskinen P, Simell S, Zawilinska B, Zgorniak-Nowosielska I, et al. Humoral beta-cell autoimmunity is rare in patients with the congenital rubella syndrome. Clin Exp Immunol. 2003;133(3):378-83.
132. Gale EA. Congenital rubella: citation virus or viral cause of type 1 diabetes? Diabetologia. 2008;51(9):1559-66.
133. Honeyman MC, Stone NL, Falk BA, Nepom G, Harrison LC. Evidence for molecular mimicry between human T cell epitopes in rotavirus and pancreatic islet autoantigens. J Immunol. 2010;184(4):2204-10.
134. Blomqvist M, Juhela S, Erkkila S, Korhonen S, Simell T, Kupila A, et al. Rotavirus infections and development of diabetes-associated autoantibodies during the first 2 years of life. Clin Exp Immunol. 2002;128(3):511-5.
135. Ward KP, Galloway WH, Auchterlonie IA. Congenital cytomegalovirus infection and diabetes. Lancet. 1979;1(8114):497.
136. Pak CY, Eun HM, McArthur RG, Yoon JW. Association of cytomegalovirus infection with autoimmune type 1 diabetes. Lancet. 1988;2(8601):1-4.
137. Hiemstra HS, Schloot NC, van Veelen PA, Willemen SJ, Franken KL, van Rood JJ, et al. Cytomegalovirus in autoimmunity: T cell crossreactivity to viral antigen and autoantigen glutamic acid decarboxylase. Proc Natl Acad Sci U S A. 2001;98(7):3988-91.
138. Numazaki K, Goldman H, Wong I, Wainberg MA. Viral infection of human fetal islets of Langerhans. Replication of human cytomegalovirus in cultured human fetal pancreatic islets. Am J Clin Pathol. 1988;90(1):52-7.
139. Hiltunen M, Hyoty H, Karjalainen J, Leinikki P, Knip M, Lounamaa R, et al. Serological evaluation of the role of cytomegalovirus in the pathogenesis of IDDM: a prospective study. The Childhood Diabetes in Finland Study Group. Diabetologia. 1995;38(6):705-10.
140. Aarnisalo J, Veijola R, Vainionpaa R, Simell O, Knip M, Ilonen J. Cytomegalovirus infection in early infancy: risk of induction and progression of autoimmunity associated with type 1 diabetes. Diabetologia. 2008;51(5):769-72.
141. Whitton JL. Immunopathology during coxsackievirus infection. Springer Semin Immunopathol. 2002;24(2):201-13.
142. Chatterjee NK, Nejman C, Gerling I. Purification and characterization of a strain of coxsackievirus B4 of human origin that induces diabetes in mice. J Med Virol. 1988;26(1):57-69.
143. Elshebani A, Olsson A, Westman J, Tuvemo T, Korsgren O, Frisk G. Effects on isolated human pancreatic islet cells after infection with strains of enterovirus isolated at clinical presentation of type 1 diabetes. Virus Res. 2007;124(1-2):193-203.
144. Stanway G, Brown F, Christian P, Hovi T, Hyypiä T, King A, et al. Family picornaviridae. Virus Taxonomy Eighth Report of the International Committee on Taxonomy of Viruses. 2005:757-78.
145. Smyth MS, Martin JH. Picornavirus uncoating. Mol Pathol. 2002;55(4):214-9.

146. van der Linden L, Wolthers KC, van Kuppeveld FJ. Replication and Inhibitors of Enteroviruses and Parechoviruses. Viruses. 2015;7(8):4529-62.
147. Sin J, Mangale V, Thienphrapa W, Gottlieb RA, Feuer R. Recent progress in understanding coxsackievirus replication, dissemination, and pathogenesis. Virology. 2015;484:288-304.
148. Chehadeh W, Kerr-Conte J, Pattou F, Alm G, Lefebvre J, Wattre P, et al. Persistent infection of human pancreatic islets by coxsackievirus B is associated with alpha interferon synthesis in beta cells. J Virol. 2000;74(21):10153-64.
149. Ylipaasto P, Klingel K, Lindberg AM, Otonkoski T, Kandolf R, Hovi T, et al. Enterovirus infection in human pancreatic islet cells, islet tropism in vivo and receptor involvement in cultured islet beta cells. Diabetologia. 2004;47(2):225-39.
150. Hodik M, Anagandula M, Fuxe J, Krogvold L, Dahl-Jorgensen K, Hyoty H, et al. Coxsackie-adenovirus receptor expression is enhanced in pancreas from patients with type 1 diabetes. BMJ Open Diabetes Res Care. 2016;4(1):e000219.
151. Chung SK, Kim JY, Kim IB, Park SI, Paek KH, Nam JH. Internalization and trafficking mechanisms of coxsackievirus B3 in HeLa cells. Virology. 2005;333(1):31-40.
152. Richardson SJ, Willcox A, Hilton DA, Tauriainen S, Hyoty H, Bone AJ, et al. Use of antisera directed against dsRNA to detect viral infections in formalin-fixed paraffin-embedded tissue. J Clin Virol. 2010;49(3):180-5.
153. Tracy S, Smithee S, Alhazmi A, Chapman N. Coxsackievirus can persist in murine pancreas by deletion of 5' terminal genomic sequences. J Med Virol. 2015;87(2):240-7.
154. Jaramillo L, Smithee S, Tracy S, Chapman NM. Domain I of the 5' non-translated genomic region in coxsackievirus B3 RNA is not required for productive replication. Virology. 2016;496:127-30.
155. Tam PE, Messner RP. Molecular mechanisms of coxsackievirus persistence in chronic inflammatory myopathy: viral RNA persists through formation of a double-stranded complex without associated genomic mutations or evolution. J Virol. 1999;73(12):10113-21.
156. Colli ML, Nogueira TC, Allagnat F, Cunha DA, Gurzov EN, Cardozo AK, et al. Exposure to the viral by-product dsRNA or Coxsackievirus B5 triggers pancreatic beta cell apoptosis via a Bim / Mcl-1 imbalance. PLoS Pathog. 2011;7(9):e1002267.
157. Clarke P, Tyler KL. Apoptosis in animal models of virus-induced disease. Nat Rev Microbiol. 2009;7(2):144-55.
158. Manning BD, Cantley LC. AKT/PKB signaling: navigating downstream. Cell. 2007;129(7):1261-74.
159. Diehl N, Schaal H. Make yourself at home: viral hijacking of the PI3K/Akt signaling pathway. Viruses. 2013;5(12):3192-212.
160. Esfandiarei M, Luo H, Yanagawa B, Suarez A, Dabiri D, Zhang J, et al. Protein kinase B/Akt regulates coxsackievirus B3 replication through a mechanism which is not caspase dependent. J Virol. 2004;78(8):4289-98.
161. Esfandiarei M, Boroomand S, Suarez A, Si X, Rahmani M, McManus B. Coxsackievirus B3 activates nuclear factor kappa B transcription factor via a phosphatidylinositol-3 kinase/protein kinase B-dependent pathway to improve host cell viability. Cell Microbiol. 2007;9(10):2358-71.
162. Elghazi L, Bernal-Mizrachi E. Akt and PTEN: beta-cell mass and pancreas plasticity. Trends Endocrinol Metab. 2009;20(5):243-51.
163. Aikin R, Hanley S, Maysinger D, Lipsett M, Castellarin M, Paraskevas S, et al. Autocrine insulin action activates Akt and increases survival of isolated human islets. Diabetologia. 2006;49(12):2900-9.
164. Lu Z, Xu S. ERK1/2 MAP kinases in cell survival and apoptosis. IUBMB Life. 2006;58(11):621-31.
165. Ramos JW. The regulation of extracellular signal-regulated kinase (ERK) in mammalian cells. Int J Biochem Cell Biol. 2008;40(12):2707-19.
166. Luo H, Yanagawa B, Zhang J, Luo Z, Zhang M, Esfandiarei M, et al. Coxsackievirus B3 replication is reduced by inhibition of the extracellular signal-regulated kinase (ERK) signaling pathway. J Virol. 2002;76(7):3365-73.

167. Wang B, Zhang H, Zhu M, Luo Z, Peng Y. MEK1-ERKs signal cascade is required for the replication of Enterovirus 71 (EV71). Antiviral Res. 2012;93(1):110-7.
168. Zhu M, Duan H, Gao M, Zhang H, Peng Y. Both ERK1 and ERK2 are required for enterovirus 71 (EV71) efficient replication. Viruses. 2015;7(3):1344-56.
169. Ma L, Chen Z, Erdjument-Bromage H, Tempst P, Pandolfi PP. Phosphorylation and functional inactivation of TSC2 by Erk implications for tuberous sclerosis and cancer pathogenesis. Cell. 2005;121(2):179-93.
170. Rodriguez-Viciana P, Warne PH, Vanhaesebroeck B, Waterfield MD, Downward J. Activation of phosphoinositide 3-kinase by interaction with Ras and by point mutation. EMBO J. 1996;15(10):2442-51.
171. Zimmermann S, Moelling K. Phosphorylation and regulation of Raf by Akt (protein kinase B). Science. 1999;286(5445):1741-4.
172. Wong WR, Chen YY, Yang SM, Chen YL, Horng JT. Phosphorylation of PI3K/Akt and MAPK/ERK in an early entry step of enterovirus 71. Life Sci. 2005;78(1):82-90.
173. Garcia M, Dogusan Z, Moore F, Sato S, Hartmann G, Eizirik DL, et al. Regulation and function of the cytosolic viral RNA sensor RIG-I in pancreatic beta cells. Biochim Biophys Acta. 2009;1793(11):1768-75.
174. Marroqui L, Lopes M, dos Santos RS, Grieco FA, Roivainen M, Richardson SJ, et al. Differential cell autonomous responses determine the outcome of coxsackievirus infections in murine pancreatic alpha and beta cells. Elife. 2015;4:e06990.
175. Takeuchi O, Akira S. Pattern recognition receptors and inflammation. Cell. 2010;140(6):805-20.
176. Takeda K, Akira S. Toll-like receptors in innate immunity. Int Immunol. 2005;17(1):1-14.
177. Chow J, Franz KM, Kagan JC. PRRs are watching you: Localization of innate sensing and signaling regulators. Virology. 2015;479-480:104-9.
178. Assmann TS, Brondani Lde A, Boucas AP, Canani LH, Crispim D. Toll-like receptor 3 (TLR3) and the development of type 1 diabetes mellitus. Arch Endocrinol Metab. 2015;59(1):4-12.
179. Takeuchi O, Akira S. MDA5/RIG-I and virus recognition. Curr Opin Immunol. 2008;20(1):17-22.
180. Mukherjee A, Morosky SA, Delorme-Axford E, Dybdahl-Sissoko N, Oberste MS, Wang T, et al. The coxsackievirus B 3C protease cleaves MAVS and TRIF to attenuate host type I interferon and apoptotic signaling. PLoS Pathog. 2011;7(3):e1001311.
181. Dabo S, Meurs EF. dsRNA-dependent protein kinase PKR and its role in stress, signaling and HCV infection. Viruses. 2012;4(11):2598-635.
182. Bluestone JA, Herold K, Eisenbarth G. Genetics, pathogenesis and clinical interventions in type 1 diabetes. Nature. 2010;464(7293):1293-300.
183. Christianson SW, Shultz LD, Leiter EH. Adoptive transfer of diabetes into immunodeficient NOD-scid/scid mice. Relative contributions of CD4+ and CD8+ T-cells from diabetic versus prediabetic NOD.NON-Thy-1a donors. Diabetes. 1993;42(1):44-55.
184. Peterson JD, Pike B, McDuffie M, Haskins K. Islet-specific T cell clones transfer diabetes to nonobese diabetic (NOD) F1 mice. J Immunol. 1994;153(6):2800-6.
185. Willcox A, Richardson SJ, Bone AJ, Foulis AK, Morgan NG. Analysis of islet inflammation in human type 1 diabetes. Clin Exp Immunol. 2009;155(2):173-81.
186. Foulis AK, Farquharson MA, Hardman R. Aberrant expression of class II major histocompatibility complex molecules by B cells and hyperexpression of class I major histocompatibility complex molecules by insulin containing islets in type 1 (insulin-dependent) diabetes mellitus. Diabetologia. 1987;30(5):333-43.
187. Rodriguez-Calvo T, Ekwall O, Amirian N, Zapardiel-Gonzalo J, von Herrath MG. Increased immune cell infiltration of the exocrine pancreas: a possible contribution to the pathogenesis of type 1 diabetes. Diabetes. 2014;63(11):3880-90.
188. Valle A, Giamporcaro GM, Scavini M, Stabilini A, Grogan P, Bianconi E, et al. Reduction of circulating neutrophils precedes and accompanies type 1 diabetes. Diabetes. 2013;62(6):2072-7.

189. Tsai S, Shameli A, Santamaria P. CD8+ T cells in type 1 diabetes. Adv Immunol. 2008;100:79-124.
190. Thomas HE, Trapani JA, Kay TW. The role of perforin and granzymes in diabetes. Cell Death Differ. 2010;17(4):577-85.
191. Szablewski L. Role of immune system in type 1 diabetes mellitus pathogenesis. Int Immunopharmacol. 2014;22(1):182-91.
192. Bingley PJ. Clinical applications of diabetes antibody testing. J Clin Endocrinol Metab. 2010;95(1):25-33.
193. Atkinson MA, Eisenbarth GS, Michels AW. Type 1 diabetes. Lancet. 2014;383(9911):69-82.
194. Richardson SJ, Willcox A, Bone AJ, Foulis AK, Morgan NG. The prevalence of enteroviral capsid protein vp1 immunostaining in pancreatic islets in human type 1 diabetes. Diabetologia. 2009;52(6):1143-51.
195. Dotta F, Censini S, van Halteren AG, Marselli L, Masini M, Dionisi S, et al. Coxsackie B4 virus infection of beta cells and natural killer cell insulitis in recent-onset type 1 diabetic patients. Proc Natl Acad Sci U S A. 2007;104(12):5115-20.
196. Coppieters KT, Wiberg A, von Herrath MG. Viral infections and molecular mimicry in type 1 diabetes. APMIS. 2012;120(12):941-9.
197. Atkinson MA, Bowman MA, Campbell L, Darrow BL, Kaufman DL, Maclaren NK. Cellular immunity to a determinant common to glutamate decarboxylase and coxsackie virus in insulin-dependent diabetes. J Clin Invest. 1994;94(5):2125-9.
198. Schloot NC, Willemen SJ, Duinkerken G, Drijfhout JW, de Vries RR, Roep BO. Molecular mimicry in type 1 diabetes mellitus revisited: T-cell clones to GAD65 peptides with sequence homology to Coxsackie or proinsulin peptides do not crossreact with homologous counterpart. Hum Immunol. 2001;62(4):299-309.
199. Horwitz MS, Bradley LM, Harbertson J, Krahl T, Lee J, Sarvetnick N. Diabetes induced by Coxsackie virus: initiation by bystander damage and not molecular mimicry. Nat Med. 1998;4(7):781-5.
200. Ashton MP, Eugster A, Walther D, Daehling N, Riethausen S, Kuehn D, et al. Incomplete immune response to coxsackie B viruses associates with early autoimmunity against insulin. Sci Rep. 2016;6:32899.
201. Christen U, Edelmann KH, McGavern DB, Wolfe T, Coon B, Teague MK, et al. A viral epitope that mimics a self antigen can accelerate but not initiate autoimmune diabetes. J Clin Invest. 2004;114(9):1290-8.
202. Filippi CM, von Herrath MG. Viral trigger for type 1 diabetes: pros and cons. Diabetes. 2008;57(11):2863-71.
203. von Herrath MG, Fujinami RS, Whitton JL. Microorganisms and autoimmunity: making the barren field fertile? Nat Rev Microbiol. 2003;1(2):151-7.
204. Oikarinen M, Tauriainen S, Oikarinen S, Honkanen T, Collin P, Rantala I, et al. Type 1 diabetes is associated with enterovirus infection in gut mucosa. Diabetes. 2012;61(3):687-91.
205. Richardson SJ, Rodriguez-Calvo T, Gerling IC, Mathews CE, Kaddis JS, Russell MA, et al. Islet cell hyperexpression of HLA class I antigens: a defining feature in type 1 diabetes. Diabetologia. 2016;59(11):2448-58.
206. Richardson SJ, Leete P, Bone AJ, Foulis AK, Morgan NG. Expression of the enteroviral capsid protein VP1 in the islet cells of patients with type 1 diabetes is associated with induction of protein kinase R and downregulation of Mcl-1. Diabetologia. 2013;56(1):185-93.
207. Olsson A, Johansson U, Korsgren O, Frisk G. Inflammatory gene expression in Coxsackievirus B-4-infected human islets of Langerhans. Biochem Biophys Res Commun. 2005;330(2):571-6.
208. Berg AK, Korsgren O, Frisk G. Induction of the chemokine interferon-gamma-inducible protein-10 in human pancreatic islets during enterovirus infection. Diabetologia. 2006;49(11):2697-703.
209. Frigerio S, Junt T, Lu B, Gerard C, Zumsteg U, Hollander GA, et al. Beta cells are responsible for CXCR3-mediated T-cell infiltration in insulitis. Nat Med. 2002;8(12):1414-20.

210. Antonelli A, Ferrari SM, Corrado A, Ferrannini E, Fallahi P. CXCR3, CXCL10 and type 1 diabetes. Cytokine Growth Factor Rev. 2014;25(1):57-65.
211. Nicoletti F, Conget I, Di Mauro M, Di Marco R, Mazzarino MC, Bendtzen K, et al. Serum concentrations of the interferon-gamma-inducible chemokine IP-10/CXCL10 are augmented in both newly diagnosed Type I diabetes mellitus patients and subjects at risk of developing the disease. Diabetologia. 2002;45(8):1107-10.
212. Roep BO, Kleijwegt FS, van Halteren AG, Bonato V, Boggi U, Vendrame F, et al. Islet inflammation and CXCL10 in recent-onset type 1 diabetes. Clin Exp Immunol. 2010;159(3):338-43.
213. Tanaka S, Nishida Y, Aida K, Maruyama T, Shimada A, Suzuki M, et al. Enterovirus infection, CXC chemokine ligand 10 (CXCL10), and CXCR3 circuit: a mechanism of accelerated beta-cell failure in fulminant type 1 diabetes. Diabetes. 2009;58(10):2285-91.
214. Christen U, McGavern DB, Luster AD, von Herrath MG, Oldstone MB. Among CXCR3 chemokines, IFN-gamma-inducible protein of 10 kDa (CXC chemokine ligand (CXCL) 10) but not monokine induced by IFN-gamma (CXCL9) imprints a pattern for the subsequent development of autoimmune disease. J Immunol. 2003;171(12):6838-45.
215. Yousef GE, Brown IN, Mowbray JF. Derivation and biochemical characterization of an enterovirus group-specific monoclonal antibody. Intervirology. 1987;28(3):163-70.
216. Oberste MS, Maher K, Kilpatrick DR, Pallansch MA. Molecular evolution of the human enteroviruses: correlation of serotype with VP1 sequence and application to picornavirus classification. J Virol. 1999;73(3):1941-8.
217. Hansson SF, Korsgren S, Ponten F, Korsgren O. Enteroviruses and the pathogenesis of type 1 diabetes revisited: cross-reactivity of enterovirus capsid protein (VP1) antibodies with human mitochondrial proteins. J Pathol. 2013;229(5):719-28.
218. Maccari G, Genoni A, Sansonno S, Toniolo A. Properties of Two Enterovirus Antibodies that are Utilized in Diabetes Research. Sci Rep. 2016;6:24757.
219. Ettischer-Schmid N, Normann A, Sauter M, Kraft L, Kalbacher H, Kandolf R, et al. A new monoclonal antibody (Cox mAB 31A2) detects VP1 protein of coxsackievirus B3 with high sensitivity and specificity. Virchows Arch. 2016;469(5):553-62.
220. Richardson SJ, Leete P, Dhayal S, Russell MA, Oikarinen M, Laiho JE, et al. Evaluation of the fidelity of immunolabelling obtained with clone 5D8/1, a monoclonal antibody directed against the enteroviral capsid protein, VP1, in human pancreas. Diabetologia. 2014;57(2):392-401.
221. Baker M. Reproducibility crisis: Blame it on the antibodies. Nature. 2015;521(7552):274-6.
222. Baker M. Antibody anarchy: A call to order. Nature. 2015;527(7579):545-51.
223. Klingel K, Hohenadl C, Canu A, Albrecht M, Seemann M, Mall G, et al. Ongoing enterovirus-induced myocarditis is associated with persistent heart muscle infection: quantitative analysis of virus replication, tissue damage, and inflammation. Proc Natl Acad Sci U S A. 1992;89(1):314-8.
224. Skog O, Ingvast S, Korsgren O. Evaluation of RT-PCR and immunohistochemistry as tools for detection of enterovirus in the human pancreas and islets of Langerhans. J Clin Virol. 2014;61(2):242-7.
225. Clements GB, Galbraith DN, Taylor KW. Coxsackie B virus infection and onset of childhood diabetes. Lancet. 1995;346(8969):221-3.
226. Oikarinen S, Martiskainen M, Tauriainen S, Huhtala H, Ilonen J, Veijola R, et al. Enterovirus RNA in blood is linked to the development of type 1 diabetes. Diabetes. 2011;60(1):276-9.
227. Mercalli A, Lampasona V, Klingel K, Albarello L, Lombardoni C, Ekstrom J, et al. No evidence of enteroviruses in the intestine of patients with type 1 diabetes. Diabetologia. 2012;55(9):2479-88.
228. Griffin M, Abu-El-Haija M, Abu-El-Haija M, Rokhlina T, Uc A. Simplified and versatile method for isolation of high-quality RNA from pancreas. Biotechniques. 2012;52(5):332-4.
229. Stanta G, Schneider C. RNA extracted from paraffin-embedded human tissues is amenable to analysis by PCR amplification. Biotechniques. 1991;11(3):304, 6, 8.

230. Masuda N, Ohnishi T, Kawamoto S, Monden M, Okubo K. Analysis of chemical modification of RNA from formalin-fixed samples and optimization of molecular biology applications for such samples. Nucleic Acids Res. 1999;27(22):4436-43.
231. Alidjinou EK, Sane F, Engelmann I, Geenen V, Hober D. Enterovirus persistence as a mechanism in the pathogenesis of type 1 diabetes. Discov Med. 2014;18(100):273-82.
232. Laiho JE, Oikarinen M, Richardson SJ, Frisk G, Nyalwidhe J, Burch TC, et al. Relative sensitivity of immunohistochemistry, multiple reaction monitoring mass spectrometry, in situ hybridization and PCR to detect Coxsackievirus B1 in A549 cells. J Clin Virol. 2016;77:21-8.
233. Gall JG, Pardue ML. Formation and detection of RNA-DNA hybrid molecules in cytological preparations. Proc Natl Acad Sci U S A. 1969;63(2):378-83.
234. Femino AM, Fay FS, Fogarty K, Singer RH. Visualization of single RNA transcripts in situ. Science. 1998;280(5363):585-90.
235. Player AN, Shen LP, Kenny D, Antao VP, Kolberg JA. Single-copy gene detection using branched DNA (bDNA) in situ hybridization. J Histochem Cytochem. 2001;49(5):603-12.
236. Wang F, Flanagan J, Su N, Wang LC, Bui S, Nielson A, et al. RNAscope: a novel in situ RNA analysis platform for formalin-fixed, paraffin-embedded tissues. J Mol Diagn. 2012;14(1):22-9.
237. Laiho JE, Oikarinen S, Oikarinen M, Larsson PG, Stone VM, Hober D, et al. Application of bioinformatics in probe design enables detection of enteroviruses on different taxonomic levels by advanced in situ hybridization technology. J Clin Virol. 2015;69:165-71.
238. Raj A, Tyagi S. Detection of individual endogenous RNA transcripts in situ using multiple singly labeled probes. Methods Enzymol. 2010;472:365-86.
239. Raj A, van den Bogaard P, Rifkin SA, van Oudenaarden A, Tyagi S. Imaging individual mRNA molecules using multiple singly labeled probes. Nat Methods. 2008;5(10):877-9.
240. Chou YY, Vafabakhsh R, Doganay S, Gao Q, Ha T, Palese P. One influenza virus particle packages eight unique viral RNAs as shown by FISH analysis. Proc Natl Acad Sci U S A. 2012;109(23):9101-6.
241. Lakdawala SS, Wu Y, Wawrzusin P, Kabat J, Broadbent AJ, Lamirande EW, et al. Influenza a virus assembly intermediates fuse in the cytoplasm. PLoS Pathog. 2014;10(3):e1003971.
242. Stellaris. Stellaris® RNA FISH Probes [Available from: http://info.biosearchtech.com/stellaris-whitepaper-download.
243. Kwon S. Single-molecule fluorescence in situ hybridization: quantitative imaging of single RNA molecules. BMB Rep. 2013;46(2):65-72.

3 Results

3.1 TLR3 activates coxsackievirus-induced chemokine secretion and apoptosis in pancreatic β-cells

Federico Paroni[1*#], Erna Domsgen[1,3#], **Niels Busse[1#]**, Amin Ardestani[1], K. Maedler[1*]

[1]Centre for Biomolecular Interactions, University of Bremen, Bremen, Germany
[2]current address: The Center for Infectious Medicine, Department of Medicine Huddinge, Karolinska Institutet, Stockholm, Sweden

[#]these authors have equally contributed to the study

This manuscript is in revision at PLOS Pathogens

My contribution:

Discussed results and wrote the paper

Designed, performed and analyzed all experiments of Fig. 5

Designed, performed and analyzed time-course of ERK activation (Fig. S4B)

Designed, performed and analyzed thapsigargin treatment of infected CM9 cells (Fig. S4C)

Revised and approved version. Changes in Figure 3E.

TLR3 activates coxsackievirus-induced chemokine secretion and apoptosis in pancreatic β-cells

Federico Paroni[1*#], Erna Domsgen[1,3#], Niels Busse[1#], Amin Ardestani[1], K. Maedler[1*]

[1]Centre for Biomolecular Interactions, University of Bremen, Bremen, Germany

[2]current address: The Center for Infectious Medicine, Department of Medicine Huddinge, Karolinska Institutet, Stockholm, Sweden

[#]these authors have equally contributed to the study

***Contact**

Kathrin Maedler, Ph.D., kmaedler@uni-bremen.de

Federico Paroni, Ph.D., ilfede74@gmail.com

Islet Biology Laboratory

Centre for Biomolecular Interactions Bremen, University of Bremen

Leobener Straße NW2, Room B2080, 28359 Bremen, Germany

phone: +49(421)218-63290

Running Title

TLR3-TBK1-AKT in CVB induced beta-cell apoptosis

Keywords

Coxsackie B virus, TLR3; TBK1; AKT, ERK, β-cells, islets, diabetes, apoptosis

BIOLOGICAL SCIENCES: Cell Biology

Abstract

Type 1 diabetes (T1D) results from a complex interplay between genetic polymorphisms, immune system and environment. Viruses, mainly enteroviruses such as members of the Coxsackie B virus (CVB) family, have been suspected to trigger diabetes for a long time. Intra-islet viral particles have been detected in pancreata from patients with type 1 and type 2 diabetes and cause β-cell dysfunction *in vitro*. The mechanisms of a correlation between virus infection, diabetes progression and β-cell destruction are still poorly understood.

Here we identified Toll-like receptor (TLR) 3 and Protein kinase R (PKR) as first defensive line during CVB infection in human islets, which directly causes apoptosis in β-cell, while in α-cells, CVB binds to TLR7 resulting in infection without induction of apoptosis.

A time course analysis of CVB-induced downstream signaling showed initial Protein kinase B (PKB/ AKT) and extracellular signal-regulated kinase (ERK) activation. When AKT was down-regulated at 24h post infection, activation of c-Jun N-terminal kinase (pJNK), and viral protein 1 (VP1) appeared together with β-cell destruction. Lack of TLR3 had a pro-survival effect in CVB3 infected human islets leading to a reduced apoptosis and inhibition of cytokine/chemokine production, VP1, JNK as well as TANK-binding kinase 1 (TBK1) phosphorylation. TBK1 linked virus induced TLR3 and AKT activation; overexpression of TLR3/TBK1 enhanced AKT phosphorylation, viral replication and cell death. In contrast, both, AKT and ERK inhibition reduced viral replication and apoptosis.

Our data show that CVB infection has a direct deleterious effect on β-cell survival; it induces apoptosis, which is potentiated through the TLR3 signaling pathway. With our present data we provide novel targets to protect the β-cell during virus infection.

Author summary

Type 1 diabetes is caused by β-cell destruction in the pancreas, and subsequently, insufficient insulin secretion leads to pathologically elevated blood glucose levels. Epidemiological studies support a causative role of viral infections during diabetes onset. Here we report that enteroviruses are directly recognized through the pattern

recognition receptor TLR3 leading to β-cell destruction, impairment in insulin secretion causing overt diabetes. This mechanism is β-cell specific; although viruses enter the neighboring glucagon producing α-cells, those did not undergo cell death.

Once the β-cells are infected, the virus initially promotes survival signaling (through AKT and ERK) to enable its own replication. Later, this is switched to cell destruction (JNK); virus is released and can go and infect the neighboring cells. Such vicious cycle leads to massive virus induced β-cell destruction.

By inhibition of TLR3 signals we reduced viral protein, cytokine and chemokine production, which promoted β-cell survival and would also inhibit immune cell attack. With our present data we provide TLR3 as a target to initially protect β-cells from virus entry and replication.

Introduction

Type 1 diabetes (T1D) is an autoimmune disease resulting in impairment of insulin secretion. The triggering cause of the loss of β-cell mass is unknown and not fully understood in its complexity. There has been a rapid rise in the incidence of childhood T1D worldwide over the past decades, the estimated average annual increase of 3.9% is too high to result only from genetic causes [1, 2]. Viral infection is one of the environmental factors triggering diabetes since disease's incidence follows a periodic pattern within the population [2-5]. Correlations of T1D with enteroviral VP1 antigen were shown in the past [6], also recent studies proved that there is a significant relationship between enterovirus infection and T1D [2, 7]. In biopsy pancreases of newly diagnosed T1D patients (3-9 weeks after T1D onset) viral protein was present in all pancreases together with human leukocyte antigen (HLA) class I expression in all patients, which indirectly confirms islet cell enteroviral infection [8].

Epidemiological studies identified an increased incidence of T1D caused by coxsackievirus B (CVB) [9-11], which possibly causes the destruction of β-cells [12]. CVB4 was also isolated from a pancreas autopsy of a 10-year-old boy with T1D [13]. Viruses that have a specific tropism within the islets could cause the onset of the disease not only by direct cytolysis but also by triggering the host immune response [14, 15]. When this occurs, i.e. the timing of enteroviral infection and T1D development, is still an open question. The mechanism of enterovirus-triggered diabetes was mainly

investigated in mice [16], used as a model for human disease, where mild insulitis is a prerequisite of the diabetic state triggered by viral infection. Virus effects are strictly dependent on the mouse conditions [13, 17-19]. Antigen specificity is a cardinal point for migration of activated T-cells within the islet [20-23]. Only a complete epitope homology can activate the immune response and diabetes onset [24]. T-cell activation through non-T-cell receptors (bystander activation) [21] is limited to viral infection [25, 26]. Such T-cell activation causes „bystander damage", where β-cell apoptosis is triggered by viral response products, e.g. cytokines and chemokines [27, 28].

The C-X-C motif chemokine 10 (CXCL10) induces human β-cell apoptosis [29]. CXCL10 is localized in infected islets [30] in both canonical and fulminant T1D and suggested as clinical marker for diabetes onset [31]. Both receptors, CXCR3 and TLR4 are present in the β-cell, CXCR3 expression is low and scattered within the pancreatic islets. TLR4 was shown to be the receptor for CXCL10 induced apoptosis [29] The innate immune response to virus infection initiates with the sensing of viral pathogen-associated molecular patterns (PAMP) as fingerprint. Such recognition is mediated by the host's pattern recognition receptors (PRR) such as Toll-like receptors (TLR) on the surface of cellular membranes and cytosolic receptors including the RIG-like receptors (RLR), the nucleotide-binding domain-leucine-rich repeat-containing molecules (NLR) and the RNA-activated protein kinase R (PKR) [32]. Many recent studies show that viruses trigger the onset of diabetes through PRRs [33-36]. From a genome wide association study the gene IFIH1 encoding the RIG-I-like receptor melanoma-associated protein 5 (MDA5) has been identified as one of the susceptibility factors for diabetes progression [37, 38]. Stronger association of TLR3 with diabetes has been proven for two polymorphisms, while others where associated with early age at diagnosis and worse glycemic control [39]. Receptors' activation is the link from immune system activation and β-cell failure. Here we show that CVB infections upregulate and activate PRRs in the β-cell, which leads to the production of pro-inflammatory cytokines and chemokines and β-cell apoptosis. CVB3 and 4 had high tropism to TLR3 expressing β-cells, but CVB4 also bound to TLR7 expressed in α-cells showing that virus sensing of TLR3 and 7 is strain and cell type specific. With our present data we provide novel insights into the mechanisms of viral recognition and β-cell destruction as well as targets towards protecting the β-cell during virus infection.

Results

Coxsackieviruses induce massive β-cell death, impaired function and CXCL10 production in human islets

Epidemiological and clinical data point to enterovirus infection, specifically by the coxsackievirus to trigger autoimmune reaction of β-cells and T1D onset [2, 6, 40-43]. Here we investigated the specific viral infection of isolated human islets. Two different coxsackievirus serotypes (CVB3, CVB4) were compared to hepatitis A virus (HAV) member of the *picornaviridae* and cytomegalovirus (CMV) of the *herpesviridae* family. First morphological changes characterized by loss of islets integrity were seen 48 hours post-infection (p.i.) in CVB (MOI of 10) infected human islets. Co-staining of the viral protein 1 (VP1) together with TUNEL and insulin revealed a strong association of islet cell infection and cell death. Both coxsackieviruses induced β-cell apoptosis (Fig.1A,B) together with an impairment in glucose stimulated insulin secretion (Fig.1C). In contrast, 72 h post infection of human islets with HAV and CMV (MOI of 10) showed apoptotic levels comparable to control (Suppl.1A). Successful infection of CVB, HAV and CMV was confirmed by PCR analysis of the viral genome (not shown). CVB's apoptotic effect was further confirmed by western blot analysis of cleaved caspase 3 and cleavage of one of its downstream substrates, poly-(ADP-ribose) polymerase (PARP) (Fig.1D). CVBs but not HAV and CMV infection led to increased production and secretion of the chemokine CXCL10 (Fig.1D, E and Suppl.1B). Expression of CXCL10 in islets is shown by co-staining of CXCL10, insulin and glucagon confirming the β-cell as source of the secreted chemokine (Fig.1F). In confirmation with previous studies [12], CVB's titers significantly increased over the time from $TCID_{50}$ of $10^{2.64}$ and $10^{3.62}$ immediately after infection to $10^{6.44}$ and $10^{5.44}$ at 24 hours p.i., respectively for CVB3 and CVB4 (Suppl.1C), showing that islets are permissive to coxsackievirus. This opened the question whether CVB triggers β-cell apoptosis by direct cytolytic or paracrine effects through secretion of cytokines/chemokines [42].

To test the latter –in vitro bystander hypothesis- we monitored the expression of interferon-stimulated genes together with cytokines. In parallel to CXCL10, a time dependent expression of interleukin 6 (IL-6), tumor necrosis factor alpha (TNFα), interferon beta 1 (IFNβ) mRNA was induced by both coxsackie virus strains (Fig.1G). Interferon gamma (IFNγ) gene expression was undetectable at any time point suggesting an IFNγ independent activation of CXCL10 (also MCP1 and IL-8 were

unchanged by the viruses; data not shown). Polyinosinic-polycytidylic acid poly(I:C), a synthetic analog of double stranded RNA was used to discriminate molecular associated pattern activation vs. viral-cycle (replication, protein synthesis, ER stress, etc.) of such response. Isolated human islets either treated or transfected with poly(I:C) led to similar chemokine production as observed for the virus (Suppl.2A,B). Chemokine and cytokine expression reached a high level of expression at 24h and slowly decreased over time probably due to the loss of the effect of the double strand analogue. Of note, IFNβ expression was higher in transfected vs. poly(I:C) treated islets. A significantly higher CXCL10 protein secretion was further confirmed in islets treated with poly(I:C) compared to untreated control islets (Suppl.2C), while only transfected but not treated poly(I:C) triggered β-cell apoptosis (Suppl.2D,E). This ruled out the *in vitro* cytotoxic paracrine effect of CXCL10 during virus infection.

Differential tropism and virus sensing in α- and β-cells

After the virus enters the cell, double stranded RNA (dsRNA) molecules are formed as intermediates of virus replication and can be recognized by several cellular sensors, leading to the activation of antiviral response linked to the host immune system. In confirmation with previous studies [70], a time-dependent investigation of PRR expression kinetics showed that mRNA of genes encoding retinoic acid-inducible gene 1 (*RIG-I*), melanoma differentiation-associated protein 5 (*MDA5*), Toll like receptor 3 (*TLR3*), protein kinase R (*PKR*) and Toll like receptor 7 (*TLR7*) increased during 48h p.i. with no difference in the pattern of activation between the two viruses (Fig.2A). This increase continued through 72h of culture, except for *TLR7* in CVB3 infected cells.

To elicit whether the host defense was triggered by the viral RNA, a similar time course analysis for PRRs was performed in poly(I:C)-treated/-transfected islets (Suppl.2F,G). With the exception of TLR7, that recognizes single stranded RNA (ssRNA), all other analyzed PRRs utilize dsRNA as pathogen-associated molecular pattern (PAMP) [44] and were therefore analyzed. Both treatment or transfection with poly(I:C) showed a similar pattern of activated PRRs (Suppl.2F,G) as virus infection (Fig.2A), only with differences seen in the kinetics of activation which are dependent on the RNA analogue/ viral load used for infection. Immunoprecipitation (IP) studies from CVB infected human islets were performed in order to identify the viral sensor that triggers the immune response upon coxsackie virus infection (Fig.2B). Classical IP using a K1 antibody against dsRNA showed that PKR but not RIG-I or MDA-5 recognized the viral

genome during the early phase of infection (Fig.2B). In contrast, reverse-IP using antibodies against TLR3 and -7 followed by RNA precipitation, reverse transcription using random primers and real time PCR showed interaction of viral RNA also with both TLR3 and -7 (Fig.2C,D). While TLR3 reverse-IP reactions showed the binding to both CVB3 and -4 RNA (+ and – strand) (Suppl.3A,B), TLR7 bound the positive but not the negative strand in CVB4 samples.

Negative controls such as the IP of non-infected human islets, the IP using unspecific antibodies, the IP performed on just sample incubated with the beads and amplification using housekeeping genes on the IP samples have been performed and showed no binding.

As proof of the method, the similar reverse-IP was performed using antibodies against each tested PRR (Suppl.Fig.3). The reverse-IP with PKR showed amplification from all primer sets, confirming the classical IP (Suppl.3A,B). While the same amount of viral RNA has been used for all IPs (Suppl.3A,B; middle and lower panels), reverse-IP reactions with RIG-I and MDA-5 displayed no obvious virus binding (under detection limit with all primer sets; data not shown). In line with the PRRs upregulation, this suggests that virus recognition starts within the endosome, where the virus is still present as ssRNA or when cytosolic replication intermediates are transported into lysosomes and then fuse with autophagosomes [45].

The binding of PRRs by both CVB3 and -4 RNAs was confirmed by long-term experiments, where human islets were first infected with lower MOI of 0.1 for 6 days and then switched to MOI of 5 for 2 days. By this “superinfection” strategy we could observe binding of all other tested PRRs to the virus RNA (MDA5, PKR, RIG-I) in addition to TLR3 and 7 (Suppl.3C,D).

A hint to the cell selective infection of the two CVB3 and -4 viruses within human islets is the difference in localization of both TLR3 and -7 in human pancreatic sections. TLR3 co-localized with insulin positive cells while TLR7 co-localized with glucagon positive cells (Fig.2E). Analysis of paraffin embedded human islet sections at different times of infection shows VP1 already 24h p.i. in 60.6%±9.6% of CVB3 infected and in 53.5%±4.9% of CVB4 infected β-cells (Fig.2F). VP1 was detected only in about 3% of the α-cells in CVB3 infected islets at 24-72h. In contrast, in CVB4 infected islets, α-cell specific VP1 staining was significantly increased, compared to CVB3 infected islets (12.1±4.0% and 8.1±2.8% at 48 and 72h, respectively; Fig.2F, Suppl.Fig.1D). As both

viruses mainly infect β-cells, we investigated whether cell death was restricted to these cells. Triple staining for insulin, glucagon and TUNEL showed significantly increased apoptosis in β-cells at 48 and 72h post infection by both CVB3 and CVB4 (Fig.2H, Suppl.Fig.1E). α-cell survival was not affected by both viruses, even under the higher infection of the CVB4 virus, suggesting a high vulnerability of the β-cells to virus induced cell death.

The AKT/JNK switch induces β-cell apoptosis as part of TLR3 signaling

TLR3 and PKR have been shown to be the first defense line against viral infection in β-cells; PKR activation by dsRNA enhanced in the presence of TLR. This is demonstrated by TLR3 overexpression in the TLR deficient cell line CM (Fig.3A). Both, transfected as well as treated poly(I:C) showed higher PKR phosphorylation compared to the TLR3 deficient cells, this was reduced by the PKR inhibitor CAS 608512-97-6 (Fig.3A). Also, CXCL10 production was dependent on TLR3 and PKR. Therefore, we further investigated the possible correlation between PKR/TLR3 and the AKT survival pathway, as Phosphatidylinositol-3 kinase (PI3K)-AKT is a well known key regulator of β-cell survival and function [46, 47].

A time course analysis of CVB3 infection of both human islets (Fig.3B) and CM cells (Suppl.4A) showed downstream activated AKT at 1 h post-infection, which lasted for several hours. At 24h p.i., AKT was downregulated together with a simultaneous up-regulation of pJNK, activation of Caspase-3, strong induction of CXCL10 and the appearance of VP1 (Fig.3B, Suppl.4A). Blockade of PI3K by LY294002 delayed, but not abrogated AKT and JNK phosphorylation, activation of caspase 3 and appearance of VP1 (Fig.3C), indicating that the PI3K pathway is required but not essential.

In human islets CVB3 and -4 also activated PKR that in turn activated eIF2α phosphorylation (Fig.3D) that leads to the block of CAP-dependent protein translation [48, 49], this was shown in the same experiment as virus induced PARP and Caspase 3 cleavage and CXCL10 production (see Fig.1D).

Tight changes in cell culture conditions and islet donors could switch the time of AKT appearance. Downregulation of PKR resulted in unchanged AKT and JNK (Fig.3E), while enhanced phosphorylation of AKT (pAKT) and JNK (pJNK) occurred with higher infection rate (Fig.3F). Independently of AKT/JNK, PKR inhibition increased virus progeny (increased capsid protein VP1) and active caspase 3 (Fig.3E,F); AKT and JNK activation were more related to viral replication than directly to PKR.

Poly(I:C) transfection of PKR-deficient CM cells showed again no effect on AKT levels; and in contrast to CVB infected islets, pJNK and cleaved caspase 3 levels were moderately reduced (Fig.3G), suggesting a contribution of PKR to β-cell apoptosis induced by the dsRNA, which is marginal in the complex virus induced scenario.

TBK1 links virus induced TLR3 and AKT activation

That TLR3 is used by the virus on its own advantage for its own amplification is shown by the effect of TLR3 on AKT. The presence of TLR3 correlated with phosphorylation of TANK binding kinase 1 (TBK1) [50], a downstream target of TLR, JNK and viral VP1 at a time when AKT phosphorylation was already diminished (Fig.4A). Overexpression of TLR3 in the TLR deficient cell line CM enhanced AKT activation together with VP1 appearance (Fig.4B). The AKT upregulation in TLR3 depleted cells (Fig.4A) and its downregulation upon virus treatment (Fig.4C) could again be explained by a time-shift in the activation event as depicted in the time course experiment (Fig.3B, C).

We postulated that TBK1 enhances AKT activation upon viral RNA/TLR3 interaction. Overexpression of TLR3/TBK1 in CM cells at earlier time points showed enhanced phosphorylation of AKT, VP1, caspase 3 cleavage and CXCL10 production (Fig.4D). Treatment with poly(I:C) led to a similar pattern but caspase 3 activation, as expected (Fig.4E).

Such outcome, once again, pointed towards a pivotal role of AKT, enhanced by TLR3, on viral replication. Blockade of AKT should then rescue β-cells from apoptosis. Indeed, treatment of isolated human islets (Fig.4F) and CM cells (Fig.4G) with the specific AKT inhibitor (AKTi) tribicine or *AKT* gene silencing by siRNA in human islets (Fig.4H) reduced viral replication and caspase 3.

ERK fosters virus replication and counterbalances AKT during virus replication

In line with previous studies showing an involvement of the MAP kinase ERK during enterovirus replication [51, 52], we observed a CVB3 induced activation pattern of ERK similar to that of AKT during a time course analysis (Suppl.Fig.4B). A CVB3-triggered activation of the two survival-pathways ERK and AKT was confirmed in CM9 cells (Fig.5A). Blockade of PI3K/ AKT action by LY294002 (Fig.5A) or the specific AKT inhibitor Tribicine (Fig.5B) led to enhanced ERK phosphorylation and reduced virus replication (VP1). Both, Poly(I:C) and CVB3 infection led to a higher ERK and JNK activation compared to that of AKT (Fig.5C). Blockade of the ERK signaling pathway by its specific inhibitor PD98059 reduced VP1, JNK and cleaved caspase 3, while AKT

was counter-regulated (Fig.5C). The decreased level of VP1 was more pronounced in cells with impaired MAP kinases than in impaired PI3K-AKT pathway. In line with these results, ERK and JNK phosphorylation levels were increased, compared to AKT, when ER-stress was reduced by 4-phenylbutyrate (4-PBA), which also increased viral replication (VP1, Fig. 5D).

On the opposite, the ER-stress inducer Thapsigargin impaired viral replication, although ERK was upregulated (Suppl.Fig.4C). To further investigate the role of ERK1 and 2 on viral replication, both proteins were overexpressed in CM9 cells and treated with or without Thapsigargin followed by CVB3 infection. As expected, overexpression of ERK1/2 positively affected viral replication (VP1).

In turn, when ER-stress was potentiated by the pre-treatment with Thapsigargin, viral replication is highly reduced. In such scenario, ERK1/2 overexpression in combination with ER-stress led to reduced virus replication (VP1), while cellular stress was also reduced as evidenced by cleaved Caspase 3, pJNK, CHOP, PARP (Fig.5E).

Silencing of TLR3 protects from cytokine secretion and β-cell death

Since TLR3 was the major PRR bound by the viruses in β-cells and viral replication as well as host cell survival dependent on the presence of TLR3, the effect of TLR3 on virus-induced cytokines, chemokines and interferons was investigated. TLR3 downregulation in human islets decreased the mRNA expression levels of *IFNβ, CXCL10, TNFα* and *IL-6* (Fig.6A) as well as CXCL10 secretion (Fig.6B), β-cell apoptosis (Fig.6C,D) and virus titer (Fig.6E), confirming results from human islet lysates (Fig.4A). A similar outcome was observed for CVB4 (Suppl.4D-F).

JNK inhibition rescues the β-cell from virus-induced apoptosis

Results from the time course approach taught us that JNK showed an intriguing opposite regulation of AKT: pJNK lowered during the early hours of infection to drastically increase together with a decrease in AKT and the appearance of VP1 and cleaved caspase 3 (Fig.3B,C), assuming JNK as a major downstream regulator of virus induced apoptosis. Isolated human islets treated with the specific JNK inhibitor SP600125 showed decreased levels of VP1 and caspase 3 activation (Fig.7A). Similarly, overexpression of a dominant negative form of JNK (DN-JNK) in isolated human islets led to a decrease in VP1 and a partial rescue from apoptosis by reducing cleaved caspase 3 (Fig.7B).

Discussion

Epidemiological and clinical studies suggest that an environmental factor, namely the infection with a group of enteroviruses, the coxsackieviruses, triggers the autoimmune reaction to the β-cell and thus the onset of T1D [53, 54]. More recently they were also described to play a role in T2D [2, 6, 55]. Our work highlights important pathways to β-cell apoptosis and induction of innate immunity. Potential harmful consequences of viral infections have been divided into molecular mimicry, antigenic spreading and bystander activation [23, 56-58]. Here we show, that CMV, which was linked to diabetes onset [59], or HAV, another member of the picornavirus family, had no effect on β-cell apoptosis, while low MOI coxsackievirus infection *in vitro* induced massive β-cell death mainly through apoptosis shown by cleavage and activation of caspase 3, which is in confirmation of previous studies [60]. Due to its high association with viral infection as well as with T1D onset [61-65], we used CXCL10 expression as an inflammation marker, which initiates the host immune activation. Our data show that only CVBs triggered significant CXCL10 production in isolated human islets; CXCL10 was the highest expressed and secreted chemokine, as shown before [66]. In contrast, secretion of IFNβ, a major antiviral response protein, which is produced by almost all cells [67] and induces an antiviral state that inhibits the spread of the viral infection, was not detectable neither by ELISA nor by a plaque reduction assay [66]. It was only increased at the mRNA level. IFNβ exerts its effect in a paracrine manner and its absence from supernatants may be due to a rapid uptake by the neighboring cells. Cytokine and chemokine expressions increased in parallel with coxsackie replication. Transfection of the double stranded RNA analogue poly(I:C) led to the up-regulation of the same genes, which confirms a direct effect of the viral genome or viral replication. In this scenario, through similar effects of the virus itself, the free RNA analogue as well as polycation-synthetic RNA complexes mimicking the sole effect of viral RNA, we hypothesized that virus entry is sensed by TLR receptors, which are present on the cell surface and within endosomes. The similar PRR activation pattern of treated and transfected poly-IC suggests that challenging of the PRRs starts already at the outer membrane level, on which treated poly-IC is able to bind. Yet, treatment with poly(I:C) only led to a poor upregulation of IFNβ, confirming previous reports showing the expression of the IFNβ gene related to intracellular sensors such RIG-I (DDX58), MDA5 (IF1H1) or PKR (EIF2AK2) [68, 69]. Human islets actively sensed the presence

of the virus with consequent up-regulation of the interferon-stimulated genes RIG-I, MDA5, TLR3 and PKR while TLR7 showed only a mild activation. A prerequisite for such viral sensing is that the viral genome interacts with the host RNA sensors. Such direct interaction between the viral genome and PRRs in islets during the early phase of infection is shown in our study. Strikingly, in β-cells, viral RNA interacts mainly with PKR and TLR3 while the RIG-like receptors MDA5 (IFIH1) and RIG-I displayed a later binding. In agreement with our hypothesis that virus sensing starts at endosome level, upregulation of RIG-like receptors could serve for a complete host-immune response in later phases of infection as shown in our "superinfection" experiments. Moreover, we show that both CVB4 and CVB3 interact with TLR7. All 5 receptors are involved in the secretion of interferons and linked to T1D progression [6, 70]. Polymorphisms in IFIH1 have been associated with type 1 diabetes onset and progression [71, 72], but not with diabetes autoimmunity [73], indicating that IFIH1 may be a rather enhancing and not initiating factor to virus load and β-cells destruction. All, TLR3 [70], PKR [6], RIG-I and MDA5 [74] are present and active in β-cells. RIG-I and MDA5 loss of function gene polymorphisms, which reduce IFN-I responses to dsRNA, are linked to the resistance to T1D [75]. A recent work shows that neither RIG-I nor MDA5 were essential by themselves for the activation of the antiviral response [76]. In contrast, absence of PKR led to defective IFNβ secretion in fibroblasts and loss of the antiviral response, assuming that IFNβ secretion is regulated by PKR. PKR in turn phosphorylates its downstream target eIF2α resulting in inhibition of translation. PKR is further involved in the formation of the stress granules, another mechanism by which the cells defend themselves from viral infection [77]. In this scenario, lack of PKR should also increase viral progeny. Indeed, PKR loss of function in infected human islets increased virus replication and β-cell death, supposing viral RNA PKR binding being rather protective for β-cell survival. In β-cells, strongest binding of the single stranded virus occurred to endosomal TLR3. In confirmation with previous studies [70, 78], we clearly show TLR3 expression in β-cells by immunostaining of frozen as well as paraffin embedded pancreatic tissue sections, both from autopsy and biopsy. Functional TLR3 was also detected by immunoprecipitation analysis, Western blotting as well as RT-PCR. Enterovirus induced TLR3 upregulation was also observed before in CVB1 infected human islets, while its expression was undetectable in the human pancreas by immunostaining [79].

The TLR3 association with T1D are proven by four receptors' polymorphisms at T1D onset; diabetes frequency correlated with the number of polymorphisms, younger age of T1D diagnosis and poor glycemic control [39]. TLR3-knockout mice are notably protected from CVB4-induced diabetes compared to the control littermates. T-lymphocyte-mediated insulitis was also less severe in TLR3$^{-/-}$-NOD mice compared to control mice [80]. Also, mice with a knockout in TRIF, a critical adaptor protein of both TLR3 and TLR4, exhibit increased blood glucose, impaired glucose tolerance and increased plasma insulin levels with no augmented insulin sensitivity pointing out that TLR signaling affects β-cell function [81].

Our immunoprecipitation studies showed a clear presence of endosomal TLR3 and TLR7 and binding to viral RNA in highly pure human islet preparations. While TLR3 was localized in both α- and β-cells, TLR7 localization was restricted to α-cells.

Similarly, CVB3 and CVB4 showed a cell-specific tropism, CVB3 infected mainly β-cells and rarely α-cells, while CVB4 was in β- as well as in a proportion of α-cells. Apoptosis mainly occurred in β-cells while α-cells appeared to be unaffected by both CVB3 and CVB4, in line with observations from a previous study [82].

Such differential tropisms of the two coxsackieviruses and the different apoptotic rate between α- and β-cells let us hypothesize that β-cells are specifically sensitive to virus induced destruction, and that α-cells could serve as reservoir for viruses during latent infection. Evidence for latent CVB infection comes from studies in murine pancreases; it involves a partial deletion naturally occurring at the 5'-terminal region of the virus genome [83-85]. Virus progeny harboring the terminal deletion originates after the acute phase of infection, thereafter displaying a slow replication rate [85]. Nonetheless slow replication could be an advantage to evade the host immune system reaction.

TLR3 is a dsRNA receptor while CVB is a positive ssRNA that forms an intermediate dsRNA during replication. TLR3 activation can occur at the endosomal level due to secondary structures present at the 5'-terminus of the viral genome [86]. It can be hypothesized that a loss in the area, either fully or partially, that forms secondary structures and interacts with TLR3 would then attenuate or eliminate virus sensing during its internalization and lowering the host immune response. CVB's infection occurs through receptor-mediated endocytosis. It is then plausible that an interaction with TLR3 and TLR7 might take place at this step. To infect cells, viruses need to attach to molecules on the cell surface. CVB's cellular entry is mediated by binding to

the coxsackie and adenovirus receptor (CAR) [87]. Binding may alter the virus structure and trigger uncoating. Several viruses, including CVBs, utilize also clathrin-mediated endocytosis [88] and are more exposed to the acidic milieu of the endosomes. Viruses may then respond to such pH decrease by undergoing changes that result in endosomal membrane penetration and viral genome release.

In support of our binding studies we show that cytokine and chemokine expression during the early phase of CVB infection in human islets is directly related to the presence of TLR3. Especially the major chemokine during CVB infection, CXCL10, was reduced to very low levels in TLR3 depleted human islets. In accordance, subjects with high risk to develop T1D as well as newly diagnosed T1D patients present elevated serum levels of the chemokine CXCL10 [89]. Furthermore, CXCL10 expression has been detected in pancreatic sections from three patients who died from fulminant T1D. All three patients showed VP1 expression in islets that were infiltrated by CXCR3+ T-cells, suggesting an important role for CXCL10 in virus induced insulitis [90]. T cell-mediated β-cells depletion is the foundation of T1D. $CXCR3^{-/-}$ mice failed to attract T-effector cells in response to CXCL10 and CXCL9 production delay diabetes onset [91]. In accordance with previous reports we show that CXCL10 is expressed in islet cells upon enterovirus infection [92].

We postulate that TLR3 activation serves the viral progeny expansion. During evolution viruses have developed various strategies to tune the host cellular pathways to generate a positive environment for their survival and propagation. Delaying or evading apoptosis serves as great advantage to the virus facilitating replication, progeny, spreading to the neighboring cells and providing protection against cellular enzymes. Such host survival programming can be achieved through activation of PI3K/AKT and ERK pathways.

Consistent with studies in HeLa cells [93], CVB infection of both isolated human islets and TLR3 overexpressing CM β-cells triggered AKT phosphorylation at Ser-473 and Thr-308 (data not shown). Previous studies showed that both the PI3K-mTOR and Ras-ERK mutually regulate each other [94]; increased activation of one pathway in absence of another could be simply caused by an abrogated inhibition [95]. Similarly we show here that lack of AKT led to increased ERK activation and vice versa. Counterbalancing of the two pathways to promote cell survival ends with improved viral replication. This support is limited and seems to favor the host instead of the pathogen

in aggravated situations. As an example, ER-stress during virus infection inhibited virus replication, but increased cell death. ERK could reverse such scenario to reduce all, viral replication and apoptotic pathways including JNK. Activation of AKT and ERK is probably required for phosphorylation of JNK, which is dependent on the amount of stress-induction, a cell can cope with. Blockade of JNK led to a decreased virus production, and protection from β-cell apoptosis, but basal apoptosis was also increased during JNK inhibition. Thus, despite its powerful effect in rescuing virus induced apoptosis in β-cells, a possible function of JNK in disease is difficult to predict due to its biphasic and contradictory role in cell survival and apoptosis.

In summary, our present study proves that coxsackie viruses highly infect pancreatic β- and α-cells and induce AKT and ERK activation to foster viral replication. β-cells are specifically sensitive to virus mediated destruction through a TLR3 dependent response, while α-cells serve as a reservoir for the virus. The full intercellular virus signaling is very complex and involves virus mediated signals to ensure its own replication and host cell survival as well as the host response, to undergo apoptosis whenever viruses are infiltrating. We postulate that a lack of TLR3 would lead to an attenuated T-cell infiltration together with β-cell protection, however, such hypothesis will need further proof in *in vivo* models.

Materials and Methods

Cell culture and treatments

Human islets from 15 donors were isolated at Lille University or Prodo Labs and cultured on extracellular matrix (ECM) coated dishes (Novamed, Jerusalem, Israel) as described previously [29]. Islet purity was greater than 95% according to dithizone staining (if this degree of purity was not achieved by routine isolation, islets were handpicked). Informed consent was obtained from all subjects or their relatives and ethical approval given to the respective institutions. The human β-cell line CM was kindly provided by Dr. Paolo Pozzilli, Barts and the London School of Medicine, Queen Mary, University of London, UK [96, 97]. FRhK-4 cell line [98] was kindly provided by Dr. Andreas Dotzauer, Institut für Virologie, University of Bremen, Germany. Human islets were cultured in complete CMRL-1066 (Invitrogen, Darmstadt, Germany) medium at 5.5 mM glucose. CM cells were cultured in complete RPMI-1640 medium at 11.1 mM glucose with 25 mM HEPES, FRhK-4 cells were cultured in Dulbecco's

modified Eagle's medium with 2 mM L-glutamine, 100 U/ml penicillin, 0.1 mg/ml streptomycin 1 mM sodium pyruvate (all PAA). All media included 10% Fetal calf serum (FCS) or 1% FCS for FRhK-4. In some experiments, cells were additionally cultured starting (if not stated otherwise) 1h before infection with 20 μM selective Phosphatidylinositol 3-kinase (PI3K) inhibitor LY294002, 20 μM AKT inhibitor V, Tribicine, selective AKT 1/2/3 inhibitor, 2 μM CAS 608512-97-6 SELECTIVE PKR INHIBITOR, 25 μM SP600125 JNK selective inhibitor, 20 μM MAPK kinase inhibitor PD98059 (all Calbiochem, San Diego, CA, USA), 25 μg poly(I:C), 1 mM ER-stress inhibitor 4-Phenybutyric acid (4-PBA), 2 μM ER-stress inducer Thapsigargin (Sigma Aldrich, Missouri, MO, USA).

Viruses and virus purification

Hepatitis A virus PI (HAV PI), Cytomegalovirus (CMV), CVB3 (Nancy) and CVB4 (JVB) were kindly provided by Dr. Andreas Dotzauer, Institut für Virologie, University of Bremen, Germany. Virus stocks were generated using FRhK-4 cells. Cells were infected in DMEM 1% FCS for 2 h and cultured for additional 3 days or until visible cytopathic effect. Cells were subjected to three freeze/thaw cycles and supernatant cleared by centrifugation 10 min at 720 x g. Purification and concentration of the virus was performed by sucrose gradient. Briefly cleared lysates were further centrifuged at 4500 x g for additional 10 min followed by ultracentrifugation for 12 h at 120000 x g in 40% sucrose gradient buffer (40% sucrose, 10 mM Tris pH 7.5 100 mM NaCl and 1 mM EDTA). The pellet was resuspended in 1X PBS.

Virus Infection of human islets or CM cells and virus titration

CM cells were infected with indicated viruses at MOI (multiplicity of infection) of 5 or 10 for human islets in 35 mm dishes. Virus stocks were diluted in FCS free medium and cells were inoculated with 750 µl for 2h at 37°C and 5% CO_2. Control cells were incubated with 750 µl of FCS free medium alone. After infection, medium was replaced with 10% FCS full medium. The $TCID_{50}$ (tissue culture infectious dose 50%) was determined using serial dilutions of virus stocks or media supernatants containing lysates from infected islets. Briefly FRhK-4 cells were infected as described with serial dilutions or either viral stocks or aliquots from infected cell culture supernatants. Each dilution was added in duplicates to 96-well plates containing 90% confluent FRhK-4 cells. Cytopathic effect was determined under light microscope and the $TCID_{50}$ calculated accordingly to the Spearman-Kärber formula [99].

Plamids and siRNA transfections of human islets and CM cells

To knock down TLR3 in human islets were transiently transfected with SMARTpool siRNA (ON-TARGETplus SMARTpool: sequences: GAACUAAAGAUCAUCGAUU, CAGCAUCUGUCUUUAAUAA, AGACCAAUCUCUCUCCAAUUU, UCACGCAAUUGGAAGAUUA, Dharmacon, GE Healthcare, Lafayette, CO, USA). To knock down AKT CM cells or human islets were transiently transfected with siRNA targeting AKT 1/2/3 (NEB, Ipswich, MA, USA). To knock down PKR CM cells were transfected with pGIPZ-PKR (pGIPZ lentiviral plasmids expressing shRNAmir against PKR and pGIPZmir; Open Biosystems, GE Healthcare, Lafayette, CO, USA). Stable clones were generated under puromycin selection (2 µg/ml). PKR silencing in human islets was achieved with infection of shPKR lentivirus system (Open Biosystems) (MOI=100). Positive clones were maintained in culture under low puromycin pressure (1 µg/ml). Overexpression was achieved with plasmids for TLR3 (pFLAg-CMV-1-hTLR3 from Dr. Carsten Kirschning, Technical University of Munich, Germany [100]), TBK1 (pEF-Bos-FLAG-TBK1), DN-JNK (pcDNA3-Flag Jnk1a1/apf, both Addgene, Cambridge, MA), Erk1 (pFLAG-CMV-hErk1 gifted from Melanie Cobb Addgene plasmid #49328), Erk2 (pCDNA3-HA-Erk2 gifted from John Blenis Addgene plasmid #8974) in both human islets and CM cells, pEGFP-N2 (GFP; fromDr. Frank Dietz, Center for Biomolecular Interaction, University of Bremen) was used as control.

An adapted transfection protocol previously described was used [101]. Briefly human islets or CM cells were incubated for 2 h before transfection in an optimized Ca^{2+}-KRH transfection medium (KCl 4.74 mM, KH_2PO_4 1.19 mM, $MgCl_26H_2O$ 1.19 mM, NaCl 119 mM, $CaCl_2$ 2.54 mM, $NaHCO_3$ 25 mM, HEPES 10 mM) at 37°C 5% CO_2. After 2h incubation the lipoplexes Lipofectamine (Invitrogen)/siRNA (ratio 1:20 pmole) or Lipofectamine/DNA (ration 2.5:1 µg) were added dropwise to the cells and incubated for additional 6 h. Transfection medium was replaced with antibiotic free CMRL-1066 or RPMI-1640 supplemented with 20% FCS. Efficiency of transfection was estimated by fluorescent microscopy of GFP or fluorescein scramble RNA (NEB).

Glucose stimulated insulin secretion

GSIS was performed with 2.8 mM glucose (basal) and 16.7 mM (stimulated) as described previously in detail [101].

Measurement of CXCL10 release

CXCL10 secretion into culture media from controls and virus infected isolated islets was assessed by BD OptEIATM Set human IP-10 (BD Biosciences, San Diego, CA, USA).

Western blot analysis

Human islets or CM cells were rinsed with ice-cold PBS and lysed using RIPA buffer (50 mM Tris HCl pH 8, 150 mM NaCl, 1% NP-40, 0.5% sodium deoxycholate, 0.1% SDS) supplemented with Protease- and phosphatase-inhibitors (Pierce, Rockford, IL, USA). Protein concentration was determined with BCA protein assay (Pierce). Equal amounts of protein were loaded and run in NuPAGE® 4 %-12 % Bis-Tris gel (Invitrogen) and blotted on PVDF membrane (Roti, Karlsruhe, Germany). After blocking the membranes were incubated over night at 4°C with primary antibodies: cleaved caspase 3, cleaved PARP, PKR, pJNK, JNK, peIf2α, pc-Jun, β-tubulin, β-actin, TBK1, pTBK1, TLR3, pAKT, AKT, pErk1/2, ERK, CHOP, GAPDH (all Cell Signaling, Beverly, MA, USA), VP1 (Clone 5-D8/1) (Dako Denmark A/S, Glostrup, Denmark), pPKR (Abcam, Cambridge, UK), CXCL10 (R&D Systems, Abingdon, UK). Membranes were developed using a chemioluminescence assay system (Immobilon Western, Millipore, Schwalbach, Germany) and analyzed with UVP BioSpectrum AC Imaging System (UVP, Upland, Canada).

Immunoprecipitation assay

Coxsackie infected human islets were immunoprecipitated with 2 µg of K1 antibody (SCICONS English and Scientific Consulting Bt, Hősök, Szirák, Hungary) as previously described in detail [101].

RNA-immunoprecipitation (RNA-IP) assay

Islets were infected as described, washed with ice-cold 1X PBS at room temperature and fixed with 1% formaldehyde in PBS at room temperature for 10 min. Cells were quickly rinsed twice in ice-cold PBS and 100 µl of lysis buffer A was added (100mM KCl, 5mM MgCl2, 10mM Hepes pH 7, 0.5% NP40, 1mM DTT, 100 U/ml RnaseOUT (Invitrogen), 400 µM vanadyl ribonucleoside complexes VRC (NEB), Protease/phosphatase inhibitor cocktail). 2 mg of total protein was used for RNA-IP. Protein-A Sepharose beads were pre-swelled in buffer B (50mM Tris-HCl pH7.4, 150mM NaCl, 1mM MgCl2, 0.05% NP-40) supplemented with 5% BSA to a final ration of 1:5 for 2h at 4°C before use. 2 µg antibodies (TLR3, TLR7 from Imgenex, Novus Biological, Cambridge, UK and MDA5, PKR, RIG-I from Cell Signaling, Danvers, MA,

USA) were added to the slurry beads and incubated overnight tumbling end over end at 4°C. The following day the antibody-coated beads were washed with ice-cold buffer B for 5 times. After the final wash the beads were resuspended in ice-cold buffer B supplemented with 200 U RNase inhibitor, 400 μM VRC, 1.2 mM DTT and 20 mM EDTA. Input fraction was saved for control. RNA-protein complexes were incubated with beads-antibody for 5h at 4°C tumbling end over end. After incubation the supernatant was saved as output fraction and the beads washed with ice-cold buffer B supplemented with 1% SDS. The beads were resuspended in buffer B supplemented with 30 μg of Proteinase K and the mixture incubated for 60 min at 55°C. RNA was isolated with PeqGold TriFast (Peqlab, Erlangen, Germany) reagent following manufacturer instructions. RNA was reverse transcribed and analysed by qPCR using CVB primers (see below). Values were expressed as logarithmic arbitrary units based on dilution standard curve.

RT and real time-PCR

500 ng of RNA were treated with DNAse I (Ferments Life Science, Waltham, MA, USA) and reverse transcribed with ReverseAid kit (Fermentas) according to manufacturer instructions. Real time PCRs reactions were prepared accordingly to Applied Biosystems guidelines using either SybrGreen or Taqman assays and performed in a StepOnePlus instrument (Applied Biosystems, Carlsbad, CA, USA). PCR efficiencies were monitored for each sample accordingly to previously described approach [102]. Results are presented as absolute or relative quantification. SybrGreen Primers used: TLR3 fw 5´ AGCCTTCAACGACTGATGCT 3´, rev 5´ TTTCCAGAGCCGTGCTAAGT 3´; MDA5 fw 5´ ACCAAATACAGGAGCCATGC 3´, rev 5´ RGCGATTTCCTTCTTTTGCAG 3´; RIG-I fw 5´ AGAGCACTTGTGGACGCTTT 3´, rev 5´ RTGCAATGTCAATGCCTTCAT 3´; PKR fw 5´ ACGCTTTGGGGCTAATTCTT 3´ rev 5´ RTTCTCTGGGCTTTTCTTCCA 3´; 18s fw 5´ AAACGGCTACCACATCCAAG 3´ rev 5´ RCCTCCAATGGATCCTCGTTA 3´; PPIA fw 5´ F TTCATCTGCACTGCCAAGAC 3´ rev 5´ TCGAGTTGTCCACAGTCAGC 3´; CVB fw 5' GGCCCCTGAATGCGGCTAAT 3', rev 5' TGGCTGCTTATGGTGACAATTG 3'; CVB (+)strand 5' GAGTCTATTGAGCTAATTGGTAAT 3'; CVB (–)strand 5' TGCCGTATTGAGTACTAAGATA 3'. Taqman assays: CXCL10 Hs00171042_m1 IFNβ Hs02621180_s1 IL-6 Hs99999032_m1 IL-1β Hs00174103_m1 TNFα Hs99999043_m1 Cyclophilin Hs99999904_m1.

Immunostaining

Pancreatic tissues were processed as previously described [103]. Briefly, human islets were fixed in 4% formaldehyde for 30 min at room temperature. Human 4 µm pancreatic or islet paraffin embedded slides were deparaffinized, rehydrated and incubated 12 h at 4°C with anti-insulin (Dako), anti-glucagon (Dako), anti-VP1 (Dako clone 5-D8/1), anti-human CXCL10 (R&D), anti-TLR3 (Imgenex, Novus Biological, Cambridge, UK), anti-TLR7 (Imgenex) antibodies followed by fluorescein isothiocyanate (FITC)-, Cy3-, Amga- or HRP-conjugated secondary antibodies (Jackson ImmunoResearch Laboratories, West Grove, PA, USA). Slides were mounted with Vectashield with 4'6-diamidino-2-phenylindole (DAPI) (Vector Labs, Burlingame, CA, USA). TLR3 and TLR7-insulin/glucagon double staining was also performed on frozen pancreas sections. β- and α-cell apoptosis for human islets sections or islets cultured on ECM dishes was analyzed by terminal deoxynucleotidyl transferase-mediated dUTP nick-end labeling (TUNEL) technique accordingly to the manufacturer's instructions (In Situ Cell Death Detection Kit, TMR red, Roche, Penzberg, Germany) and double stained for insulin or glucagon. Fluorescence was analyzed using a Nikon MEA53200 (Nikon GmbH, Düsseldorf, Germany) microscope and images were acquired using NIS-Elements software (Nikon).

Statistics

Samples were evaluated in a randomized manner by a single investigator (E.D.; blinded to the treatment conditions). Data were analyzed by paired Student's t-test.

Ethics Statement

Research with human islets from brain dead donors applies to NIH regulations PHS 398, exemption 4. Informed consent was obtained from all subjects or their relatives and ethical approval given to the respective institutions. Ethical approval for the use of islets has been granted by the University of Bremen ethical committee.

Acknowledgements

We thank Julie Kerr-Conte and Francois Pattou, European Genomic Institute for Diabetes, INSERM UMR 1190, Lille, France and ProdoLabs for the high quality human islet isolations, Jennifer Bergemann and Katrischa Hennekens for excellent technical assistance, Andreas Dotzauer for the help with the viruses and providing the FRhK-4 cells (all University of Bremen) and Annalisa Riccardi (Strathclyde University,

Schotland, UK) for help with real time data analysis. Human insulinoma CM cell line by Paolo Pozzilli (Barts and the London School of Medicine, Queen Mary, University of London, UK), pFLAg-CMV-1-hTLR3 from Carsten Kirschning (Technical University of Munich, Germany) and pEGFP-N2 from Frank Dietz (University of Bremen). Human islets were provided through the JDRF award 31-2008-413 (ECIT Islet for Basic Research program) and by the integrated islet distribution program (IIDP). Frozen pancreases were obtained from the National Disease Research Interchange NDRI, supported from the NIDDK.

1. Hyoty H, Taylor KW (2002) The role of viruses in human diabetes. Diabetologia 45:1353–1361. doi: 10.1007/s00125-002-0852-3
2. Yeung W-CG, Rawlinson WD, Craig ME (2011) Enterovirus infection and type 1 diabetes mellitus: systematic review and meta-analysis of observational molecular studies. BMJ 342:d35.
3. ADAMS SF (1926) THE SEASONAL VARIATION IN THE ONSET OF ACUTE DIABETES: THE AGE AND SEX FACTORS IN 1,000 DIABETIC PATIENTS. Archives of Internal Medicine 37:861. doi: 10.1001/archinte.1926.00120240133010
4. Oikarinen M, Tauriainen S, Oikarinen S, et al (2012) Type 1 Diabetes Is Associated With Enterovirus Infection in Gut Mucosa. Diabetes. doi: 10.2337/db11-1157
5. Stene LC, Oikarinen S, Hyöty H, et al (2010) Enterovirus infection and progression from islet autoimmunity to type 1 diabetes: the Diabetes and Autoimmunity Study in the Young (DAISY). Diabetes 59:3174–3180. doi: 10.2337/db10-0866
6. Richardson SJ, Willcox A, Bone AJ, et al (2009) The prevalence of enteroviral capsid protein vp1 immunostaining in pancreatic islets in human type 1 diabetes. Diabetologia 52:1143–1151. doi: 10.1007/s00125-009-1276-0
7. Oikarinen M, Tauriainen S, Honkanen T, et al (2007) Detection of enteroviruses in the intestine of type 1 diabetic patients. Clin Exp Immunol 151:71–75. doi: 10.1111/j.1365-2249.2007.03529.x
8. Krogvold L, Edwin B, Buanes T, et al (2014) Detection of a low-grade enteroviral infection in the islets of Langerhans of living patients newly diagnosed with type 1 diabetes. Diabetes 64:1682–1687. doi: 10.2337/db14-1370
9. Christen U, Herrath von MG (2011) Do viral infections protect from or enhance type 1 diabetes and how can we tell the difference? Cell Mol Immunol. doi: 10.1038/cmi.2010.71
10. Rodriguez-Calvo T, Herrath von MG (2015) Enterovirus infection and type 1 diabetes: closing in on a link? Diabetes 64:1503–1505. doi: 10.2337/db14-1931
11. Rodriguez-Calvo T, Sabouri S, Anquetil F, Herrath von MG (2016) Autoimmunity Reviews. Autoimmun Rev 1–6. doi: 10.1016/j.autrev.2016.07.019
12. Chehadeh W, Kerr-Conte J, Pattou F, et al (2000) Persistent infection of human

pancreatic islets by coxsackievirus B is associated with alpha interferon synthesis in beta cells. J Virol 74:10153–10164. doi: 10.1128/JVI.74.21.10153-10164.2000
13. Yoon J-W, Austin M, Onodera T, Notkins AL (1979) Isolation of a virus from the pancreas of a child with diabetic ketoacidosis. N Engl J Med 300:1173–1179. doi: 10.1056/NEJM197905243002102
14. Yoon J-W, Jun H-S (2006) Viruses cause type 1 diabetes in animals. Annals of the New York Academy of Sciences 1079:138–146. doi: 10.1196/annals.1375.021
15. Shimada A, Maruyama T (2004) Encephalomyocarditis-virus-induced diabetes model resembles “fulminant” type 1 diabetes in humans. Diabetologia 47:1854–1855. doi: 10.1007/s00125-004-1538-9
16. Coppieters KT, Boettler T, Herrath von M (2012) Virus infections in type 1 diabetes. Cold Spring Harb Perspect Med 2:a007682. doi: 10.1101/cshperspect.a007682
17. Serreze DV, Ottendorfer EW, Ellis TM, et al (2000) Acceleration of type 1 diabetes by a coxsackievirus infection requires a preexisting critical mass of autoreactive T-cells in pancreatic islets. Diabetes 49:708–711.
18. Tracy S, Drescher KM, Chapman NM, et al (2002) Toward testing the hypothesis that group B coxsackieviruses (CVB) trigger insulin-dependent diabetes: inoculating nonobese diabetic mice with CVB markedly lowers diabetes incidence. J Virol 76:12097–12111.
19. Filippi CM, Estes EA, Oldham JE, Herrath von MG (2009) Immunoregulatory mechanisms triggered by viral infections protect from type 1 diabetes in mice. J Clin Invest 119:1515–1523. doi: 10.1172/JCI38503
20. Lennon GP, Bettini M, Burton AR, et al (2009) T cell islet accumulation in type 1 diabetes is a tightly regulated, cell-autonomous event. Immunity 31:643–653. doi: 10.1016/j.immuni.2009.07.008
21. Horwitz MS, Bradley LM, Harbertson J, et al (1998) Diabetes induced by Coxsackie virus: initiation by bystander damage and not molecular mimicry. Nat Med 4:781–785.
22. Schloot NC, Willemen SJ, Duinkerken G, et al (2001) Molecular mimicry in type 1 diabetes mellitus revisited: T-cell clones to GAD65 peptides with sequence homology to Coxsackie or proinsulin peptides do not crossreact with homologous counterpart. Hum Immunol 62:299–309.
23. Kaufman DL, Erlander MG, Clare-Salzler M, et al (1992) Autoimmunity to two forms of glutamate decarboxylase in insulin-dependent diabetes mellitus. J Clin Invest 89:283–292. doi: 10.1172/JCI115573
24. Sevilla N, Homann D, Herrath von M, et al (2000) Virus-induced diabetes in a transgenic model: role of cross-reacting viruses and quantitation of effector T cells needed to cause disease. J Virol 74:3284–3292.
25. Ehl S, Hombach J, Aichele P, et al (1997) Bystander activation of cytotoxic T cells: studies on the mechanism and evaluation of in vivo significance in a transgenic mouse model. J Exp Med 185:1241–1251.
26. Zarozinski CC, Welsh RM (1997) Minimal bystander activation of CD8 T cells during the virus-induced polyclonal T cell response. J Exp Med 185:1629–1639.
27. Nair S, Leung K-C, Rawlinson WD, et al (2010) Enterovirus infection induces cytokine and chemokine expression in insulin-producing cells. J Med Virol 82:1950–1957. doi: 10.1002/jmv.21900

28. Seewaldt S, Thomas HE, Ejrnaes M, et al (2000) Virus-induced autoimmune diabetes: most beta-cells die through inflammatory cytokines and not perforin from autoreactive (anti-viral) cytotoxic T-lymphocytes. Diabetes 49:1801–1809.
29. Schulthess FT, Paroni F, Sauter NS, et al (2009) CXCL10 Impairs b Cell Function and Viability in Diabetes through TLR4 Signaling. Cell Metabolism 9:125–139. doi: 10.1016/j.cmet.2009.01.003
30. Berg A-K, Korsgren O, Frisk G (2006) Induction of the chemokine interferon-gamma-inducible protein-10 in human pancreatic islets during enterovirus infection. Diabetologia 49:2697–2703. doi: 10.1007/s00125-006-0429-7
31. Christen U, McGavern DB, Luster AD, et al (2003) Among CXCR3 chemokines, IFN-gamma-inducible protein of 10 kDa (CXC chemokine ligand (CXCL) 10) but not monokine induced by IFN-gamma (CXCL9) imprints a pattern for the subsequent development of autoimmune disease. J Immunol 171:6838–6845.
32. Takeuchi O, Akira S (2010) Pattern recognition receptors and inflammation. Cell 140:805–820. doi: 10.1016/j.cell.2010.01.022
33. Aida K, Nishida Y, Tanaka S, et al (2011) RIG-I- and MDA5-initiated innate immunity linked with adaptive immunity accelerates beta-cell death in fulminant type 1 diabetes. Diabetes 60:884–889. doi: 10.2337/db10-0795
34. Lee AS, Ghoreishi M, Cheng WK, et al (2011) Toll-like receptor 7 stimulation promotes autoimmune diabetes in the NOD mouse. Diabetologia 54:1407–1416. doi: 10.1007/s00125-011-2083-y
35. Tannahill GM, O'Neill LAJ (2011) The emerging role of metabolic regulation in the functioning of Toll-like receptors and the NOD-like receptor Nlrp3. FEBS Letters 585:1568–1572. doi: 10.1016/j.febslet.2011.05.008
36. Dasu MR, Devaraj S, Park S, Jialal I (2010) Increased toll-like receptor (TLR) activation and TLR ligands in recently diagnosed type 2 diabetic subjects. Diabetes Care 33:861–868. doi: 10.2337/dc09-1799
37. Smyth DJ, Cooper JD, Bailey R, et al (2006) A genome-wide association study of nonsynonymous SNPs identifies a type 1 diabetes locus in the interferon-induced helicase (IFIH1) region. Nat Genet 38:617–619. doi: 10.1038/ng1800
38. Nejentsev S, Walker N, Riches D, et al (2009) Rare variants of IFIH1, a gene implicated in antiviral responses, protect against type 1 diabetes. Science 324:387–389. doi: 10.1126/science.1167728
39. Assmann TS, Brondani LDA, Bauer AC, et al (2014) Polymorphisms in the TLR3 gene are associated with risk for type 1 diabetes mellitus. European Journal of Endocrinology 170:519–527. doi: 10.1530/EJE-13-0963
40. Dotta F, Sebastiani G (2014) Enteroviral Infections and Development of Type 1 Diabetes: The Brothers Karamazov Within the CVBs. Diabetes 63:384–386. doi: 10.2337/db13-1441
41. Morgan NG, Richardson SJ (2014) Enteroviruses as causative agents in type 1 diabetes: loose ends or lost cause? Trends in Endocrinology & Metabolism 1–9. doi: 10.1016/j.tem.2014.08.002
42. Herrath von M, Filippi C, Coppieters K (2011) How viral infections enhance or prevent type 1 diabetes-from mouse to man. J Med Virol 83:1672–1672. doi: 10.1002/jmv.22063
43. Afonso G, Mallone R (2013) Infectious triggers in type 1 diabetes: is there a case for epitope mimicry? Diabetes Obes Metab 15 Suppl 3:82–88. doi: 10.1111/dom.12166
44. Kawasaki T, Kawai T, Akira S (2011) Recognition of nucleic acids by pattern-recognition receptors and its relevance in autoimmunity. Immunol Rev 243:61–

73. doi: 10.1111/j.1600-065X.2011.01048.x
45. Lee HK, Lund JM, Ramanathan B, et al (2007) Autophagy-dependent viral recognition by plasmacytoid dendritic cells. Science 315:1398–1401. doi: 10.1126/science.1136880
46. Elghazi L, Bernal-Mizrachi E (2009) Akt and PTEN: β-cell mass and pancreas plasticity. Trends in Endocrinology & Metabolism 20:243–251. doi: 10.1016/j.tem.2009.03.002
47. Aikin R, Hanley S, Maysinger D, et al (2006) Autocrine insulin action activates Akt and increases survival of isolated human islets. Diabetologia 49:2900–2909. doi: 10.1007/s00125-006-0476-0
48. Elde NC, Child SJ, Geballe AP, Malik HS (2009) Protein kinase R reveals an evolutionary model for defeating viral mimicry. Nature 457:485–489. doi: doi:10.1038/nature07529
49. Colli ML, Nogueira TC, Allagnat F, et al (2011) Exposure to the viral by-product dsRNA or Coxsackievirus B5 triggers pancreatic beta cell apoptosis via a Bim / Mcl-1 imbalance. PLoS Pathog 7:e1002267. doi: 10.1371/journal.ppat.1002267.g007
50. Yu T, Yi Y-S, Yang Y, et al (2012) The pivotal role of TBK1 in inflammatory responses mediated by macrophages. Mediators Inflamm 2012:979105. doi: 10.1155/2012/979105
51. Wang B, Zhang H, Zhu M, et al (2012) MEK1-ERKs signal cascade is required for the replication of Enterovirus 71 (EV71). Antiviral Res 93:110–117. doi: 10.1016/j.antiviral.2011.11.001
52. Zhu M, Duan H, Gao M, et al (2015) Both ERK1 and ERK2 Are Required for Enterovirus 71 (EV71) Efficient Replication. Viruses 7:1344–1356. doi: 10.3390/v7031344
53. ADAMS SF (1926) THE SEASONAL VARIATION IN THE ONSET OF ACUTE DIABETES. Archives of Internal Medicine 37:861. doi: 10.1001/archinte.1926.00120240133010
54. Gamble DR, Taylor KW (1969) Seasonal incidence of diabetes mellitus. Br Med J 3:631–633. doi: 10.1136/bmj.3.5671.631
55. Dezayee ZMI (2012) The status of serum γ-interferonand antiviral antibodies in patients with type I and type 2 diabetes: A comparative study. J Res Med Sci 17:855–858.
56. Herrath von MG, Fujinami RS, Whitton JL (2003) Opinion: Microorganisms and autoimmunity: making the barren field fertile? Nat Rev Microbiol 1:151–157. doi: 10.1038/nrmicro754
57. Horwitz MS, Bradley LM, Harbertson J, et al (1998) Diabetes induced by Coxsackie virus: Initiation by bystander damage and not molecular mimicry. Nat Med 4:781–785. doi: 10.1038/nm0798-781
58. Seewaldt S, Thomas HE, Ejrnaes M, et al Virus-induced autoimmune diabetes: most beta-cells die through inflammatory cytokines and not perforin from autoreactive (anti-viral) cytotoxic T-lymphocytes.
59. Nicoletti F, Scalia G, Lunetta M, et al (1990) Correlation between islet cell antibodies and anti-cytomegalovirus IgM and IgG antibodies in healthy first-degree relatives of type 1 (insulin-dependent) diabetic patients. Clin Immunol Immunopathol 55:139–147.
60. Tauriainen S, Oikarinen S, Oikarinen M, Hyöty H (2010) Enteroviruses in the pathogenesis of type 1 diabetes. Semin Immunopathol 33:45–55. doi: 10.1007/s00281-010-0207-y

61. Shimada A, Morimoto J, Kodama K, et al (2001) Elevated serum IP-10 levels observed in type 1 diabetes. Diabetes Care 24:510–515.
62. Nicoletti F, Di Mauro M, et al (2002) Serum concentrations of the interferon--inducible chemokine IP-10/CXCL10 are augmented in both newly diagnosed Type I diabetes mellitus patients and subjects at risk of developing the disease. Diabetologia 45:1107–1110. doi: 10.1007/s00125-002-0879-5
63. Nakagawa Y, Shimada A, Oikawa Y, et al (2003) Two cases of “fulminant” type 1 diabetes suggesting involvement of autoimmunity. Annals of the New York Academy of Sciences 1005:359–361.
64. Xin Y, Zhao Y-Q, Zhao Y-X, Zhang L-H (2007) [The changes of serum interferon-inducible protein-10 levels in children with type 1 diabetes mellitus]. Zhonghua Er Ke Za Zhi 45:853–855.
65. Antonelli A, Fallahi P, Ferrari SM, et al (2008) Serum Th1 (CXCL10) and Th2 (CCL2) chemokine levels in children with newly diagnosed Type 1 diabetes: a longitudinal study. Diabetic Med 25:1349–1353. doi: 10.1111/j.1464-5491.2008.02577.x
66. Schulte BM, Lanke KHW, Piganelli JD, et al (2012) Cytokine and Chemokine Production by Human Pancreatic Islets Upon Enterovirus Infection. Diabetes 61:2030–2036. doi: 10.2337/db11-1547
67. Ivashkiv LB, Donlin LT (2014) Regulation of type I interferon responses. Nat Rev Immunol 14:36–49. doi: 10.1038/nri3581
68. Wolferstatter M, Schweneker M, Spath M, et al (2014) Recombinant Modified Vaccinia Virus Ankara Generating Excess Early Double-Stranded RNA Transiently Activates Protein Kinase R and Triggers Enhanced Innate Immune Responses. J Virol 88:14396–14411. doi: 10.1128/JVI.02082-14
69. Luthra P, Sun D, Silverman RH, He B (2011) Activation of IFN-b expression by a viral mRNA through RNase L and MDA5. Proc Natl Acad Sci U S A 108:2118–2123. doi: 10.1073/pnas.1012409108
70. Ylipaasto P, Kutlu B, Rasilainen S, et al (2005) Global profiling of coxsackievirus- and cytokine-induced gene expression in human pancreatic islets. Diabetologia 48:1510–1522. doi: 10.1007/s00125-005-1839-7
71. Liu S, Wang H, Jin Y, et al (2009) IFIH1 polymorphisms are significantly associated with type 1 diabetes and IFIH1 gene expression in peripheral blood mononuclear cells. Hum Mol Genet 18:358–365. doi: 10.1093/hmg/ddn342
72. Field LL, Bonnevie-Nielsen V, Pociot F, et al (2005) OAS1 splice site polymorphism controlling antiviral enzyme activity influences susceptibility to type 1 diabetes. Diabetes 54:1588–1591.
73. Winkler C, Lauber C, Adler K, et al (2011) An interferon-induced helicase (IFIH1) gene polymorphism associates with different rates of progression from autoimmunity to type 1 diabetes. Diabetes 60:685–690. doi: 10.2337/db10-1269
74. García M, Dogusan Z, Moore F, et al (2009) Regulation and function of the cytosolic viral RNA sensor RIG-I in pancreatic beta cells. Biochim Biophys Acta 1793:1768–1775. doi: 10.1016/j.bbamcr.2009.09.005
75. Shigemoto T, Kageyama M, Hirai R, et al (2009) Identification of loss of function mutations in human genes encoding RIG-I and MDA5: implications for resistance to type I diabetes. J Biol Chem 284:13348–13354. doi: 10.1074/jbc.M809449200
76. Sen A, Pruijssers AJ, Dermody TS, et al (2011) The Early Interferon Response to Rotavirus Is Regulated by PKR and Depends on MAVS/IPS-1, RIG-I, MDA-

5, and IRF3. J Virol 85:3717–3732. doi: 10.1128/JVI.02634-10
77. Zhang P, Li Y, Xia J, et al (2014) IPS-1 plays an essential role in dsRNA-induced stress granule formation by interacting with PKR and promoting its activation. J Cell Sci 127:2471–2482. doi: 10.1242/jcs.139626
78. Rasschaert J, Ladriere L, Urbain M, et al (2005) Toll-like receptor 3 and STAT-1 contribute to double-stranded RNA plus interferon-gamma-induced apoptosis in primary pancreatic beta-cells. J Biol Chem 280:33984–33991. doi: 10.1074/jbc.M502213200
79. Anagandula M, Richardson SJ, Oberste MS, et al (2013) Infection of human islets of langerhans with two strains of coxsackie B virus serotype 1: Assessment of virus replication, degree of cell death and induction of genes involved in the innate immunity pathway. J Med Virol 86:1402–1411. doi: 10.1002/jmv.23835
80. McCall KD, Thuma JR, Courreges MC, et al (2014) Toll-Like Receptor 3 is Critical for Coxsackievirus B4–Induced Type 1 Diabetes in Female NOD Mice. Endocrinology en.2013–2006. doi: 10.1210/en.2013-2006
81. Hutton MJH, Soukhatcheva G, Johnson JD, Verchere CB (2010) Role of the TLR signaling molecule TRIF in β-cell function and glucose homeostasis. Islets 2:104–111. doi: 10.4161/isl.2.2.11209
82. Marroqui L, Lopes M, Santos dos RS, et al (2015) Differential cell autonomous responses determine the outcome of coxsackievirus infections in murine pancreatic α and β cells. Elife. doi: 10.7554/eLife.06990
83. Tracy S, Smithee S, Alhazmi A, Chapman N (2014) Coxsackievirus can persist in murine pancreas by deletion of 5' terminal genomic sequences. J Med Virol 87:240–247. doi: 10.1002/jmv.24039
84. Kim K-S, Chapman NM, Tracy S (2008) Replication of coxsackievirus B3 in primary cell cultures generates novel viral genome deletions. J Virol 82:2033–2037. doi: 10.1128/JVI.01774-07
85. Kim K-S, Tracy S, Tapprich W, et al (2005) 5'-Terminal Deletions Occur in Coxsackievirus B3 during Replication in Murine Hearts and Cardiac Myocyte Cultures and Correlate with Encapsidation of Negative-Strand Viral RNA. J Virol 79:7024–7041. doi: 10.1128/JVI.79.11.7024-7041.2005
86. Tatematsu M, Nishikawa F, Seya T, Matsumoto M (2013) Toll-like receptor 3 recognizes incomplete stem structures in single-stranded viral RNA. Nat Comms 4:1833–1833. doi: 10.1038/ncomms2857
87. Shafren DR, Williams DT, Barry RD (1997) A decay-accelerating factor-binding strain of coxsackievirus B3 requires the coxsackievirus-adenovirus receptor protein to mediate lytic infection of rhabdomyosarcoma cells. J Virol 71:9844–9848.
88. Chung S-K, Kim J-Y, Kim I-B, et al (2005) Internalization and trafficking mechanisms of coxsackievirus B3 in HeLa cells. Virology 333:31–40. doi: 10.1016/j.virol.2004.12.010
89. Antonelli A, Ferrari SM, Giuggioli D, et al (2013) Chemokine (C–X–C motif) ligand (CXCL)10 in autoimmune diseases. Autoimmun Rev. doi: 10.1016/j.autrev.2013.10.010
90. Tanaka S, Nishida Y, Aida K, et al (2009) Enterovirus infection, CXC chemokine ligand 10 (CXCL10), and CXCR3 circuit: a mechanism of accelerated beta-cell failure in fulminant type 1 diabetes. Diabetes 58:2285–2291. doi: 10.2337/db09-0091
91. (2002) β cells are responsible for CXCR3-mediated T-cell infiltration in insulitis.

8:1414–1420. doi: 10.1038/nm792
92. Roep BO, Kleijwegt FS, van Halteren AGS, et al (2010) Islet inflammation and CXCL10 in recent-onset type 1 diabetes. Clin Exp Immunol 159:338–343. doi: 10.1111/j.1365-2249.2009.04087.x
93. Esfandiarei M, Luo H, Yanagawa B, et al (2004) Protein kinase B/Akt regulates coxsackievirus B3 replication through a mechanism which is not caspase dependent. J Virol 78:4289–4298. doi: 10.1128/JVI.78.8.4289–4298.2004
94. Mendoza MC, Er EE, Blenis J (2011) The Ras-ERK and PI3K-mTOR pathways: cross-talk and compensation. Trends Biochem Sci 36:320–328. doi: 10.1016/j.tibs.2011.03.006
95. Zimmermann S, Moelling K (1999) Phosphorylation and regulation of Raf by Akt (protein kinase B). Science 286:1741–1744.
96. (null), Pozzilli P, (null), (null) (2008) Insulinoma CM cell line as in vitro model for beta-cell. J Cell Physiol 216:568–568. doi: 10.1002/jcp.21409
97. Baroni MG, Cavallo MG, Mark M, et al (1999) Beta-cell gene expression and functional characterisation of the human insulinoma cell line CM. J Endocrinol 161:59–68.
98. Bell YC, Semler BL, Ehrenfeld E (1999) Requirements for RNA replication of a poliovirus replicon by coxsackievirus B3 RNA polymerase. J Virol 73:9413–9421.
99. G K (1931) Beitrag zur kollektiven Behandlung pharmakologischer Reihenversuche. Arch Exp Pathol Pharmakol. Arch Exp Pathol Phamakol 1–6.
100. Gibbert K, Dietze KK, Zelinskyy G, et al (2010) Polyinosinic-polycytidylic acid treatment of Friend retrovirus-infected mice improves functional properties of virus-specific T cells and prevents virus-induced disease. J Immunol 185:6179–6189. doi: 10.4049/jimmunol.1000858
101. Ardestani A, Paroni F, Azizi Z, et al (2014) MST1 is a key regulator of beta cell apoptosis and dysfunction in diabetes. Nat Med 20:385–397. doi: 10.1038/nm.3482
102. Rutledge RG, Stewart D (2010) Assessing the performance capabilities of LRE-based assays for absolute quantitative real-time PCR. PLoS ONE 5:e9731. doi: 10.1371/journal.pone.0009731
103. Shu L, Sauter NS, Schulthess FT, et al (2008) Transcription factor 7-like 2 regulates beta-cell survival and function in human pancreatic islets. Diabetes 57:645–653. doi: 10.2337/db07-0847

Fig.1: Coxsackieviruses induce massive β-cell death, impaired function and CXCL10 production in human islets

Isolated human islets infected with CVB3 or -4 (MOI=10) for 48h **(A-F).** Immunostaining for TUNEL, insulin and VP1 **(A),** quantification of β-cell apoptosis **(B)** and GSIS with 2.8 mM (basal) and 16.7 mM (stimulated) glucose for 1h. Results are presented as stimulated/basal (stimulatory index) **(C)**. Western blot analysis of PARP, cleaved caspase 3, CXCL10, VP1 in control and infected isolated human islets **(D)**. CXCL10 secretion measured by ELISA of control and infected isolated human islet supernatants **(E)**. Immunostaining of insulin, glucagon, CXCL10 of control and infected human islets. Merged images show colocalization of insulin and CXCL10 **(F)**. Time course mRNA analysis of the host immune response from human islets infected with CVB3 or -4 (MOI=5) for 24, 48 and 72h normalized on peptidylpropyl isomerase A (PPIA) **(G)**. Data are means ± SE or representative data from at least three independent experiments from three different donors; *p<0.05 compared to control (magnification x400).

Fig.2: Differential tropism and virus sensing in α- and β-cells

Time course analyses of mRNA encoding PRRs. Human pancreatic islets were infected with CVB3 or 4 (MOI=5). RNA extracted at 24, 48 and 72h post infection, reverse transcribed and analyzed by real time PCR (normalized to 18S) **(A)**. Immunoprecipitation of uninfected (control) and CVB3 and 4 infected islets 24h p.i.. Equal protein concentrations were incubated with antibody against double strand RNA (K1) and sepharose beads. IP, output and input fractions were analyzed for the presence of RIG-I, MDA5 and PKR **(B)**. Reverse-IP from control, CVB3 and CVB4 infected human islets 24 and 48h p.i.. Equal amount of cell lysates were incubated with either TLR3 or TLR7 antibody and sepharose beads and ethanol precipitated RNA reverse transcribed using random primers. Logarithmic scale shows arbitrary units based on dilution curve using CVB primers **(C, D)**. Fluorescence and bright field immunostaining for TLR3 (upper panel) or for TLR7 (lower panel) of paraffin embedded pancreatic sections from healthy donors. Merged image shows colocalization of insulin or glucagon and TLR3 (upper panel) or insulin or glucagon and DAPI and TLR7 (lower panel) **(E)**. Paraffin embedded human islets infected with CVB3 or CVB4 (MOI=5) for 24, 48 and 72h were stained for insulin, glucagon and VP1 **(F)** or insulin, TUNEL and DAPI **(H).** Results are expressed as percentage of VP1 positive α- or β-cells (**F)** and

as percentage of TUNEL positive α- or β-cells **(G)**. Data are means ± SE or representative data from at least three independent experiments from three different donors; *p<0.05 compared to non-infected control; #p<0.05 compared to CVB3 (magnification x400).

Fig.3: AKT/JNK switch induces β-cell apoptosis as part of TLR3 signaling

CM cells overexpressing TLR3 or GFP were treated or transfected with 25 or 5 μg of poly(I:C) for 24h and treated with 2 μM CAS 608512-97-6 (PKRi). Western blot analysis performed of pPKR, TLR3, CXCL10 **(A)**. Human islets were infected with CVB3 (MOI=5) for 24 **(B)** or 48h **(C)** and treated with 20 μM PI3K inhibitor LY294002 starting 1 h before infection **(C)**. Time course western blot of pro- and antiapoptotic signals pAKT, pJNK, cleaved Caspase-3, CXCL10 and the appearance of viral protein VP1 **(B,C).** Western blot analysis of human islets infected with CVB3 and -4 (MOI=10) for 48h for pPKR and peIF2a; this is the same experiment shown in Fig.1D; the same loading control was used **(D)**. The human β-cell line CM9 stably overexpressing shScr control or shPKR was infected with CVB3 **(E)** or transfected with 5 μg poly(I:C) **(G)**. 24h post infection cells were lysed and western blot analysis of pPKR, pAKT, pJNK, VP1, cleaved Caspase 3 (clC3) was performed **(E,G)**. Human islets were infected with shScr or shPKR for 48 h and with CVB3 (MOI=5) for 24 h and western blot analysis performed of total PKR, pPKR, pAKT, pJNK, VP1 **(F)**. Results are from at least three independent experiments (CM cells, islets) from three different donors (A-D) or from two independent experiments (CM; G) or one (islets; F). β-actin or GAPDH were analyzed for house keeping control.

Fig.4: TBK1 links virus induced TLR3 and AKT activation

Human islets transfected with specific of TLR3 siRNA (siTLR3) or scramble siRNA (siScr) for 48 h and infected with CVB3 (MOI=5) for 24 h and western blot analysis performed of TLR3, pTBK1, pAKT, pJNK, VP1, cleaved Caspase 3 **(A)**. CM cells overexpressing TLR3 or GFP (Ctrl) or wildtype CM cells (WT) were CVB3 infected (MOI=5) for 24 h and western blot analysis performed of TLR3, pAKT and VP1 **(B)**. Human islets infected with CVB3 (MOI=5) for 16h and western blot analysis performed of TLR3, pTBK1, pAKT, pJNK, VP1, cleaved Caspase 3 **(C)**. CM cells overexpressing TLR3 or TLR3/TBK1 were infected with CVB3 (MOI=5) **(D)** or treated with 25 μg of

poly(I:C) **(E)** for 16 h. Western blot analysis of TLR3, TBK1, pTBK1, pAKT, cleaved Caspase 3, CXCL10 **(D,E)** and VP1 **(D only)**. Human islets **(F)** and CM cells overexpressing TLR3 or TLR3/TBK1 **(G)** were treated with 20 μM AKT inhibitor Tribicine starting 1h before infection with CVB3 (MOI=5). Western blot analysis of pPKR, pAKT, pJNK, VP1, cleaved caspase 3, TLR3, TBK1, pTBK1 **(F,G)**. Human islets were transfected with specific siRNA against AKT (siAKT) or scramble (siScr) for 48 h and infected with CVB3 for 24h. Western blot analysis of pAKT, total AKT, pJNK, VP1, cleaved Caspase 3 **(H)**. Results are from three independent experiments of three different donors. β-tubulin or GAPDH were analyzed for house keeping control.

Fig.5. ERK fosters virus replication and counterbalances AKT during virus replication

The human β-cell line CM was treated with 1.9 μM PI3K inhibitor (LY294002, **A**), 20 uM AKT inhibitor (tribicine) **(B)** or 20 μM ERK inhibitor (PD98059; **C**) starting 1h before infection with CVB3 (MOI=5) for 24h and analyzed for pAKT, pERK, VP1 **(A-C)** and pJNK **(C)** by western blotting. CM cells were treated with 1mM of the ER stress inhibitor 4-phenylbutyrate (4-PBA) starting 1h before infection with CVB3 (MOI=5) for 24h and analyzed for pERK, VP1, pAKT and pJNK by western blotting **(D).** CM cells overexpressing GFP, GFP/Flag-ERK1, GFP/HA-ERK2 or Flag-ERK1/HA-ERK2 were treated with 2 μM ER stress inducer Thapsigargin, starting 2h before infection with CVB3 (MOI=5) for 24h and analyzed for pERK, HA, cleaved Caspase3, PARP, VP1, total ERK (tERK) and pJNK by western blotting (E).

Fig.6: Silencing of TLR3 protects from cytokine secretion and β-cell death

Isolated human islets were transfected with small interference RNA against TLR3 (siTLR3) or scramble control (siScr) for 48h and infected with CVB3 for 24 h **(A-E)**. IFNβ, CXCL10, TNFα and IL-6 mRNA expression were analyzed by RT-PCR and normalized to PPIA from three independent experiments from three different donors; *p<0.05 compared to control **(A)**. Supernatants from the same islets were analyzed using a CXCL10 ELISA **(B)**. TUNEL and insulin double-positive cells were quantified; results are expressed as percentage of TUNEL positive β-cells from one experiment from 4 dishes/ treatment **(C)**. TUNEL staining is shown in bright field (black nuclei), (magnification x400) **(D)**. Serial dilutions of cleared supernatants were titrated on

FRhK-4 cells. Results show % change of $TCID_{50}$/ml in siTLR3 compared to siScr treated islets ± SE of three independent experiments from three different donors; *p<0.05 compared to control **(E).**

Fig.7: JNK inhibition rescues the β-cell from virus-induced apoptosis

Human islets were either treated with 25 uM JNK inhibitor (SP600125) starting 1h before infection (**A**) or transfected with dnJNK- or GFP-plasmid for 48 h **(B)** and transfected with CVB3 or -4 (MOI=5) for 24 h and analyzed for pAKT, pc-JUN, total JNK, VP1 and cleaved Caspase 3 by western blotting. Results are from three independent experiments of three different donors. β-actin was analyzed for house keeping control.

Our hypothetical view on the events during early infection of coxsackievirus in human pancreatic islets **(C)**. Virus enters α- and β-cells and TLR7/TLR3-virus interaction occurs either at the endosomal level mediated by secondary structures at 5'-term or lysosome/autophagosome level due to sensing of double stranded nucleic acid. TLR3 activates TBK1 that in turn potentiates AKT activation. AKT and ERK can counterbalance each other to maintain cell survival and facilitate viral replication. Virus replication intermediates activate PKR that lead to phosphorylation of eIF2α and block of translation, as well as further ERK activation. At a certain amount of intracellular virus, the balance tips towards cell death, further activating JNK and Caspase 3 and mediating viral release-a vicious cycle starts. Acute infection does not necessarily and immediately leads to apoptosis, but chronically to cell lysis, cell death and subsequent virus release. TLR3 downstream signaling activates the host immune response with increasing cytokine and chemokine production promoting activation of immune system activation and further β-cell killing. Infected α-cells serve as reservoir of virus during latent infection.

Supplementary Fig.1: Isolated human islets were infected with CMV, HAV, CVB3, CVB4 (MOI=10) and mock control. 72 h p.i. β-cell apoptosis was monitored and quantified by triple staining (TUNEL, insulin, VP1); data are expressed as percentage of TUNEL/insulin positive cells **(A)**. CXCL10 secretion from supernatants from the same cells was monitored by ELISA **(B)**. Human islets infected with CVB3 and -4

(MOI=5) were lysed immediately after the 2-hinfection period (0h) and 24, 48 and 72h p.i.. Serial dilutions of cleared supernatants were titrated on FRhK-4 cells, results show the $TCID_{50}$/ml in logarithmic scale **(C).** *p<0.05 compared to control.
Paraffin embedded human islets infected with CVB3 or CVB4 (MOI=5) for 24, 48 and 72h were stained for insulin, glucagon and VP1 **(D)** or insulin, TUNEL and DAPI **(E).** Merged images show colocalization of VP1 with insulin for CVB3 (middle panel) and insulin, glucagon and VP1 for CVB4 (lower panel; **D)**.

Supplementary Fig.2: Human pancreatic islets either treated **(A,C,D,E,F)** or transfected **(B,D,G)** with 25 or 5 μg poly(I:C). RNA was extracted at 24, 48 and 72 h p.i.. Time course real time PCR of cytokines/chemokines, normalized to PPIA **(A, B)** and of PRRs, normalized to 18S **(F,G)**. CXCL10 secretion from islet supernatants treated with poly(I:C) after 72 h measured by ELISA **(C),** western blot analysis of VP1 and cleaved Caspase 3 from control, CVB3 infected, poly(I:C) treated or transfected human islets 48 h p.i. or post treatment **(D)**. Quantification of β-cell apoptosis monitored by double staining for TUNEL and insulin **(E)**.

Supplementary Fig.3: Human pancreatic islets were infected with CVB3 and -4 (MOI=5) for 48 h. Reverse-IP carried out by incubating equal amounts of protein with either PKR, TLR3, TLR 7, MDA5 or RIG-I antibodies and sepharose beads. RNA was precipitated and reverse transcribed using either random or specific primers to detect the negative CVB RNA strand ("-") or the positive CVB RNA strand ("+"). MDA5 and RIG-I showed no amplification (not shown). Logarithmic scale shows arbitrary units based on dilution curve using CVB primers. Data are representative from at least three independent experiments from three different donors **(A, B)**. Human pancreatic islets were infected with CVB3 and -4 (MOI=0.1) for 6 days and re-infected (MOI=5) for additional 48 h. Fresh media was replaced daily. Reverse-IP carried out incubating equal amounts of protein with either PKR, TLR3, TLR7, MDA5 or RIG-I antibodies and sepharose beads. RNA was precipitated and reverse transcribed using either random primers or specific primers for positive or negative CVB RNA strands. MDA5 and RIG-I showed no amplification (not shown). Logarithmic scale shows arbitrary units based on dilution curve using CVB primers **(C, D)**. 18S loading PCR controls from reverse-IP output fraction confirm integrity and equal amount of RNA used for real time PCR (**A-**

D, middle panels). Viral RNA controls from reverse-IP output fraction confirm intact equal amount of RNA used for real time PCR analysis (**A-D**, lower panels). Results expressed as Ct values.

Supplementary Fig.4: CM cells were infected with CVB3 (MOI=5) for 24 h and western blot analysis performed of pAKT, pJNK, VP1, cleaved Caspase 3. Results are representative of three independent experiments. β-actin was analyzed as house keeping control **(A).** Human islets were infected with CVB3 (MOI=5) for 24h **(B)**. Time course western blot of pERK and the appearance of viral protein VP1 **(B).** CM cells were treated with 2μM ER stress inducer Thapsigargin, starting 2h before infection with CVB3 (MOI=5) for 24h and analyzed in parallel (1) for CHOP and pJNK, and (2) for cleaved Caspase 3, pERK, VP1 and tubulin as house keeping controls. Since this experiment included a time course study, we only show the results, when Thapsigargin induced ER-stress was confirmed after 24h **(C).**
Isolated human islets were transfected with small interference RNA against TLR3 (siTLR3) or scramble control (siScr) for 48h and infected with CVB4 for 24 h **(D-F)**. TUNEL and insulin double-positive cells were quantified; results are expressed as percentage of TUNEL positive β-cells **(D)**. TUNEL staining is shown in bright field (black nuclei), (magnification x400) **(E)**. Supernatants from the same islets were analyzed using a CXCL10 ELISA **(F)**.

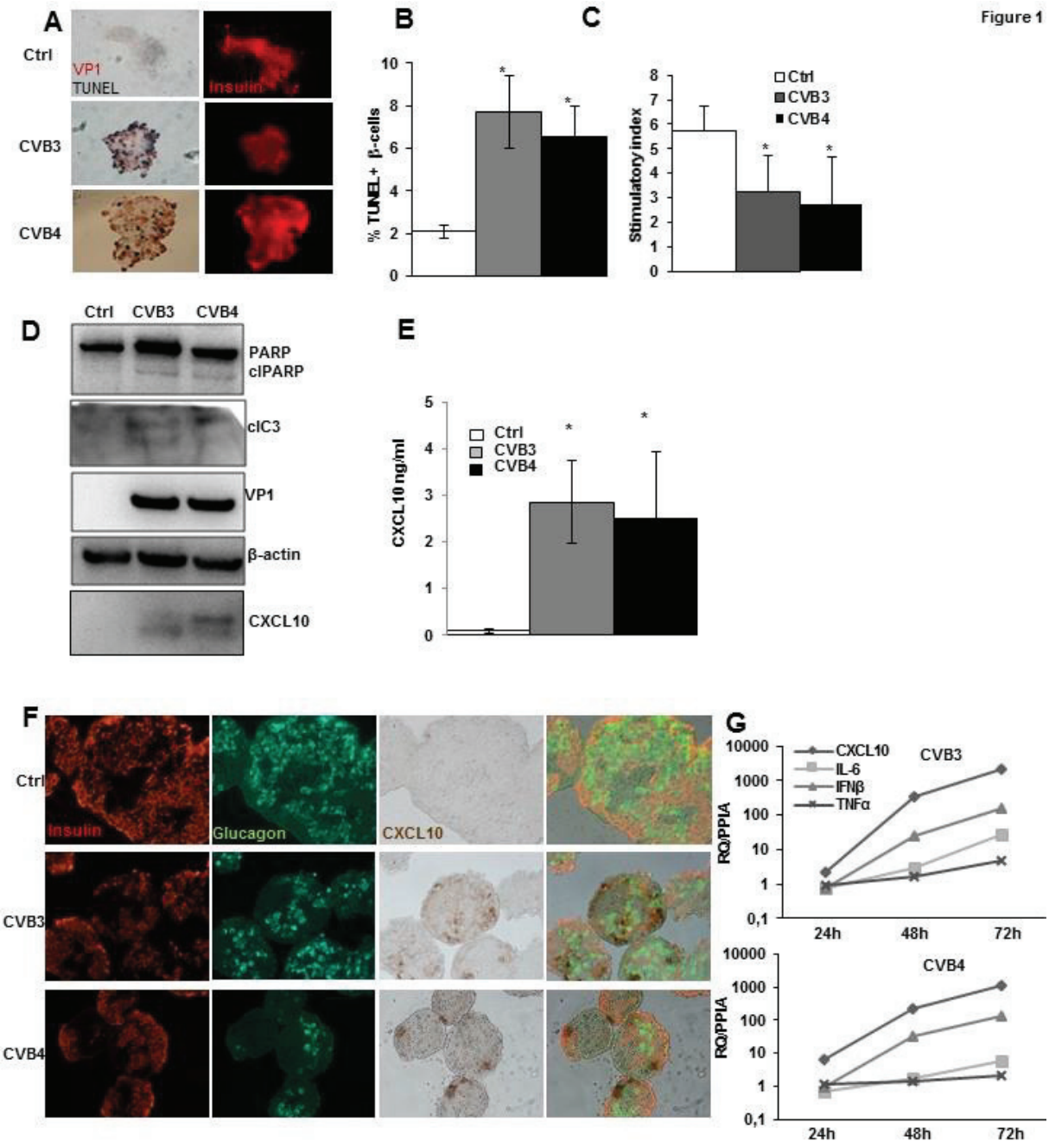
A
Ctrl
CVB3
CVB4
VP1
TUNEL
Insulin
B
% TUNEL+ β-cells
C
Stimulatory index
Ctrl
CVB3
CVB4
D
Ctrl CVB3 CVB4
PARP
cIPARP
cIC3
VP1
β-actin
CXCL10
E
CXCL10 ng/ml
F
Insulin
Glucagon
CXCL10
G
CXCL10
IL-6
IFNβ
TNFα
CVB3
CVB4
RQ/PPIA
24h
48h
72h

Figure 1

Figure 2

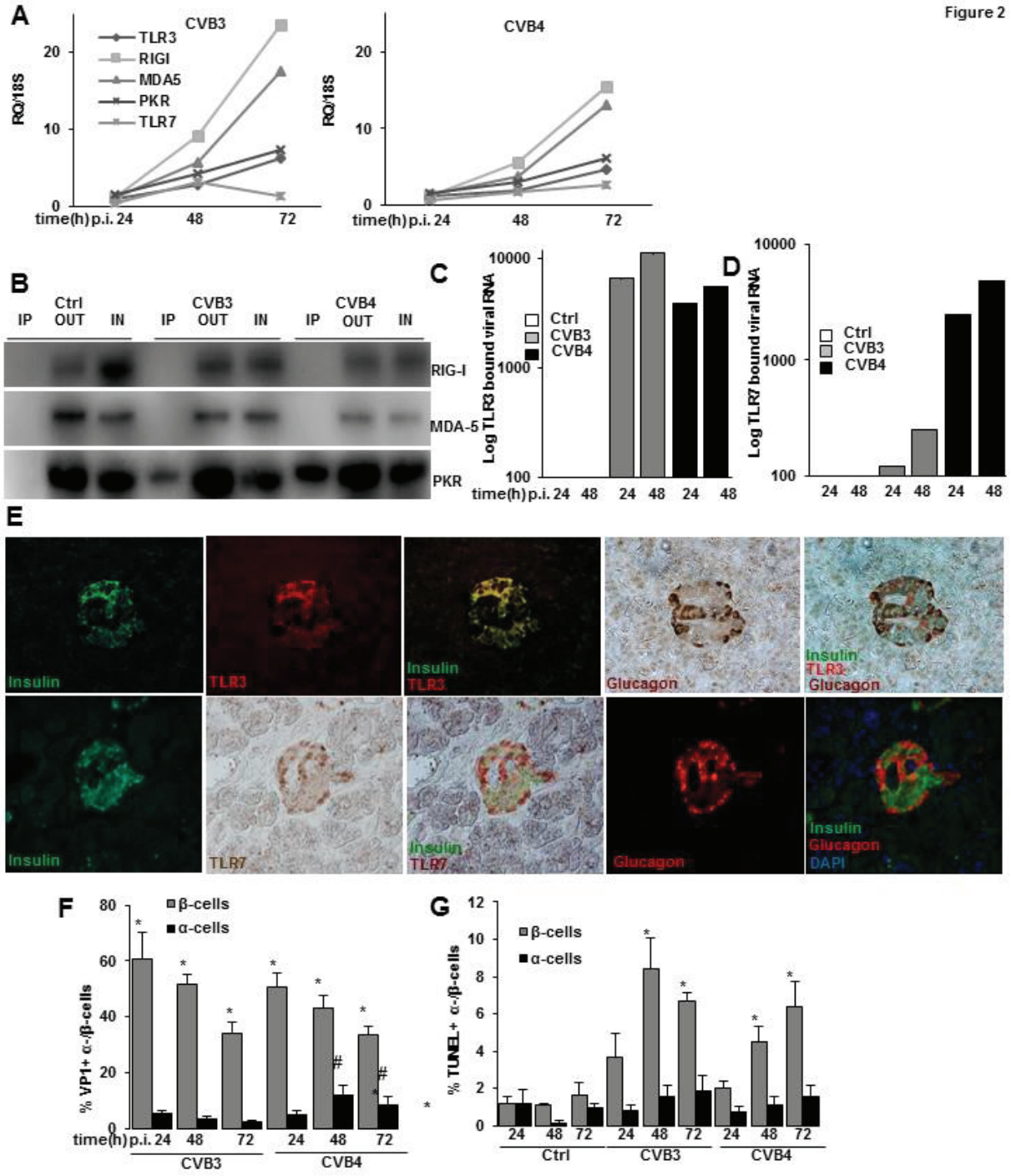
A
CVB3
TLR3
RIGI
MDA5
PKR
TLR7
RQ/18S
time(h) p.i. 24 48 72
CVB4
B
Ctrl
CVB3
CVB4
IP OUT IN IP OUT IN IP OUT IN
RIG-I
MDA-5
PKR
C
Log TLR3 bound viral RNA
Ctrl
CVB3
CVB4
time(h) p.i. 24 48 24 48 24 48
D
Log TLR7 bound viral RNA
Ctrl
CVB3
CVB4
24 48 24 48 24 48
E
Insulin
TLR3
Insulin
TLR3
Glucagon
Insulin
TLR3
Glucagon
Insulin
TLR7
Insulin
TLR7
Glucagon
Insulin
Glucagon
DAPI
F
β-cells
α-cells
% VP1+ α-/β-cells
time(h) p.i. 24 48 72 24 48 72
CVB3
CVB4
G
β-cells
α-cells
% TUNEL+ α-/β-cells
24 48 72 24 48 72 24 48 72
Ctrl
CVB3
CVB4

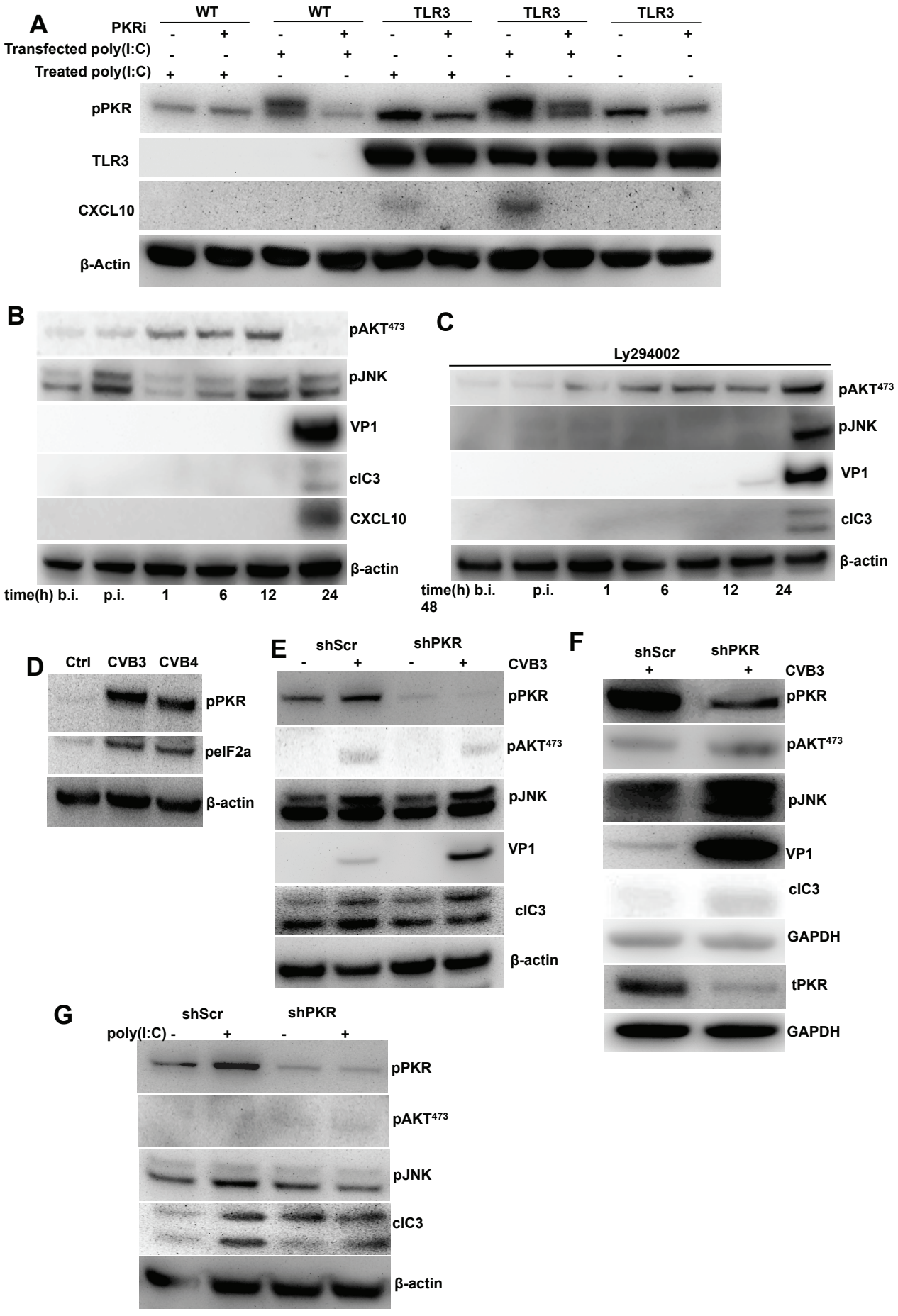
A
PKRi
WT
WT
TLR3
TLR3
TLR3
Transfected poly(I:C)
Treated poly(I:C)
pPKR
TLR3
CXCL10
β-Actin
B
pAKT473
pJNK
VP1
cIC3
CXCL10
β-actin
time(h) b.i. p.i. 1 6 12 24
C
Ly294002
pAKT473
pJNK
VP1
cIC3
β-actin
time(h) b.i. p.i. 1 6 12 24
48
D
Ctrl CVB3 CVB4
pPKR
peIF2a
β-actin
E
shScr
shPKR
CVB3
pPKR
pAKT473
pJNK
VP1
cIC3
β-actin
F
shScr
shPKR
CVB3
pPKR
pAKT473
pJNK
VP1
cIC3
GAPDH
tPKR
GAPDH
G
shScr
shPKR
poly(I:C)
pPKR
pAKT473
pJNK
cIC3
β-actin

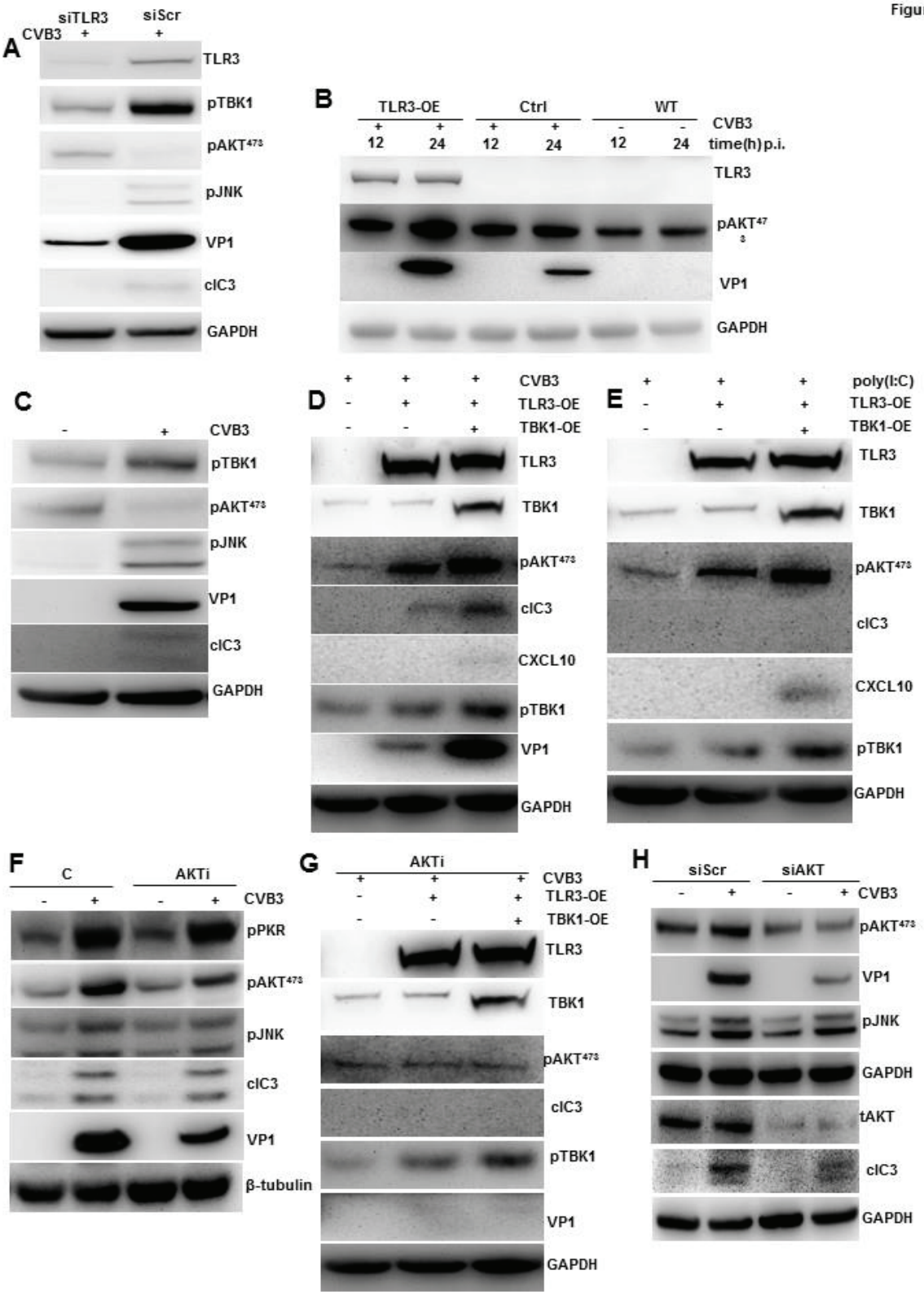
A
siTLR3
siScr
CVB3 + +
TLR3
pTBK1
pAKT473
pJNK
VP1
cIC3
GAPDH
B
TLR3-OE
Ctrl
WT
CVB3
12 24 12 24 12 24 time(h)p.i.
TLR3
pAKT473
VP1
GAPDH
C
CVB3
pTBK1
pAKT473
pJNK
VP1
cIC3
GAPDH
D
CVB3
TLR3-OE
TBK1-OE
TLR3
TBK1
pAKT473
cIC3
CXCL10
pTBK1
VP1
GAPDH
E
poly(I:C)
TLR3-OE
TBK1-OE
TLR3
TBK1
pAKT473
cIC3
CXCL10
pTBK1
GAPDH
F
C
AKTi
CVB3
pPKR
pAKT473
pJNK
cIC3
VP1
β-tubulin
G
AKTi
CVB3
TLR3-OE
TBK1-OE
TLR3
TBK1
pAKT473
cIC3
pTBK1
VP1
GAPDH
H
siScr
siAKT
CVB3
pAKT473
VP1
pJNK
GAPDH
tAKT
cIC3
GAPDH

Figure 5

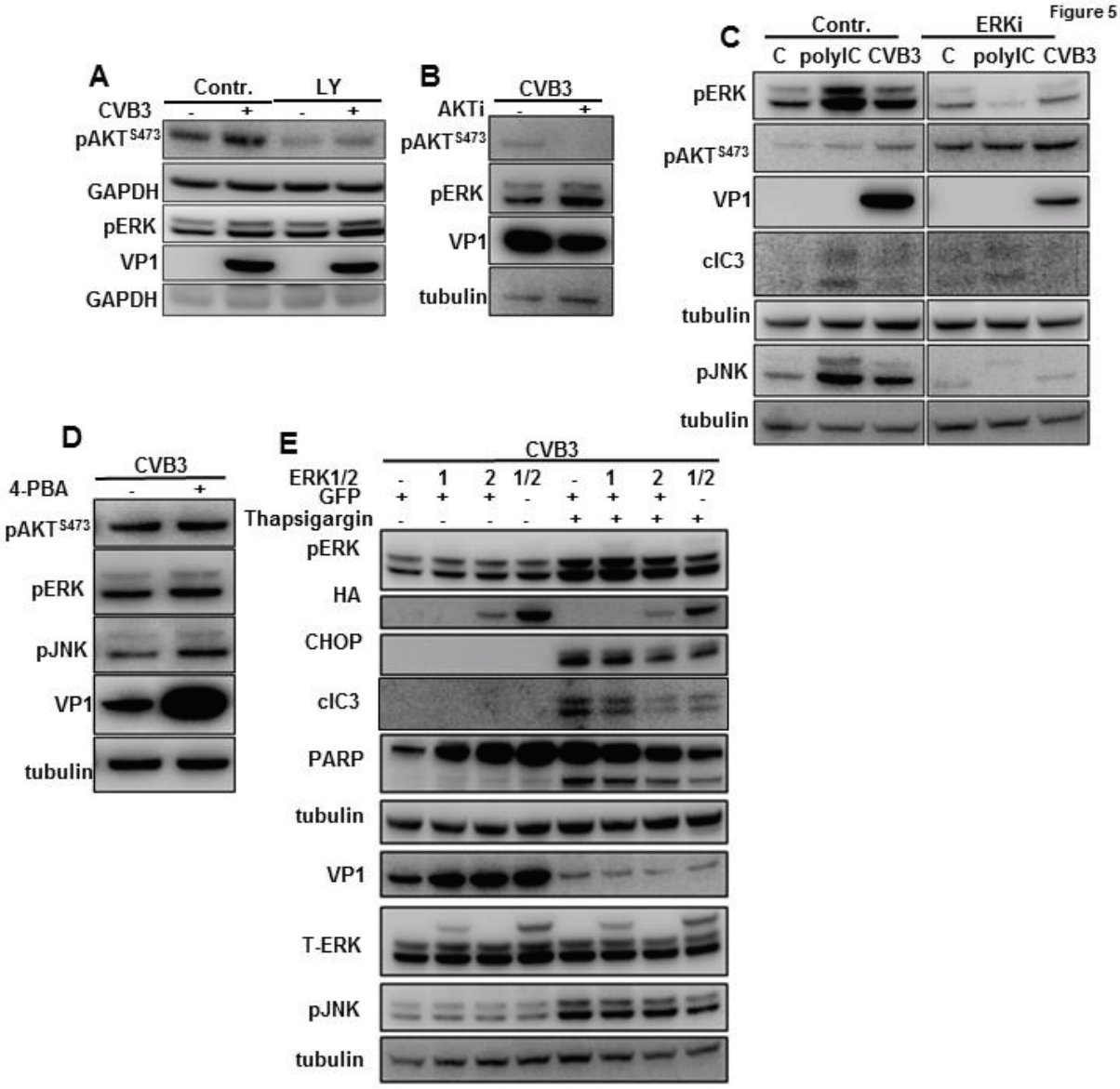
A
Contr.
LY
CVB3
- + - +
pAKT S473
GAPDH
pERK
VP1
GAPDH
B
CVB3
AKTi
- +
pAKT S473
pERK
VP1
tubulin
C
Contr.
ERKi
C polyIC CVB3 C polyIC CVB3
pERK
pAKT S473
VP1
cIC3
tubulin
pJNK
tubulin
D
CVB3
4-PBA
- +
pAKT S473
pERK
pJNK
VP1
tubulin
E
CVB3
ERK1/2 - 1 2 1/2 - 1 2 1/2
GFP + + + - + + + -
Thapsigargin - - - - + + + +
pERK
HA
CHOP
cIC3
PARP
tubulin
VP1
T-ERK
pJNK
tubulin

Figure 6

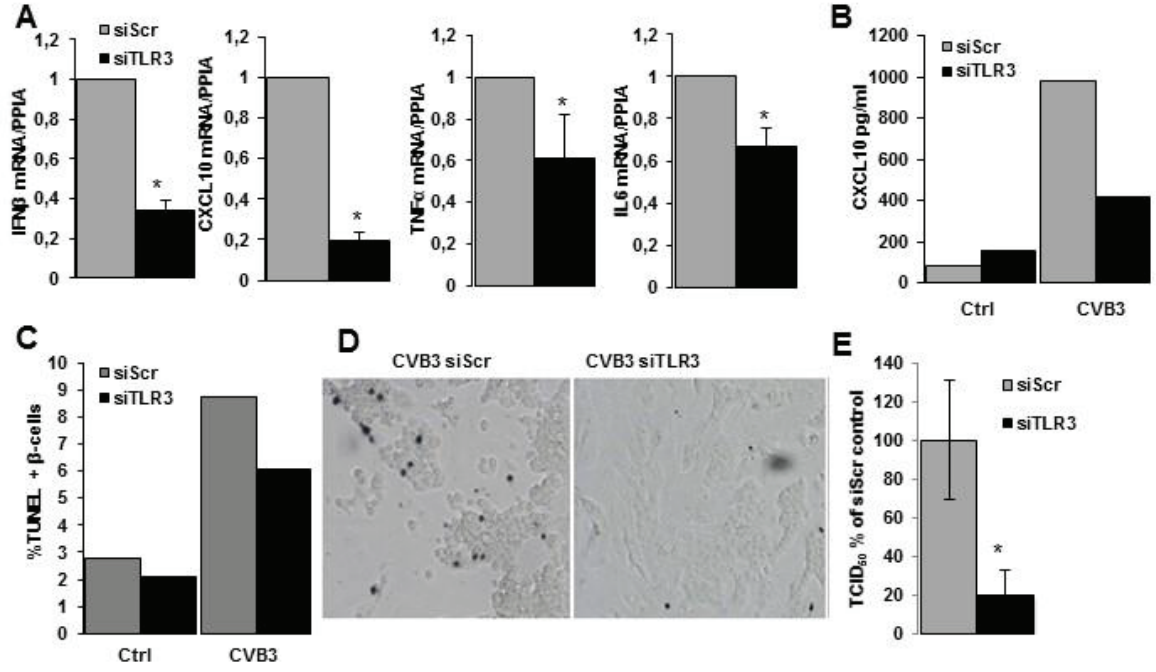
A
siScr
siTLR3
IFNβ mRNA/PPIA
CXCL10 mRNA/PPIA
TNFα mRNA/PPIA
IL6 mRNA/PPIA
B
CXCL10 pg/ml
Ctrl
CVB3
C
%TUNEL + β-cells
D
CVB3 siScr
CVB3 siTLR3
E
TCID50 % of siScr control

Figure 7

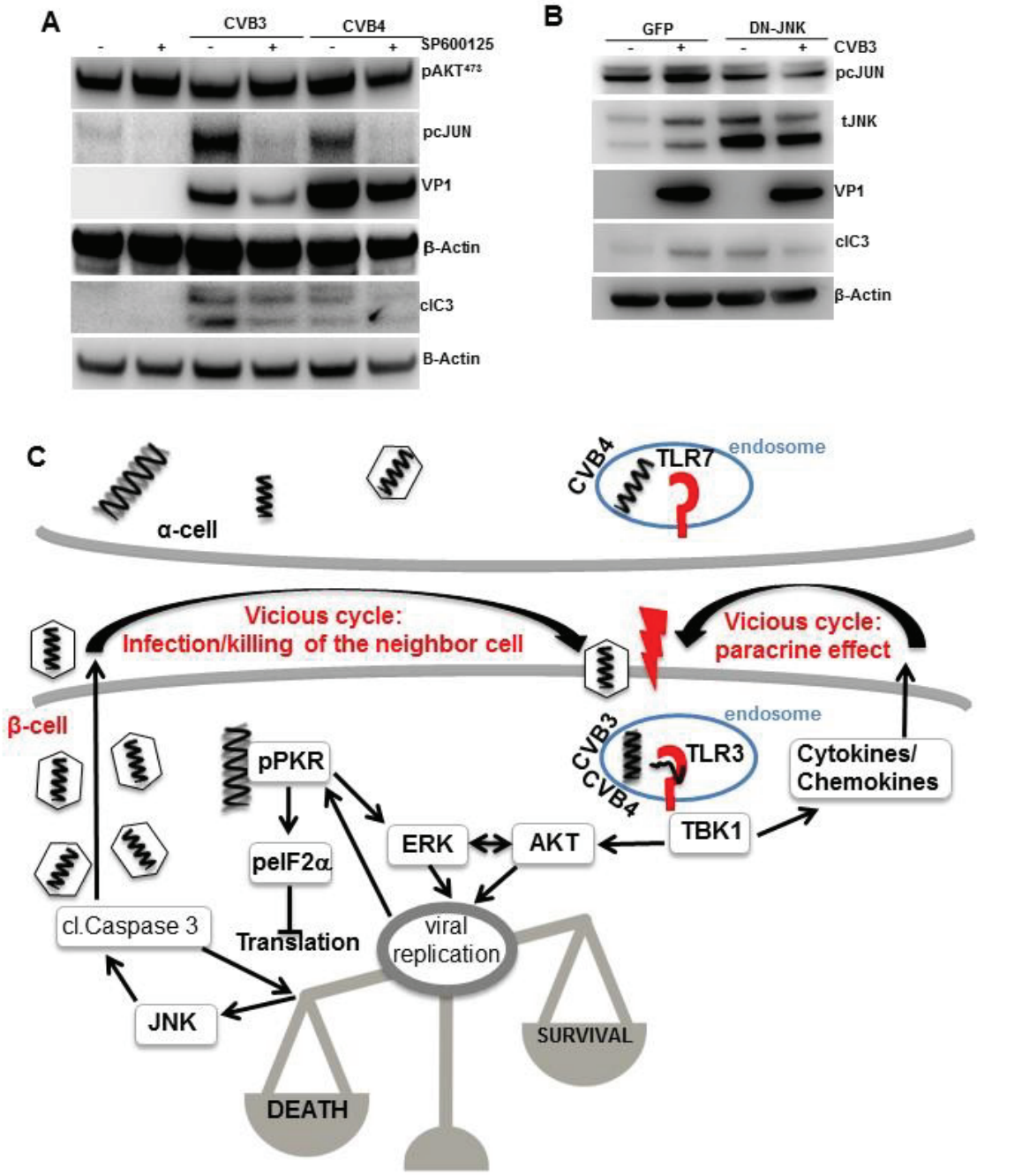
A
CVB3
CVB4
SP600125
pAKT473
pcJUN
VP1
β-Actin
cIC3
B-Actin
B
GFP
DN-JNK
CVB3
pcJUN
tJNK
VP1
cIC3
β-Actin
C
α-cell
CVB4
TLR7
endosome
Vicious cycle:
Infection/killing of the neighbor cell
Vicious cycle:
paracrine effect
β-cell
endosome
CVB3
CVB4
TLR3
Cytokines/
Chemokines
pPKR
peIF2α
ERK
AKT
TBK1
cl.Caspase 3
Translation
viral
replication
JNK
SURVIVAL
DEATH

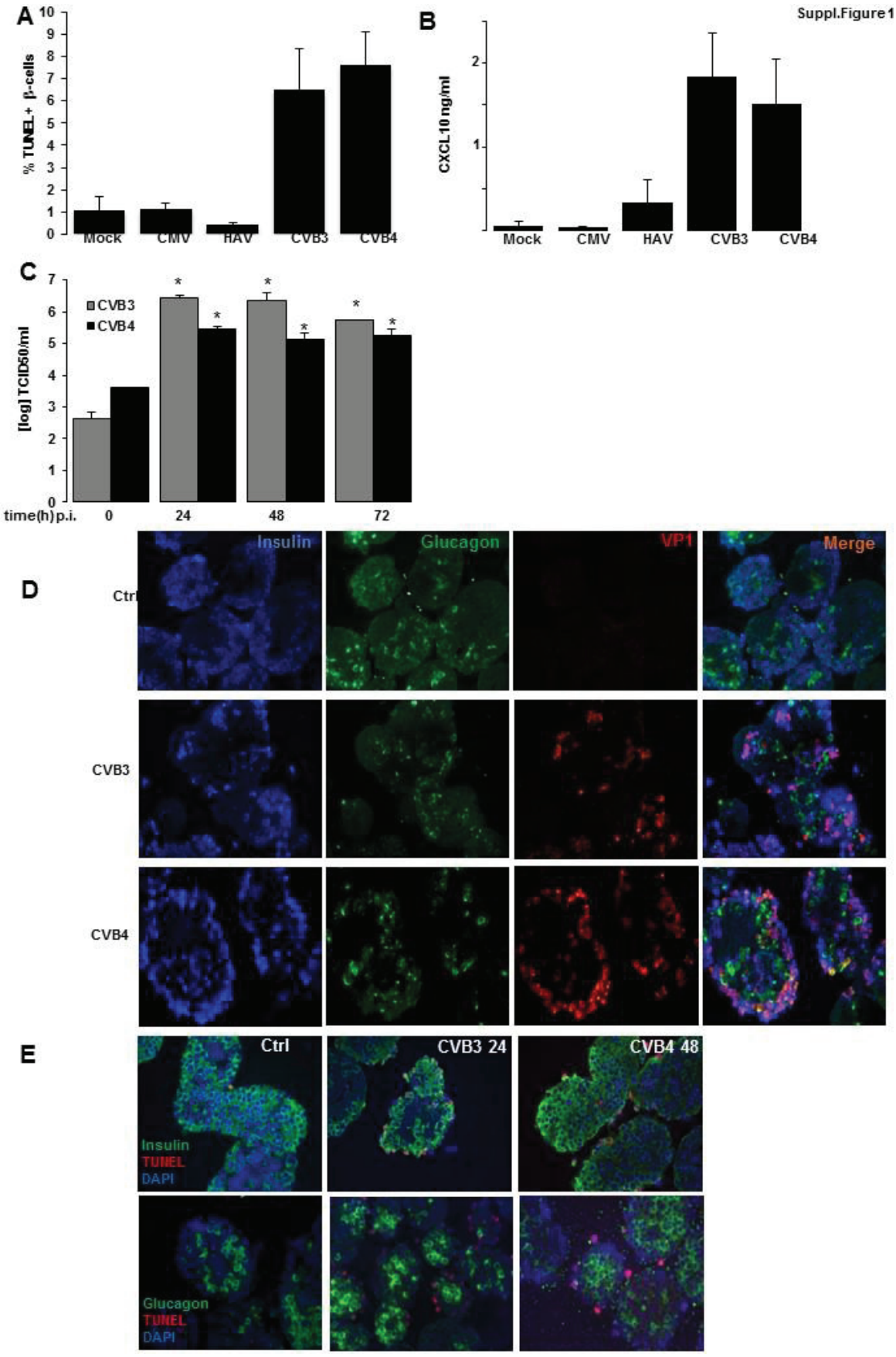
Suppl.Figure 1
A
% TUNEL+ β-cells
Mock
CMV
HAV
CVB3
CVB4
B
CXCL10 ng/ml
C
[log] TCID50/ml
CVB3
CVB4
time(h) p.i.
0
24
48
72
D
Insulin
Glucagon
VP1
Merge
Ctrl
CVB3
CVB4
E
Ctrl
CVB3 24
CVB4 48
Insulin
TUNEL
DAPI
Glucagon
TUNEL
DAPI

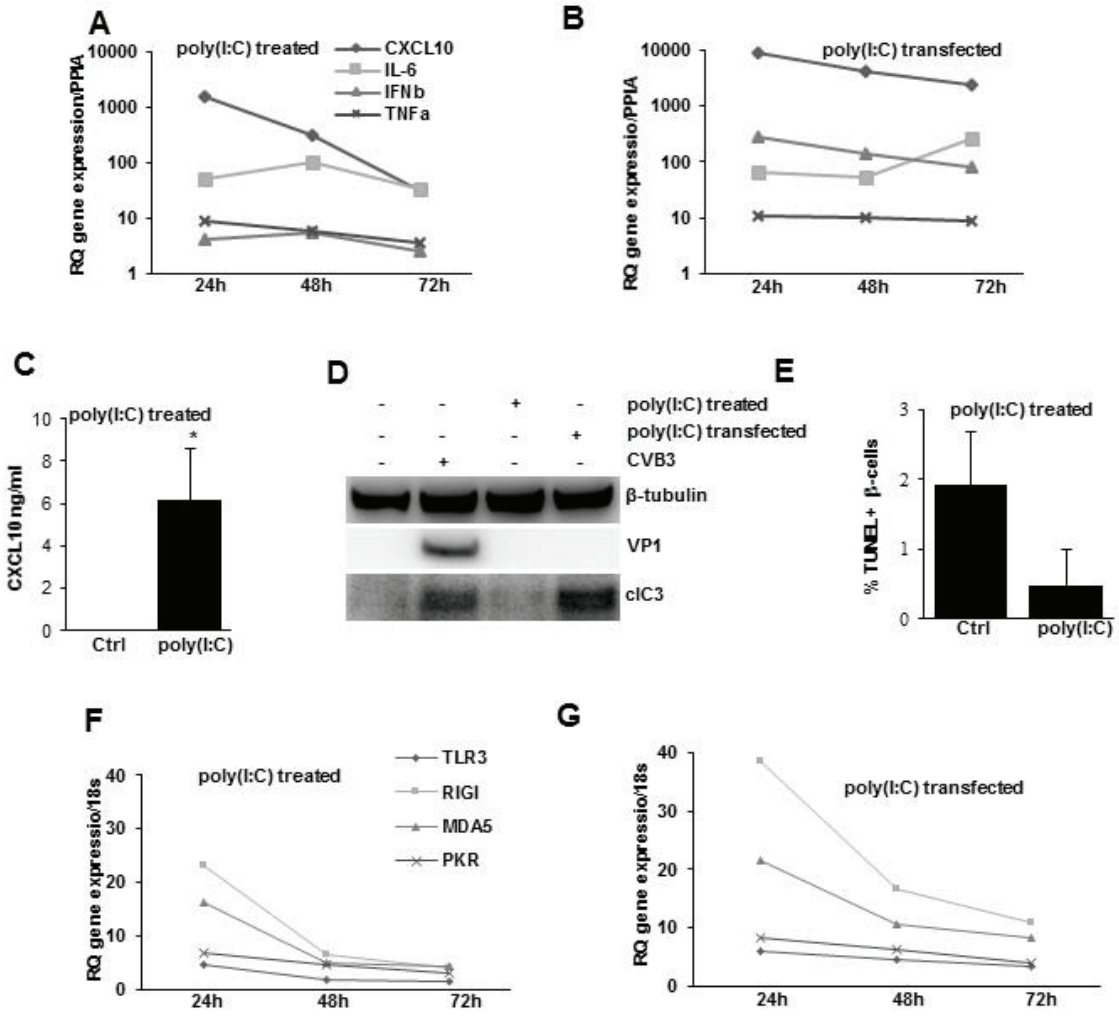
A
poly(I:C) treated
CXCL10
IL-6
IFNb
TNFa
RQ gene expression/PPIA
10000
1000
100
10
1
24h
48h
72h
B
poly(I:C) transfected
RQ gene expressio/PPIA
C
poly(I:C) treated
CXCL10 ng/ml
Ctrl
poly(I:C)
D
poly(I:C) treated
poly(I:C) transfected
CVB3
β-tubulin
VP1
cIC3
E
poly(I:C) treated
% TUNEL+ β-cells
F
poly(I:C) treated
TLR3
RIGI
MDA5
PKR
RQ gene expressio/18s
G
poly(I:C) transfected

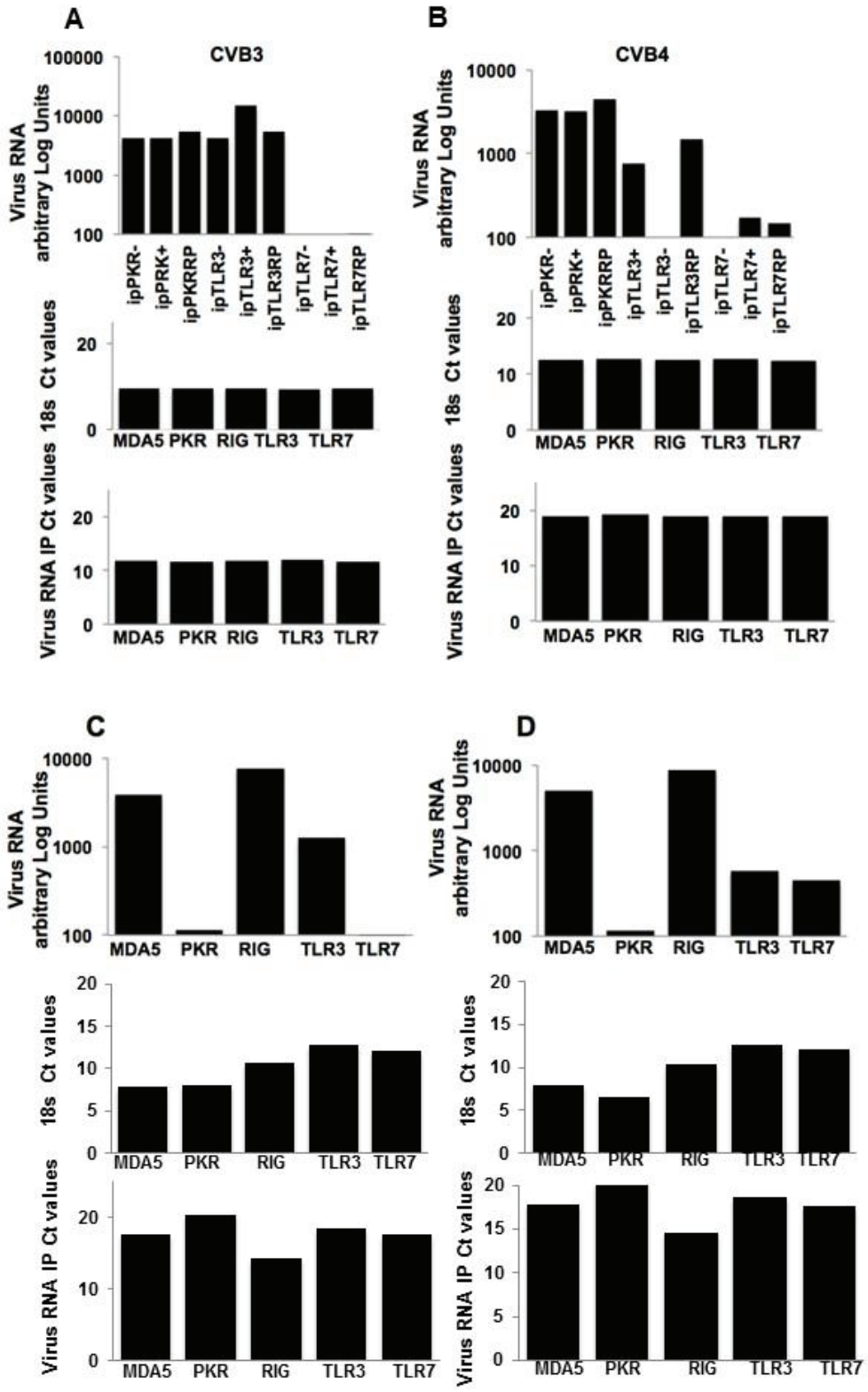
A
CVB3
Virus RNA arbitrary Log Units
100000
10000
1000
100
ipPKR-
ipPRK+
ipPKRRP
ipTLR3-
ipTLR3+
ipTLR3RP
ipTLR7-
ipTLR7+
ipTLR7RP
18s Ct values
20
0
MDA5 PKR RIG TLR3 TLR7
Virus RNA IP Ct values
20
10
0
MDA5 PKR RIG TLR3 TLR7
B
CVB4
Virus RNA arbitrary Log Units
10000
1000
100
ipPKR-
ipPRK+
ipPKRRP
ipTLR3+
ipTLR3-
ipTLR3RP
ipTLR7-
ipTLR7+
ipTLR7RP
18s Ct values
20
10
0
MDA5 PKR RIG TLR3 TLR7
Virus RNA IP Ct values
20
10
0
MDA5 PKR RIG TLR3 TLR7
C
Virus RNA arbitrary Log Units
10000
1000
100
MDA5 PKR RIG TLR3 TLR7
18s Ct values
20
15
10
5
0
MDA5 PKR RIG TLR3 TLR7
Virus RNA IP Ct values
20
10
0
MDA5 PKR RIG TLR3 TLR7
D
Virus RNA arbitrary Log Units
10000
1000
100
MDA5 PKR RIG TLR3 TLR7
18s Ct values
20
15
10
5
0
MDA5 PKR RIG TLR3 TLR7
Virus RNA IP Ct values
20
15
10
5
0
MDA5 PKR RIG TLR3 TLR7

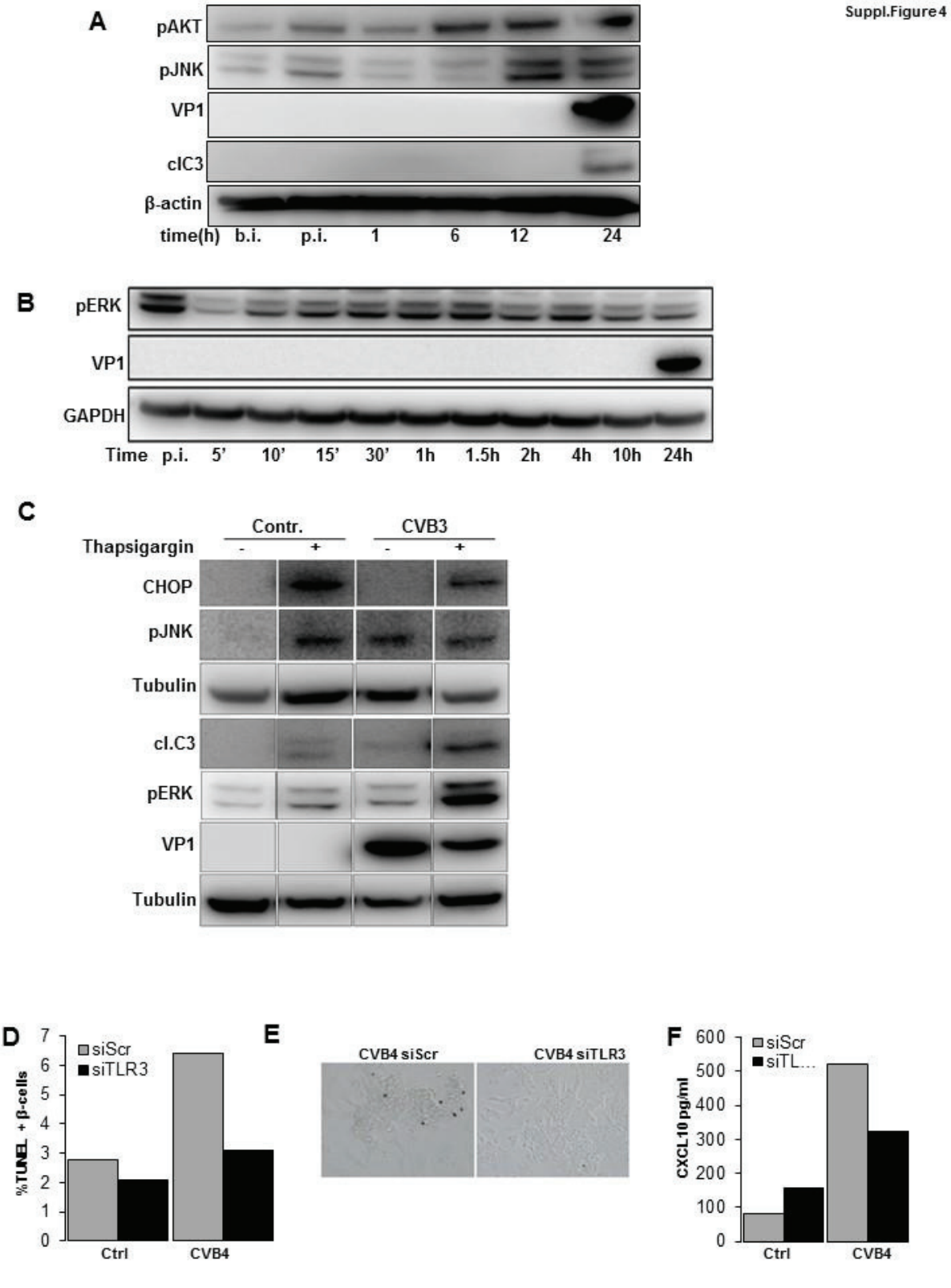
A
pAKT
pJNK
VP1
cIC3
β-actin
time(h) b.i. p.i. 1 6 12 24
B
pERK
VP1
GAPDH
Time p.i. 5' 10' 15' 30' 1h 1.5h 2h 4h 10h 24h
C
Contr.
CVB3
Thapsigargin - + - +
CHOP
pJNK
Tubulin
cl.C3
pERK
VP1
Tubulin
D
siScr
siTLR3
%TUNEL + β-cells
0 1 2 3 4 5 6 7
Ctrl
CVB4
E
CVB4 siScr
CVB4 siTLR3
F
siScr
siTL...
CXCL10 pg/ml
0 100 200 300 400 500 600
Ctrl
CVB4

3.2 Detection and localization of viral infection in the pancreas of patients with type 1 diabetes using short fluorescently-labelled oligonucleotide probes

N. Busse[1*], F. Paroni[1*], S.J. Richardson[2], J.E. Laiho[3], M. Oikarinen[3], G. Frisk[4], H. Hyöty[3, 5], Eelco de Koning[6], N.G. Morgan[2], K. Maedler[1,7]

[1]Islet Biology Laboratory, University of Bremen, Germany,
[2]Islet Biology Exeter (IBEx), University of Exeter Medical School, UK,
[3]Department of Virology, School of Medicine, University of Tampere, Tampere, Finland.
[4]Department of Immunology, Genetics and Pathology, Uppsala University, Sweden,
[5]Fimlab Laboratories, Pirkanmaa Hospital District, Tampere, Finland
[6]Leiden University Medical Center, Department of Nephrology, Leiden and University Medical Center Utrecht, Hubrecht Institute, Utrecht, The Netherlands
[7]German Center for Diabetes Research (DZD) project partner, University of Bremen, Bremen, Germany

[*]shared first authors

This manuscript is in minor revision at Oncotarget.

My contribution:

Designed and performed all experiments, analyzed data, wrote the paper.

Detection and localization of viral infection in the pancreas of patients with type 1 diabetes using short fluorescently-labelled oligonucleotide probes

N. Busse[1*], F. Paroni[1*], S.J. Richardson[2], J.E. Laiho[3], M. Oikarinen[3], G. Frisk[4], H. Hyöty[3, 5], Eelco de Koning[6], N.G. Morgan[2], K. Maedler[1]

[1]Islet Biology Laboratory, University of Bremen, Germany,
[2]Islet Biology Exeter (IBEx), University of Exeter Medical School, UK,
[3]Department of Virology, School of Medicine, University of Tampere, Tampere, Finland.
[4]Department of Immunology, Genetics and Pathology, Uppsala University, Sweden,
[5]Fimlab Laboratories, Pirkanmaa Hospital District, Tampere, Finland
[6]Leiden University Medical Center, Department of Nephrology, Leiden and University Medical Center Utrecht, Hubrecht Institute, Utrecht, The Netherlands

[*]shared first authors

Contact:
Federico Paroni, Ph.D. (federicoparoni@yahoo.it)
Kathrin Maedler, Ph.D. (kmaedler@uni-bremen.de)
Islet Biology Laboratory
Centre for Biomolecular Interactions Bremen, University of Bremen
Leobener Straße NW2, Room B2080, 28359 Bremen, Germany
phone: +49(421)218-63290

Keywords: enteroviruses, Type 1 Diabetes, pancreas, islets, oligonucleotide probes, FISH

Running title: Viral RNA in T1D

Authors´ contribution:
Designed and performed all experiments, analyzed data, wrote the paper: NB, FP
Supervised the project, wrote the paper: KM
Provided cell arrays, pancreas sections, evaluated and discussed results, edited the manuscript: SJR, GF, JEL, MO, HH, NGM

Abstract
Enteroviruses, specifically of the Coxsackie B virus family, have been implicated in triggering islet autoimmunity and type 1 diabetes, but their presence in pancreata of patients with diabetes has not been fully confirmed.
To detect the presence of very low copies of the virus genome in tissue samples from T1D patients, we designed a panel of fluorescently labeled oligonucleotide probes, each of 17-22 nucleotides in length with a unique sequence to specifically bind to the enteroviral genome of the picornaviridae family.
With these probes enteroviral RNA was detected with high sensitivity and specificity in infected cells and tissues, including in FFPE pancreas sections from patients with T1D. Detection was not impeded by variations in sample processing and storage thereby overcoming the potential limitations of fragmented RNA. Co-staining of small RNA probes in parallel with classical immunstaining enabled virus detection in a cell-specific manner and more sensitive than by viral protein.

Introduction
Type 1 diabetes (T1D) is a chronic multifaceted disorder that results from selective autoimmune-mediated destruction of the insulin producing β-cells. Environmental factors (1), together with genetic predisposition (2), interact cooperatively to initiate chronic islet autoimmunity (3).
Viruses have been proposed as possible initiators of islet autoimmunity and were first implicated as long ago as the nineteenth century although it was not until much later that a clear association was established between mumps and diabetes (4-6). Improvements in molecular biology subsequently broadened the panel of viruses which are implicated in causing diabetes (7, 8) and the weight of evidence now suggests that coxsackieviruses (9) play a role. In support of this, a clear correlation between enterovirus infection and the onset of T1D was revealed in association studies (10) and via a comprehensive meta-analysis (11).
Coxsackieviruses belong to the *Picornaviridiae*, and are small positive-sense single stranded RNA viruses, which have been shown recently to induce a persistent, slowly-replicating infection in both myocardium and pancreas. This may result from alteration to the viral genome during the progress of infection including the generation of naturally occurring 5'-deletions (12-14). Several direct (immunohistochemistry) and indirect (serology, isolation of viruses from patients) approaches have confirmed the presence of enterovirus both in the circulation and in the islets of T1D patients (15-20). Enteroviruses in the pancreas were detected by immunostaining for viral protein (VP1) (17, 21), which is highly expressed under acute viral infection and diminishes in persistent infection and may not be detected under circumstances where viral replication is compromised (22). Also, non-specific interaction of the VP1 antibody with other cellular proteins has been reported (23, 24).
A well-characterized cohort of human pancreatic donor tissue has been established by nPOD (Network for Pancreatic Organ Donors with Diabetes) and is available, similar

as other cohorts, in the majority as formalin fixed, paraffin embedded samples (FFPE) (25). This method ensures preservation of the samples for many years, but a limiting factor is the relatively poor RNA integrity often associated with FFPE preservation which means that analysis of tissue samples by PCR can be difficult (26). Also, detection of the viral genome in the pancreas has been challenging and more sensitive and reliable methods are required.

This has created pressure to develop alternative (accurate and equally sensitive) methods to allow the detection of RNA in single cells within FFPE tissue samples. An obvious candidate is *in situ* hybridization, where labeled oligonucleotide probes specifically pair with target nucleic acids via Watson-Crick base pairing and some success has been gained using long probes (~50-100nts) labeled with either radioisotopes or enzymes catalyzing chromogenic reactions The detection of coxsackievirus RNA in cardiac tissue by in situ hybridization. However, this approach also has limitations in the face of samples with poor RNA integrity or very low target RNA copy numbers. Thus, improved RNA FISH methods have been developed to overcome these hurdles. Enteroviral RNA was detected by a new generation of RNA probes (QuantiGene® ViewRNA Assay), which depend on signal amplification (25). This approach offers the advantage of signal amplification via the use of branched secondary probes but, theoretically, may be affected by several conditions. To create a docking site for the branched probes, two probes must sit adjacent to one-another on the target sequence, effectively lengthening the de facto short probes. However, RNA degradation can still affect the docking of probes and hence signal enhancement. Flexibility in choosing the binding site with the best thermodynamic characteristics may also be compromised.

Because of such limitations to the detection of enteroviruses with high accuracy and sensitivity, we present here an adapted method to target single RNA molecules with short (~20nts) fluorescently labeled oligonucleotides *in situ* that anneal to common regions of the RNA genome of members of the coxsackievirus family. Such short singly labeled oligo RNA probes are resistant to RNAse and RNA detection is less affected by target RNA degradation, making these probes more versatile while retaining sensitivity and specificity. Because their binding to the target sequences occurs independently for each probe, this gives probe combinations the advantage that there is a degree of freedom in their positioning without risk of the loss of stringency, efficiency or specificity.

To generate a distinct fluorescent signal above background noise, a sufficient amount of labeled probes must bind in close proximity (27-29), thereby ensuring high specificity and considerable flexibility of detection after hybridisation. The use of small contiguous RNA species also overcomes the potential limitation of fragmented target RNA. With our newly established protocol, we successfully detect viral RNA in both cell culture and FFPE tissue sections, in combination with classical immunostaining. Short probes were able to detect viral infection at lower viral loads than classical immunostaining and the method is comparable in sensitivity to that of semi-nested PCR (30).

Results

An established protocol for short RNA-oligoprobe labeling in FFPE tissue sections

In order to develop a robust protocol for RNA-oligoprobe labeling of FFPE pancreatic tissue sections, we initially tested a commercially available probe set targeting the housekeeping gene (GAPDH) in cultured HEK293 cells and in isolated FFPE human islets (Fig.1). Natural, as well as fixative-derived signal noise, is a major problem when employing fluorescence microscopy to detect probes targeting RNA molecules, especially when these are present in low abundance. Thus, while our test probes gave a very specific signal in cultured HEK293 cells (Fig.1A), probing of FFPE human islets generated high background noise both in the absence of probes (Fig.1B) and with the GAPDH probes (Fig.1C), when following the standard protocol. Reduction in the FFPE-derived background signal was achieved by the removal of any remaining paraffin wax crystals (see material and methods). This involved the use of a protocol in which xylene washes were undertaken at high temperatures prior to a step utilizing pepsin/HCl to separate proteins from nucleic acids. In addition, Sudan black was included to reduce the overall FFPE-derived background fluorescence.

Using this modified protocol, single positive dots (representing hybridization to as few as one RNA molecule) could be detected within the Abbe-diffraction limit and were easily discriminated from any residual background noise (Fig.1D).

RNA-oligonucleotide probe design and specificity

Probe set CVB_1 included a wide range of group B coxsackieviruses; it consisted of a mixture of 40 short oligonucleotides, each comprising 17-22 nucleotides covering the whole viral genome (see material and methods and Fig.2A). This enabled to target single RNA molecules. To detect a positive signal, it was determined that at least 17 of the probes must bind to their target sequence with only one mismatch allowed with respect to the stringency parameters [25].

To test the specificity of the probe set CVB_1, HEK293 cells were fixed and processed after either culture without viruses or following infection with coxsackieviruses CVB3 and CVB2 (Fig.2B) which share a sequence similarity of about 79%. Cells were infected for 2h at an MOI of 5 and the viruses allowed to replicate for 24h prior to fixation and analysis. Probes efficiently detected viral genomes within infected cells (Fig.2B, CVB3 and CVB2) whereas signal was absent from uninfected cells (Fig.2B, non-infected), confirming that the virus-specific probe set had no off-target effects.

The specificity of the probe set was further tested in HEK293 cells infected with cytomegalovirus (CMV), a DNA virus of the *herpesviridae* family (Fig.2B, CMV) or hepatitis A virus (HAV), a positive ssRNA virus of the *picornaviridae* family (Fig.2B, HAV). Following infection at an MOI of 5 and incubation for 4 days to ensure viral replication, there was no visible cytopathic effect. The presence of virus was confirmed by RT-PCR (Suppl.Fig.1A), although the CMV appeared not to be in an active phase of replication as no signal was generated by RT-PCR of DNAse-treated samples. In neither HAV nor CMV infected cells were probe-specific hybridization spots detected,

confirming the probe specificity. HAV shares partial sequence similarity with CVB3 (<45%) while CMV is a DNA virus; for each, the number of “on target” probes was below the detection limit of the assay.
The likelihood that the signals detected in samples were non-specific was further excluded by staining CVB3 infected islets in the absence of the probe set and by staining uninfected cells with the probe set. In each case, the negative controls delivered no staining, whereas virally infected cells yielded positive signals (Suppl.Fig.1B). RNAse A treatment abolished the signal from infected cells and confirmed that the probe set is specific to viral RNA (Suppl.Fig.1B).
We further tested the CVB_1 probe set on an array of cell lines previously generated for use with Quantigene® ViewRNA virus probes [21]. Green monkey kidney cells (GMK and Vero), the human cervix (HeLa), alveolar (A549) epithelial carcinomic and rhabdomyosarcoma (RD) muscle cells were infected with viruses from the enterovirus groups A and B or adenovirus (DNA virus) [21] (Table 1 and Suppl.Fig.2). In line with the results obtained with Quantigene® ViewRNA by Laiho et al. [21] the CVB_1 probe set yielded positive staining for viruses of both groups A and B, while it did not stain cells infected with adenovirus and human parechovirus 1 (HPeV1) (0/ 40 probes binding). Also, there was no binding to sequences from coxsackievirus A5 (11/40 probes theoretically match the virus sequence).

RNA-oligonucleotide probe sensitivity and consistency

Next, we evaluated sensitivity of the CVB_1 probe set. Our RNA-FISH system was compared with two of the most widely used and well established techniques for virus detection: RT-PCR and immunohistochemistry using an antibody against the viral capsid protein 1 (VP1). RT-PCR is the most powerful and specific tool for RNA detection; but RNA accessibility and degradation are two important limiting factors. To compare the sensitivity of the RNA probes with analysis by PCR, the pancreatic line CM9 (31) and HEK293 cells were infected with CVB3. Since both RT-PCR and RNA-FISH can, in principle, detect the presence of a single RNA molecule, we used successive 10-fold serial dilutions of virus prior to infect cells and to compare the sensitivity of the methods. Cells were plated in duplicates and the virus (CVB3; starting MOI of 100) was centrifugally inoculated at 16˚C for 1h to synchronize the infection. After inoculation, any unbound viruses were removed by washing and the cells incubated at 37˚C for an additional hour, to allow virus internalization and genome release from the capsid, before fixation or cell lysis for RNA extraction. Both RNA-FISH (Fig.3A,B and Suppl.Table1) and RT-PCR (Fig.3C and Suppl.Table2) were able to detect the presence of viral genomes, even at the highest dilution (10^{-8}) (Fig.3B,C). Using RNA-FISH probes, single RNA molecules were detected and a plateau reached at a dilution of 10^{-3} virus by both visual counting and RT-PCR (Fig.3B-C). The specificity of the RT-PCR results were confirmed by examination of dissociation curves, which were identical in all cases while samples from non-infected cells showed no signal (data not shown).

We next compared the efficiency of the CVB_1 probe set with the widely used VP1 (clone 5-D8/1, Dako cytomations) antibody, using a cell array of the human alveolar basal epithelial cell line A549 infected with CVB1 for 2, 4 and 6 h to generate a population representing different stages of infection [27]. After infection, cells were serially diluted with uninfected A549 cells to achieve a range from undiluted to 10^{-8}. The cells were then fixed and paraffin embedded. When employed at a dilution of 1:2000 (which ensures specificity and minimizes the possibility of false positives (23, 24)), the VP1 antibody yielded positive signals only at dilutions of 10^{-1} or lower, whereas the RNA-FISH probes were able to detect viral RNA even at the highest dilution of 10^{-8}, (Fig.3D,E).
The design of the RNA-FISH system should circumvent the problem of RNA degradation since it employs multiple probes to detect the target RNA. RNA fragmentation frequently occurs in, for example, autopsy samples, where processing and storage under RNAse free conditions is unlikely. We therefore tested FFPE CVB1-infected GMK cell sections, which had been infected and processed at the same time, but then cut and processed at different times (covering periods between 2012 and 2015) and stored at room temperature. The probes showed similar signals in all three samples regardless of the processing and storage time. Importantly, uninfected controls were negative (Suppl.Fig.3).

Coupling RNA-FISH and Immunohistochemistry

Important advantages of the use of RNA-FISH probes relate not only to their high sensitivity and specificity but also their ability to localize RNA molecules within specific cells of tissues such as the pancreas. We, therefore, investigated the localization and distribution of the signal emanating from the viral probes within the pancreas and compared this with detection by immunohistochemistry with the widely used VP1 antibody.
Fig.4A shows a schematic representation of the expected profile of virus-staining: RNA probes (red) are not expected to anneal to the viral RNA while it is packaged within the capsid. However, once released within the cell, the probes should bind. Conversely, the VP1 antibody (green) should always bind to the capsid surface or, conceivably, to free VP1 which has not been incorporated into capsids. To visualize any differential labeling, human CM9 cells were infected with centrifugally inoculated CVB3 at an MOI of 1000. (Fig.4B). Anti-VP1 was detected at the plasma membrane and in the cytoplasm while RNA probes were localized exclusively in the cytoplasmic area (Fig.4B, middle panel and Suppl.Fig.4 for enhanced signals). As depicted at larger magnification, signals from the RNA molecules co-localized, or were in close proximity with those arising from the capsid protein, but the two were not superimposed. To verify the staining patterns, we also performed VP1 immunohistochemistry prior to cell permeabilization and subsequent RNA-FISH, so that the signals should not co-localize. As shown in Fig.4B (right panel), under these conditions the signals arising from each method of detection were clearly separate. Uninfected CM9 cells were used as controls and showed no nonspecific signal for either anti-VP1 or the RNA-probes (Fig.4B).

Successful double staining of viral RNA and VP1 was confirmed in FFPE infected mouse spleen. Spleen sections from mice infected with CVB1 were stained with the CV_1 probe set to detect the viral genome and subsequently with anti-VP1 in an additional round of staining of the same section. Both techniques showed positive staining within the same regions of the samples (Suppl.Fig.5A).
Double staining of FFPE CVB3 infected cultured rat INS1-E cells for insulin and virus probes showed co-localization of viral RNA within insulin positive INS-1E cells (Fig.4E). Close proximity of viral RNA and insulin was also found in a Coxsackie infected neonatal mouse pancreas (Fig.4C), confirming the established double-staining protocol also in $HgCl_2$ fixed and paraffin embedded cells. To demonstrate efficacy for virus staining in various tissues, we stained a section from a coxsackie-infected neonatal heart and found cells displaying a strong signal corresponding to viral RNA (Suppl.Fig.5B).

Viral RNA localization in the pancreas in T1D

Having established the validity of our approach, we then used an enterovirus genome alignment (Suppl.Fig.6) to design two additional probe sets (CVB_2 and CVB_3; Suppl.Tables 4,5), which would complement the first set and allow detection of the entire range of group B enteroviruses. A scheme of the binding positions of the newly designed probe sets is shown in Fig.5A. We then used a combination of the three probe sets for a blinded analysis of autopsy pancreatic tissue recovered from nondiabetic and T1D patients having remaining residual β-cells from a UK cohort [31, 32]. As shown in table 2, we were able to detect the presence of enteroviruses in 7 of 8 pancreas samples from T1D patients and in 2 of 8 nondiabetic controls. While viral RNA was found within the insulin-positive islet area in 6 of 8 T1D patients (Table 2 and Fig.5B), 5 of 8 pancreata also yielded positive signals for enteroviral RNA in the exocrine area. A single T1D patient from the UK collection had viral RNA exclusively in the exocrine area of the pancreas and not in the islets (although in this patient, only 1 fragmented and 2 normal islets were found throughout the whole section). Similarly, this distribution of viral RNA was also observed in a patient with T1D from the nPOD cohort (Fig.5C). In one nondiabetic control, we also found viral RNA in islets. Comparison of our results with anti-VP1 staining on the same samples performed separately in Exeter, 66% concordance was achieved. Thus, while virus was detected using viral probes in 6 out of 8 T1D pancreata, VP1 staining was present in only 4/8 pancreata.

Discussion

In this study we present a robust method to identify and localize enteroviral RNA in FFPE tissue, which was established for the analysis of viral infection in pancreata from patients with T1D. The use of RNA probes allowed the discrimination of virally-encoded RNA from virus replication loci with high fidelity and sensitivity. Adapting a method from Raj et al. (28, 29), we created a set of short fluorescently labeled oligonucleotide probes that anneal to common regions of the coxsackievirus family *in situ* to target

single RNA molecules.
Probe sets are easily developed using the online Stellaris® RNA FISH Probe Designer. With three different sets of probes we were able to localize viral RNA in all tested tissue including FFPE tissues from patients with proven coxsackievirus infection and in the pancreas of 7 of 8 patients with T1D.
Use of our probe sets with the method described can be routinely applied for virus identification in the pancreas (and, in principle, in any other tissue). It should also now be possible, to increase the specificity of the probe sets for particular virus strains in order to specifically characterize the infection of pancreatic islets in patients with T1D. This is a major undertaking, but is possible using the well-preserved and -characterized FFPE tissues available within the nPOD initiative.
Although enteroviruses (including members of the Coxsackie B virus/ CVB family), have been suspected as potential triggers of T1D for a long time, firm evidence of viral genome expression in the pancreas has been largely elusive.
Most evidence supporting a causative role for enteroviral infections in diabetes onset have come from epidemiological studies (4-6, 11) or from the identification of viral antigens in fixed pancreatic tissue (32, 33). By contrast, there have been few successful attempts to detect viral genome, except in isolated islet samples or in a small number of samples where positive signals were seen by in situ hybridisation.
For long time the approach to identify the disease's trigger has been based on the four Koch's postulates (34), which were formulated only considering acute infection but are unfitted when the infection has been encountered long before manifestation of the disease. From tail biopsies of living newly diagnosed T1D patients of the DiViD study (3-9 weeks after T1D onset), VP1 was detected in the pancreas in all patients in 1.7% of the islets. This 100% association of VP1 and T1D could lay in the VP1 characteristics, which is highly expressed at acute viral infection and diminishes in persistent infection (17). Indirect evidence has been provided to confirm islet cell enteroviral infection by the demonstration of human leukocyte antigen (HLA) class I expression in all patients. In contrast to HLA class I and VP1, viral genome was found in less; 4 of 6 patients at very low concentrations (by PCR, >40 cycles). Although this was a very small study, it was the first showing full correlation of viral RNA by at least one method (17) and convinces that a pancreatic enterovirus infection occurs before or at the time of T1D onset and may be causative for β-cell destruction.

Several hypotheses have been proposed to explain why the viral genome has proven so difficult to detect in the islets of patients with T1D (1): (i) viral infection could act as an initial trigger to activate autoimmunity but the infection may not sustain for long periods; one or multiple viruses can act in concert or in waves leading slowly to β-cell failure. (ii) The virus genome may be modified such that it becomes persistent with very low copy numbers present in infected cells being then difficult to detect (1). In this context, coxsackieviruses have been shown to establish persistent infections in human heart (22) and in the mouse pancreas (35) via a process involving deletion of the 5'-UTR of the viral genome (14), viruses would be undetected by classical PCR/VP1 staining approaches. Whether this happens in human pancreas has been

yet not verified.
In the present work, we have overcome these difficulties by deploying our highly sensitive FISH method to provide firm evidence that enteroviral genome can be detected more frequently in the pancreas of patients with T1D than in equivalent controls.
The technique applied in this study combines the advantages associated with access to FFPE samples (which retain tissue morphology and allow precise localization of cellular and tissue structures) with a highly sensitive detection method. The sensitivity of detection was much greater than that achieved with classical immunohistochemistry to detect the viral capsid protein, VP1, implying that it is ideal for use in circumstances where viral replication may be compromised (35).
To verify these conclusions, we compared directly results obtained by RNA-FISH with those employing a widely used anti-VP1 (clone 5-D8/1) antibody in infected FFPE material. We carefully established optimized conditions for specific virus detection to avoid interactions of VP1 antibody with other cellular proteins. As a result, we were able to identify viral RNA with much greater sensitivity such that a single RNA molecule was labelled. The use of other sensitive techniques, which might match the sensitivity achieved here (such as PCR, either direct or nested), is limited because of the low accessibility and stability of nucleic acids (26). By contrast, improvements in *in situ* hybridization (ISH) and fluorescent *in situ* hybridization (FISH) have increased both the sensitivity and specificity of RNA detection such that they now represent a valid alternative to PCR, with the advantage that they can spatially localize particular RNA molecules within fixed cells (25).
The unique advantage of the small contiguous probe sets presented in this study is that RNA duplexes are detected via microscopy, because of direct conjugation of fluorophores to the probe (29). In order to obtain a detectable signal, multiple probes must then bind to their target RNA to allow the close apposition of sufficient fluorophores for detection under the microscope. A key advantage of this approach is that the potential “off-target” binding of a few oligonucleotides from the probe pool will be either undetectable or where it is detected, can be readily distinguished from the much brighter spots that correspond to the true targets. A minimum of 17 out of 40 probes must bind in order to generate a specific signal in accordance with the Abbe diffraction limit (29).
A significant problem in fluorescence microscopy can be a high background signal, generated either intrinsically from cellular molecules or induced by the fixatives (36, 37). This high background often precludes accurate analysis of immunostained pancreatic islets in FFPE tissue and is also enhanced by their high auto-fluorescence (38). The interference from natural fluorescence relates to the tissue type and is due to the presence of endogenous molecules such as flavins, lipofuscins, reticulins, reduced NADP(H), collagen, elastin (36). Pancreatic tissue has low accretion of flavins and lipofuscins (37), yet the fixatives used to preserve tissue morphology could increase signal background. FFPE samples are highly susceptible to this because of wax crystals and formaldehyde forming covalent bonds with adjacent amino-groups

via through Schiff reactions. This can result in an intense fluorescent background with a typical emission between 450 and 650 nm (36, 37). Here, we refined the de-waxing and hybridization conditions to decrease the background fluorescence and to enhance signal detection.

Of note, our modified deparaffinization/ hybridization protocol had no effect on either tissue morphology or the signal intensity at different wavelengths as shown, for example, by the strongly retained DAPI staining.

Despite the labour-intensive pre-hybridisation protocol employed to ensure background signal reduction, the use of small contiguous RNA-labelled oligonucleotide probes offers several advantages when compared to either classical FISH (using long probes of >100nt) or indirect FISH that relies on intense signal amplification. Firstly, the strength of the bonds between the probe and the target is influenced by various factors such as formamide, salt concentration, temperature and pH. All these factors are easier to control for short than for long sequences. Secondly, systems which use branched probes for signal amplification may be more influenced by RNA degradation, because of the reduced freedom in positioning and flexibility that is allowed for the docking of two consecutive probes.

Sensitivity and specificity of our probe set was tested on different virus strains as well as on various embedding procedures and was compared with indirect FISH on a set of previously analysed samples (25) as well as on newly prepared samples (30). Our viral probes showed a sensitivity comparable to that of PCR analysis of cell lines when tested in infected cell lines.

Probe specificity was further tested in cell culture conditions and on a cell array (25). We were able to successfully detect all the viruses with a probe-sequence homology of greater than 60%. From the alignment of our CVB_1 set probes with CVA5 and HPeV1, only 11/40 and 0/40 oligos showed a perfect match and, as expected, these viruses were not detectable by our probe set.

As mentioned above, with the use of small contiguous RNA probes we were able to overcome the issue of RNA stability/degradation in samples, which had been stored over long periods of time. In particular, no signal loss occurred in samples processed at various points over a time course of 3 years.

To test the utility of our probes in archive pancreatic tissue we undertook a blinded evaluation of T1D pancreata from a UK (39, 40) cohort, and expanded our CVB_1 probe set with the addition of 2 complementary sets, namely CVB_2 and CVB_3. This broadened the opportunity to detect enteroviruses across the entire group B when used in combination. By this approach, we detected viral RNA in 7 of 8 T1D pancreata; 6 of which had also given positive signals using immunohistochemical analysis of VP1 expression.

Among the group of 7 RNA positive individuals, 6 had viral RNA in insulin-containing cells whereas only 4 were also immune-positive for VP1 (the parameter used to define “T1D VP1+” in this concordance study). The two pancreata which were negative for viral RNA within islets using FISH probes were also immunonegative for enteroviral VP1. Typically, 1-2 islets per section showed viral genome staining but, unlike

immunoreactive VP1, enteroviral RNA was not restricted solely to insulin positive cells. Viral RNA was detected in two young non-diabetic control pancreata, but at a much lower prevalence than among patients with T1D. Thus, enteroviral infection may not be absolutely unique to the islets of patients with T1D and it remains possible that cellular response to viral infection (rather than infection per se) is a critical determinant of autoimmunity.

In conclusion, we have developed a stringent and highly specific method for the detection of enteroviral genome in fixed pancreatic tissue with high sensitivity. We have used this method to confirm that viral RNA is detected in the pancreas in 7 of 8 patients with T1D and in only 2 of 8 controls. We propose that this new method may find wide applicability in future studies of the viral aetiology of type 1 diabetes.

Materials and Methods

Cell culture and Viruses

Human islets were isolated and cultured as previously described (41), HEK 293 and FHRK-4 were cultured in Dulbecco's Modified Eagle's Medium (DMEM) at 5.5 mM glucose, CM9 and INS-1E in RPMI-1640 (Lonza) at 11.1 mM glucose. All media were supplemented with 1% penicillin/streptomycin and 10% fetal calve serum (FCS) or 1% FCS (FHRK-4). All cellular experiments were performed at 37°C and 5% CO_2, if not stated otherwise.

All viruses were propagated in FHRK-4 cells and purified in a sucrose gradient (40% sucrose, 10mM Tris pH 7,5, 100mM NaCl and 1mM EDTA), aliquots were stored at -80°C as previously described (42). Cells were grown to confluency of 80-90% and infected with multiplicity of infection (MOI) of 5 supplemented growth media without FCS. Virus-containing media was replaced with 1% FCS fresh media after 2h of infection (post-infection).

Probe design

Premade Stellaris® FISH Probes recognizing human GAPDH labeled with Quasar 570 (Catalog #SMF-2026-1-BS) and custom Stellaris® FISH Probes, each recognizing various enteroviral strains, labeled with Quasar 570 were purchased from Biosearch Technologies, Inc. (Petaluma, CA). Briefly, the initial set of custom RNA FISH oligonucleotides (CVB_1) was designed based on CVB3 consensus based sequence (M33854.1). The consensus sequence was generated from a ClustalW alignment of several coxsackieviruses to localize conserved regions, with thermodynamic characteristics fitted to the probe design [26]; in total, 50 regions of about 20 nucleotides (nts) in length with 2 nucleotides gap between adjacent regions and 45% GC content. Suitability of the regions for probe design were then verified using the Stellaris® RNA FISH Probe Designer (Biosearch Technologies, Inc., Petaluma, CA) available online at www.biosearchtech.com/stellarisdesigner. As result, 40 probes (Fig.S4) distributed throughout the whole target genome were generated. For the CVB_2 and _3 probe sets design, 106 genome sequences of viruses belonging to the enterovirus group B family were aligned (Fig.S6) and divided into three subgroups based on sequence similarities. For each subgroup probes were designed based on

newly generated consensus sequences as described before [26]. From the pool, 35 and 36 oligo probes were selected as CVB_2 and -3 pool for a sequential combinatorial approach to detect all the members of the enterovirus group B.

RNA FISH in FFPE tissue samples

The pre- and post-hybridization protocol for RNA fluorescent in situ hybridization (FISH) was modified based on the manufacturer's instructions available online at www.biosearchtech.com/stellarisprotocols (version 11.04.2013).

We adapted the pre-hybridization procedure by increasing the temperature of the xylene bath, in order to also access older FFPE tissue libraries (40). The melting temperature for low-melting point paraffin is around 52°C and for normal paraffin is around 65-70°C (43, 44). Melted paraffin can remain on the section forming wax crystals at lower temperatures (~57°C). Residual paraffin particles and wax crystals from the embedding procedure were removed by a series of Xylene washes (20 min at 70°C; 10 min at 70°C; 10 min at room temperature), followed by rehydration in an ethanol (EtOH) gradient (100%, 100% and 95%) for 10 min each and for 1 h in 70% EtOH at room temperature. Finally, sections were rinsed twice with H_2O for 1 min. All steps were performed with constant steering.

Slides fixed with $HgCl_2$ where washed with iodine to remove mercury, before the deparaffinization protocol. To facilitate probe annealing, sections were incubated for 20 min in 0.2M HCl (room temperature) and washed with 2x SSC Buffer (15 min, 70°C, slightly shaking) and PBS (2x 1 min, room temperature). Pepsin (Sigma) was applied and washed off after 10 min incubation at 37°C with PBS (2 times 1 min, room temperature). To quench any remaining autofluorescence of biological molecules 0.5-1% Sudan Black (Sigma-Aldrich) in 70% EtOH was added for 20 min (room temperature) and thoroughly washed off with PBS (3x times 5 min, room temperature). Tissues were equilibrated with washing buffer (10% formamide, 2xSSC, 2x, 5 min at room temperature) before hybridization. Stellaris® FISH Probes (GAPDH 0,125 μM; viral RNA 0,25 μM) were diluted in hybridization buffer (10% w/v Dextran sulfate, 10% formamide, 2xSSC) and samples incubated overnight at 37°C in a humidified chamber. Hybridization mix was aspirated and sections were washed extensively. Stringency was increased with each washing step to remove any unspecific probe binding, thus reducing background noise and increasing relative signal intensity. Slides were washed at 37°C with constant agitation; twice with 2xSSC and 10% formamide for 20 min, twice with 2xSSC for 15 min, twice with 1xSSC for 15 min, once with 0.1x SCC for 15 min and 5 min. VECTASHIELD® antifade mounting medium (Vector laboratories) including 4',6-Diamidin-2-phenylindol (DAPI) was immediately added and images were acquired with a Nikon Ti MEA53200 (NIKON GmbH, Düsseldorf, Germany) microscope. A 60x oil-immersion objective (N.A. 1,4). TRITC filter (ex. 520-560nm) was used to acquire images of the Quasar 570 labeled probes. Control images were always taken with the FITC filter (ex. 465- 495nm) at the same exposure time to ensure no false-positive signals caused by a bleed-through from one channel to another. NIS-Elements BR (NIKON GmbH, Düsseldorf, Germany) and ImageJ (NIH, USA) were used for image analysis.

RNA FISH in cell lines

Cells were cultivated on 13x13 mm #1 microscope cover glasses (Marienfeld GmbH & Co. KG, Lauda-Königshofen, Germany) in 24-well plates till a confluency of 80-90% and treated as indicated. Further processing followed manufacturer's instructions available online at www.biosearchtech.com/stellarisprotocols (11.04.2013). Briefly, cover glasses were rinsed with PBS and cells were fixed (3,7% formaldehyde, 1x PBS) for 10 min at room temperature, followed by two washes with PBS (room temperature). To permeabilize the cellular membrane 70% EtOH was added for overnight incubation at 4°C. EtOH was removed, cells were equilibrated with washing Buffer (5 min, room temperature) and respective RNA FISH probe mix was added for overnight hybridization at 37°C in a humidified chamber. Hybridization mix was aspirated; cells were washed twice with washing buffer (20 min, 37°C) and rinsed with 2xSSC (room temperature). Cover glasses were placed on glass slides with VECTASHIELD® antifade mounting medium (Vector laboratories) including DAPI and analyzed as described above.

Immunohistochemistry

FFPE sections were deparaffinized as described above. Antigen retrieval was performed in heated unmasking solution (Vector laboratories) in three consecutive 5 min microwave cycles (full power). Sections were blocked (TBS, 3% BSA IgG free, 0.2% Tween) for 1h at room temperature and primary anti-VP1 (DAKO, clone 5-D8/1, dilution 1/2000) was applied for over night incubation at 4°C. FITC anti-mouse (1/100) for 1h at room temperature was used as secondary antibody.

Co-immunostaining of insulin and RNA-FISH

Samples were first probed for RNA targets and analyzed as described above. Afterwards, the coverslip was gently removed, slides were immersed in washing buffer and anti-insulin (DAKO) was applied for overnight incubation at 4°C. Sections were washed three times with washing buffer (5 min, room temperature), incubated for 1h at room temperature with fluorescein isothiocyanate (FITC) anti-guinea pig, were washed 3x with 2xSSC (5 min, room temperature) and mounted with VECTASHIELD® antifade mounting medium (Vector laboratories) including DAPI.

Co-immunostaining of VP1 and RNA-FISH

Cells were infected with CVB3 (MOI 1000) for 1h (16°C). Media was changed and temperature shifted to 37°C. Cells were fixed 30 min post-infection using a solution of 3,7% formaldehyde in 1x PBS for 10 min. Cells were permeabilized with 70% EtOH overnight at 4°C and probed with RNA probes as described above. Cells were washed and stained for VP1 (1/2000; 1h; RT) and FITC anti-mouse as secondary antibody.

RNA isolation, reverse transcription and real time PCR

RNA was extracted using Trizol® reagent (Invitrogen, Darmstadt, Germany) according to manufacturer's protocol. Extracted RNA was treated with DNAse I (Ferments Life Science, Waltham, MA, USA) and reverse transcribed with ReverseAid kit (Fermentas) according to manufacturer's instructions. Real time PCRs reactions were prepared according to Applied Biosystems guidelines using SybrGreen assay and performed in a StepOnePlus instrument (Applied Biosystems, Carlsbad, CA, USA). PCR efficiencies

were monitored for each sample according to a previously described approach [42]. Results are presented as relative quantification. SybrGreen Primers used:
CVB fw 5' GGCCCCTGAATGCGGCTAAT 3',
CVB rev 5' TGGCTGCTTATGGTGACAATTG 3';
Microglobulin β2 fw 5´TTTACTCACGTCATCCAGCAG A 3';
Microglobulin β2 rev 5´CGGCAGGCATACTCATCTTT 3'.

RNAse treatment

CVB3 infected FFPE human islets sections were prepared as described above. To digest any viral or endogenous RNA 100μg/ml RNAse A (Macherey-Nagel) in 2xSSC buffer or 2xSSC Buffer alone was applied to the sections for 1h at 37°C. At this salt-concentration (150mM NaCl) single-stranded, as well as double-stranded RNA, is enzymatically cleaved by RNase A (45).

Viral dilution and FISH analysis

CVB 3 was diluted in RPMI-1640 media in logarithmic steps, starting from 10^2 (MOI 100) to 10^-8. Infection media was added to respective cells in a 24-well plate either grown on coverslips or without. Cells were directly transferred to a tabletop centrifuge and spun for 1h at 16°C and 105 rcf., followed by 1.5h (HEK 293) or 3h (CM9) post-infection at 37°C. Afterwards one set of cells was used for RNA isolation and the other for microscopical analysis. Ten images were acquired for each condition, choosing the same areas of the slide for every dilution.

Acknowledgements

We would like to thank Katrischa Hennekens (Uni Bremen) for excellent technical assistance. Human islets were provided through the JDRF award 31-2008-416 (ECIT Islet for Basic Research program). We are grateful to our collaborators for providing the cell lines and viruses for this study; HEK293 and FHRK-4 cells and all viruses (cytomegalovirus (CMV), hepatitis-A-Virus (HAV), coxsackievirus B3 (Nancy) and B2 were kindly provided by Dr. Andreas Dotzauer, Institute for Virology, University of Bremen, Germany. CM9 cells were kindly provided by Dr. Paolo Pozzilli, Barts and the London School of Medicine, Queen Mary, University of London, UK. INS-1E cells were kindly provided by Dr. Claes Wollheim, Universities of Geneva, Switzerland and Lund, Sweden.

Financial support

This study was supported by nPOD and JDRF. The funders had no role in study design, data collection and analysis, decision to publish, or preparation of the manuscript.

Competing interests

The authors declare no competing interest

References

1. Rodriguez-Calvo T, von Herrath MG. Enterovirus infection and type 1 diabetes: closing in on a link? Diabetes. 2015;64(5):1503-5.
2. Pociot F, Lernmark A. Genetic risk factors for type 1 diabetes. Lancet. 2016;387(10035):2331-9.
3. Redondo MJ, Jeffrey J, Fain PR, Eisenbarth GS, Orban T. Concordance for islet autoimmunity among monozygotic twins. N Engl J Med. 2008;359(26):2849-50.
4. Harris HF. A Case of Diabetes Mellitus Quickly Following Mumps. . N Engl J Med 1899;140(140):465–9.
5. Patrick A. Acute Diabetes Following Mumps. Br Med J. 1924;2(3331):802.
6. Gundersen E. Is diabetes of infectious origin? . Journal of Infectious Diseases 1927;41:197–202.
7. Gamble DR, Taylor KW. Seasonal incidence of diabetes mellitus. Br Med J. 1969;3(5671):631-3.
8. Clements GB, Galbraith DN, Taylor KW. Coxsackie B virus infection and onset of childhood diabetes. Lancet. 1995;346(8969):221-3.
9. Coppieters KT, Boettler T, von Herrath M. Virus infections in type 1 diabetes. Cold Spring Harb Perspect Med. 2012;2(1):a007682.
10. Beyerlein A, Donnachie E, Jergens S, Ziegler AG. Infections in Early Life and Development of Type 1 Diabetes. Jama. 2016;315(17):1899-901.
11. Yeung WC, Rawlinson WD, Craig ME. Enterovirus infection and type 1 diabetes mellitus: systematic review and meta-analysis of observational molecular studies. BMJ. 2011;342:d35.
12. Hober D, Sane F. Enteroviruses and type 1 diabetes. BMJ. 2011;342:c7072.
13. Sane F, Caloone D, Gmyr V, Engelmann I, Belaich S, Kerr-Conte J, et al. Coxsackievirus B4 can infect human pancreas ductal cells and persist in ductal-like cell cultures which results in inhibition of Pdx1 expression and disturbed formation of islet-like cell aggregates. Cell Mol Life Sci. 2013;70(21):4169-80.
14. Tracy S, Smithee S, Alhazmi A, Chapman N. Coxsackievirus can persist in murine pancreas by deletion of 5' terminal genomic sequences. J Med Virol. 2015;87(2):240-7.
15. Richardson SJ, Leete P, Bone AJ, Foulis AK, Morgan NG. Expression of the enteroviral capsid protein VP1 in the islet cells of patients with type 1 diabetes is associated with induction of protein kinase R and downregulation of Mcl-1. Diabetologia. 2013;56(1):185-93.
16. Oikarinen S, Tauriainen S, Hober D, Lucas B, Vazeou A, Sioofy-Khojine A, et al. Virus antibody survey in different European populations indicates risk association between coxsackievirus B1 and type 1 diabetes. Diabetes. 2014;63(2):655-62.
17. Krogvold L, Edwin B, Buanes T, Frisk G, Skog O, Anagandula M, et al. Detection of a low-grade enteroviral infection in the islets of langerhans of living patients newly diagnosed with type 1 diabetes. Diabetes. 2015;64(5):1682-7.
18. Dezayee ZM. The status of serum gamma-interferonand antiviral antibodies in patients with type I and type 2 diabetes: A comparative study. J Res Med Sci. 2012;17(9):855-8.
19. Alberti AM, Amato C, Candela A, Costantino F, Grandolfo ME, Lombardi F, et al. Serum antibodies against Coxsackie B1-6 viruses in type 1 diabetics. Acta Diabetol Lat. 1985;22(1):33-8.
20. Oikarinen S, Martiskainen M, Tauriainen S, Huhtala H, Ilonen J, Veijola R, et al. Enterovirus RNA in blood is linked to the development of type 1 diabetes. Diabetes. 2011;60(1):276-9.
21. Richardson SJ, Willcox A, Bone AJ, Foulis AK, Morgan NG. The prevalence of enteroviral capsid protein vp1 immunostaining in pancreatic islets in human type 1 diabetes. Diabetologia. 2009;52(6):1143-51.
22. Klingel K, Hohenadl C, Canu A, Albrecht M, Seemann M, Mall G, et al. Ongoing enterovirus-induced myocarditis is associated with persistent heart muscle infection: quantitative analysis of virus replication, tissue damage, and inflammation. Proc Natl Acad Sci U S A. 1992;89(1):314-8.

23. Richardson SJ, Leete P, Dhayal S, Russell MA, Oikarinen M, Laiho JE, et al. Evaluation of the fidelity of immunolabelling obtained with clone 5D8/1, a monoclonal antibody directed against the enteroviral capsid protein, VP1, in human pancreas. Diabetologia. 2014;57(2):392-401.
24. Hansson SF, Korsgren S, Ponten F, Korsgren O. Enteroviruses and the pathogenesis of type 1 diabetes revisited: cross-reactivity of enterovirus capsid protein (VP1) antibodies with human mitochondrial proteins. J Pathol. 2013;229(5):719-28.
25. Laiho JE, Oikarinen S, Oikarinen M, Larsson PG, Stone VM, Hober D, et al. Application of bioinformatics in probe design enables detection of enteroviruses on different taxonomic levels by advanced in situ hybridization technology. J Clin Virol. 2015;69:165-71.
26. Skog O, Ingvast S, Korsgren O. Evaluation of RT-PCR and immunohistochemistry as tools for detection of enterovirus in the human pancreas and islets of Langerhans. J Clin Virol. 2014;61(2):242-7.
27. Femino AM, Fay FS, Fogarty K, Singer RH. Visualization of single RNA transcripts in situ. Science. 1998;280(5363):585-90.
28. Raj A, Tyagi S. Detection of individual endogenous RNA transcripts in situ using multiple singly labeled probes. Methods Enzymol. 2010;472:365-86.
29. Raj A, van den Bogaard P, Rifkin SA, van Oudenaarden A, Tyagi S. Imaging individual mRNA molecules using multiple singly labeled probes. Nat Methods. 2008;5(10):877-9.
30. Laiho JE, Oikarinen M, Richardson SJ, Frisk G, Nyalwidhe J, Burch TC, et al. Relative sensitivity of immunohistochemistry, multiple reaction monitoring mass spectrometry, in situ hybridization and PCR to detect Coxsackievirus B1 in A549 cells. J Clin Virol. 2016;77:21-8.
31. Gragnoli C. The CM cell line derived from liver metastasis of malignant human insulinoma is not a valid beta cell model for in vitro studies. Journal of cellular physiology. 2008;216(2):569-70.
32. Dotta F, Galleri L, Sebastiani G, Vendrame F. Virus Infections: Lessons from Pancreas Histology. Curr Diabetes Rep. 2010;10(5):357-61.
33. Morgan NG, Richardson SJ. Enteroviruses as causative agents in type 1 diabetes: loose ends or lost cause? Trends Endocrinol Metab. 2014;25(12):611-9.
34. KOCH R. Ueber bakteriologische Forschung. . Verhandlungen des X Internationalen Medichinischen Congresses, Berlin 1890, August Hirshwald, Berlin, Germany, 10th International Congress of Medicine, Berlin, Germany 1. 1891.
35. Chapman NM, Kim KS. Persistent coxsackievirus infection: enterovirus persistence in chronic myocarditis and dilated cardiomyopathy. Curr Top Microbiol Immunol. 2008;323:275-92.
36. Viegas MS, Martins TC, Seco F, do Carmo A. An improved and cost-effective methodology for the reduction of autofluorescence in direct immunofluorescence studies on formalin-fixed paraffin-embedded tissues. Eur J Histochem. 2007;51(1):59-66.
37. Erben T, Ossig R, Naim HY, Schnekenburger J. What to do with high autofluorescence background in pancreatic tissues - an efficient Sudan black B quenching method for specific immunofluorescence labelling. Histopathology. 2016;69(3):406-22.
38. Van de Winkle M, Maes E, Pipeleers D. Islet cell analysis and purification by light scatter and autofluorescence. Biochem Biophys Res Commun. 1982;107(2):525-32.
39. Willcox A, Richardson SJ, Bone AJ, Foulis AK, Morgan NG. Analysis of islet inflammation in human type 1 diabetes. Clin Exp Immunol. 2009;155(2):173-81.
40. Foulis AK, Liddle CN, Farquharson MA, Richmond JA, Weir RS. The histopathology of the pancreas in type 1 (insulin-dependent) diabetes mellitus: a 25-year review of deaths in patients under 20 years of age in the United Kingdom. Diabetologia. 1986;29(5):267-74.
41. Ardestani A, Paroni F, Azizi Z, Kaur S, Khobragade V, Yuan T, et al. MST1 is a key regulator of beta cell apoptosis and dysfunction in diabetes. Nat Med. 2014;20(4):385-97.
42. Brack K, Frings W, Dotzauer A, Vallbracht A. A cytopathogenic, apoptosis-inducing variant of hepatitis A virus. J Virol. 1998;72(4):3370-6.
43. Abhat A. Low temperature latent heat thermal energy storage: heat storage materials. . Solar energy. 1983;30(4):313-32.

44. Olert J, Wiedorn KH, Goldmann T, Kuhl H, Mehraein Y, Scherthan H, et al. HOPE fixation: a novel fixing method and paraffin-embedding technique for human soft tissues. Pathol Res Pract. 2001;197(12):823-6.
45. Ausubel FM, Brent R, Kingston RE. Short Protocols in Molecular Biology. John Wiley & Sons. 2003.

Figure Legends

Figure 1. An established protocol for short RNA-oligoprobe labeling in FFPE tissue sections

(A) GAPDH oligonucleotides were tested in the cell line HEK 293. Single fluorescent spots, each representing one single RNA molecule, are clearly visible. **(B)** Normal deparaffinization procedure shows high background noise in FFPE islet sections even without probes (No Probes) and does not allow clear distinction of probe signal and background, when GAPDH oligonucleotides were added (**C**; Standard Protocol). Modification of the deparaffinization and post-hybridisation protocol leads to background reduction and increased signal intensity of GAPDH oligonucleotides (**D**; Modified Protocol). RNA Probes are labeled with Quasar 570 (red) and nuclei were stained with DAPI (blue), scale bar depicts 10µm.

Figure 2. RNA-oligonucleotide probe design and specificity

(**A**) Scheme of custom-designed oligonucleotide (CVB_1) annealing throughout the viral genome. (**B**) Viral RNA probes were tested against non-infected, CVB3 and CVB2 (100% and 79% similarity to consensus sequence, respectively; positive control), CMV, (DNA virus; negative control) and HAV (<45% similarity to consensus sequence) infected HEK 293 cells. Cells were infected with an MOI of 5 and harvested after 24h (control, CVB3, CVB2) or 4 days (CMV, HAV) post-infection. RNA Probes are labeled with Quasar 570 (red) and nuclei were stained with DAPI (blue), scale bar depicts 10µm.

Figure 3. RNA-oligonucleotide probe sensitivity

(A) CM 9 and HEK 293 were infected with a dilution series (MOI 10^{2}–10^{-8}) of CVB3 and stained with custom-designed oligonucleotides (CVB_1). Representative images of CM9 and HEK293 cells infected with either the highest or lowest dilution of CVB3 of the series are shown. White arrows highlight single viral spots. (**B)** Ten single images were acquired for each dilution and single fluorescent spots were manually counted. Results for HEK 293 (diamonds) and CM 9 (squares) are displayed as single spots per cell in logarithmic scale. In total, viral particles were counted in 4470 HEK293 cells and CM9 cells. (**C)** Viral RNA from a parallel experiment was extracted and analyzed by PCR; MOI of 100 (10^{2}) was set as 100%. (**D)** Viral RNA (red) and VP1 (1/2000; green) staining on a CVB1-dilution array of FFPE infected GMK cells mixed with uninfected cells. RNA Probes were labeled with Quasar 570 (red) and nuclei were stained with DAPI (blue), scale bar depicts 10µm. (**E**) Summary of the viral RNA and VP1 signals obtained from a CVB1-dilution array of FFPE infected GMK cells.

Figure 4. Coupling RNA-FISH and Immunohistochemistry

(A) Theoretical scheme of viral RNA and VP1 co-staining. Initially, labeled oligonucleotides cannot bind viral RNA within the capsid, but only when the virus is released. On the other hand, VP1 antibody can bind to the capsid surface. Over time as more RNA is released, more probes can anneal to their target sequence. When a

sufficient amount of oligonucleotides is bound, green (VP1) and red (RNA) signal are visible in close proximity. **(B)** CM9 cells were infected with CVB3 (MOI 1000) for 1h at 4°C, fixed and probed for viral RNA and VP1. VP1 (green) was found in close proximity with viral RNA (red), when capsid and RNA were present in the cytosol area (**B;** middle panel). When VP1 staining was performed before cell permeabilization no colocalization of viral RNA/VP1 was detected (**B;** right panel). No cross-reactivity was found with cellular proteins or RNAs (**B;** left panel). **(C)** Co-staining and localization of viral RNA (red) and insulin (green) in CVB3-infected INS-1E cells and $HgCl_2$ fixed paraffin embedded CVB-infected neonatal pancreas. Samples were stained with RNA FISH probes first, analyzed and then stained for insulin. The non-granular insulin staining in this slide appeared also by classical single insulin immunohistochemistry and is caused by the tissue condition. Nuclei were visualized by DAPI staining (blue); scale bar depicts 10µm.

Figure 5. Viral RNA within an islet of a T1D patient
(A) The original probe set CVB_1 was complemented with two additional sets (CVB_2 and CVB_3). Scheme of custom-designed probe sets annealing throughout the viral genome. Arrows show localization of CVB_1, lines show the positions of CVB_2 and CVB_3 probe sets. **(B,C)** Representative images of donors E375 and E514 form the UK cohort and of donor 3626 from the nPOD cohort. Virus RNA was found within the endocrine area **(B)** and outside the islets **(C)** shown by the co-staining of viral RNA probes (combination of CVB_1, CVB_2 and CVB3) (red) and insulin (Green). Tissues were first probed for viral RNA, analyzed and then stained for insulin. Nuclei were visualized by DAPI staining (blue); scale bar depicts 10µm.

Figure S1. Specificity of viral RNA probes
(A) Confirmation of viral-infection in the probe sensitivity test of Fig.2. DNA and RNA of CMV, HAV, CVB3 and CVB2 were isolated and analyzed for the presence of viral genome. Each sample was processed in parallel with or without DNAse digestion. **(B)** CVB3 infected or uninfected FFPE human islets were either stained with buffer or CVB_1 oligos (left panel) or treated with 100ug/ml RNAse A or 2xSSC Buffer (control) for 1h at 37°C before hybridization with RNA FISH probes (right panel). Nuclei were stained with DAPI (blue); scale bar depicts 10µm.

Figure S2. Summary of custom RNA oligonucleotide staining of different picornaviridae and control viruses.
Representative images of the viral RNA (red) staining on the cell array shown in Table 1. Nuclei were stained with DAPI (blue), scale bar depicts 10µm.

Figure S3. RNA-oligonucleotide labelling is consistent despite sample conditions

GMK cells FFPE sections of different age from non-infected (2015 and 2013) and CVB1-infected (2015, 2013 and 2012) were probed for viral RNA (red). Nuclei were stained with DAPI (blue); scale bar depicts 10µm.

Figure S4. Coupling RNA-oligonucleotide labelling and immunohistochemistry
Magnified and enhanced image from Fig.4B, middle panel showing colocalization of VP1 (green) and viral RNA oligonucleotide probes (red).

Figure S5. Custom viral RNA oligonucleotides bind tissue- and fixative-independent
(A) Detection of viral RNA (red) and viral protein 1 (VP1) (green) in the same region of an FFPE spleen sample. Tissue was first stained for viral RNA, analyzed and probed for VP1. (**B**) CVB-infected neonatal heart FFPE section was tested positive for viral RNA with fluorescent-labeled oligonucleotides (red). (**C**) RNA-FISH probes perform independent of the fixative used in human pancreatic sections as shown in the concordance study (Table 3). Nuclei were stained with DAPI (blue); scale bar depicts 10µm.

Figure S6. Genome alignment.
Enterovirus genome alignment for the design of CVB_2 and CVB_3 probe sets (Geneious version (9.1.5) (http://www.geneious.com) (46)).

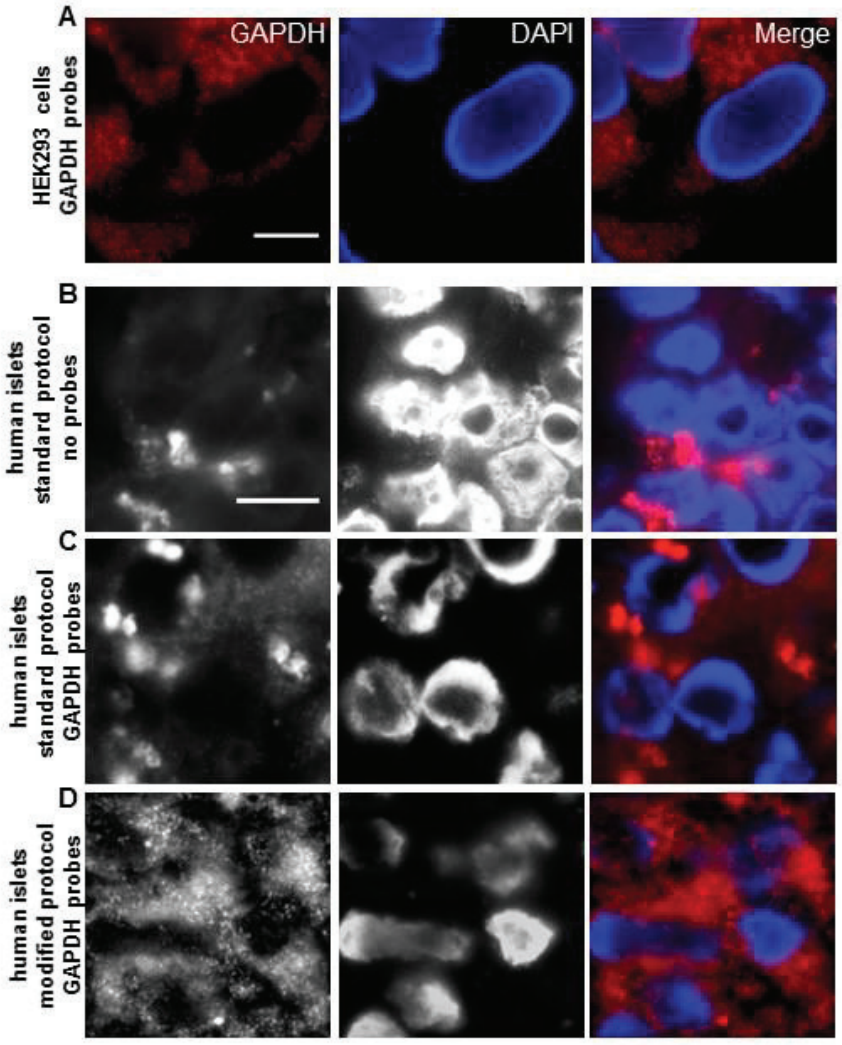
A
GAPDH
DAPI
Merge
HEK293 cells
GAPDH probes
B
human islets
standard protocol
no probes
C
human islets
standard protocol
GAPDH probes
D
human islets
modified protocol
GAPDH probes

Figure 1

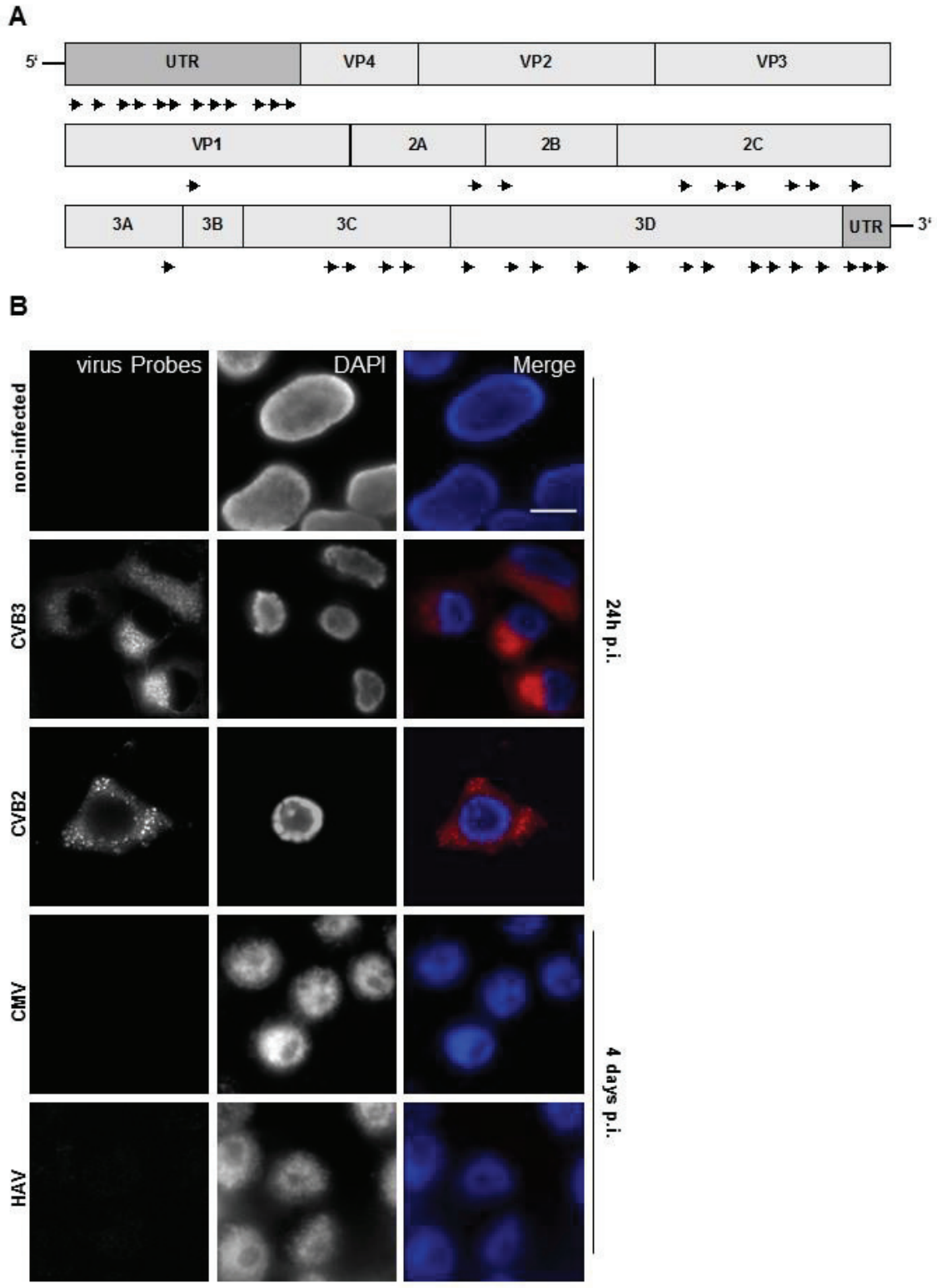
A
5'
UTR
VP4
VP2
VP3
VP1
2A
2B
2C
3A
3B
3C
3D
UTR
3'
B
virus Probes
DAPI
Merge
non-infected
CVB3
CVB2
CMV
HAV
24h p.i.
4 days p.i.

Figure 2

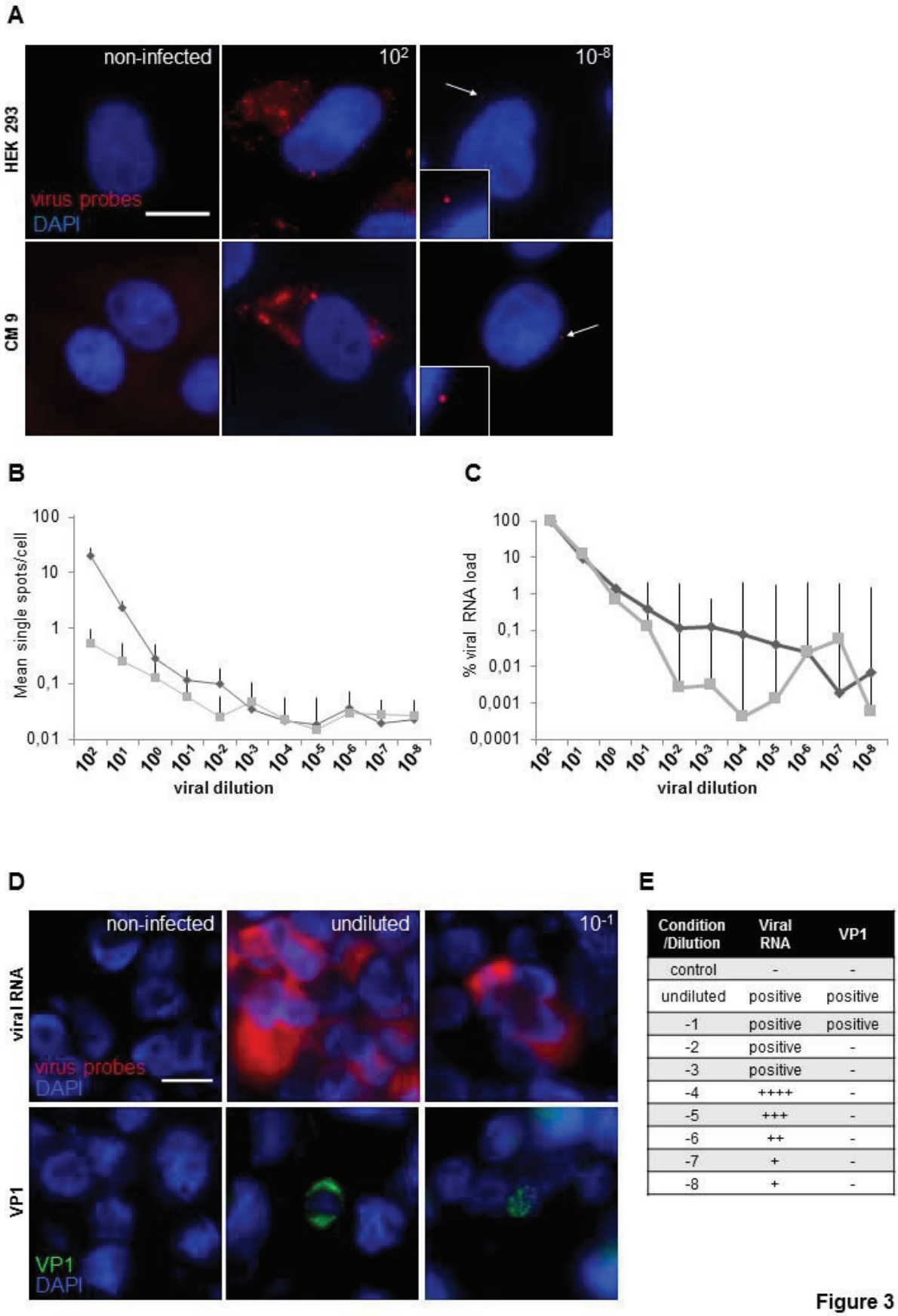

E

Condition /Dilution	Viral RNA	VP1
control	-	-
undiluted	positive	positive
-1	positive	positive
-2	positive	-
-3	positive	-
-4	++++	-
-5	+++	-
-6	++	-
-7	+	-
-8	+	-

Figure 3

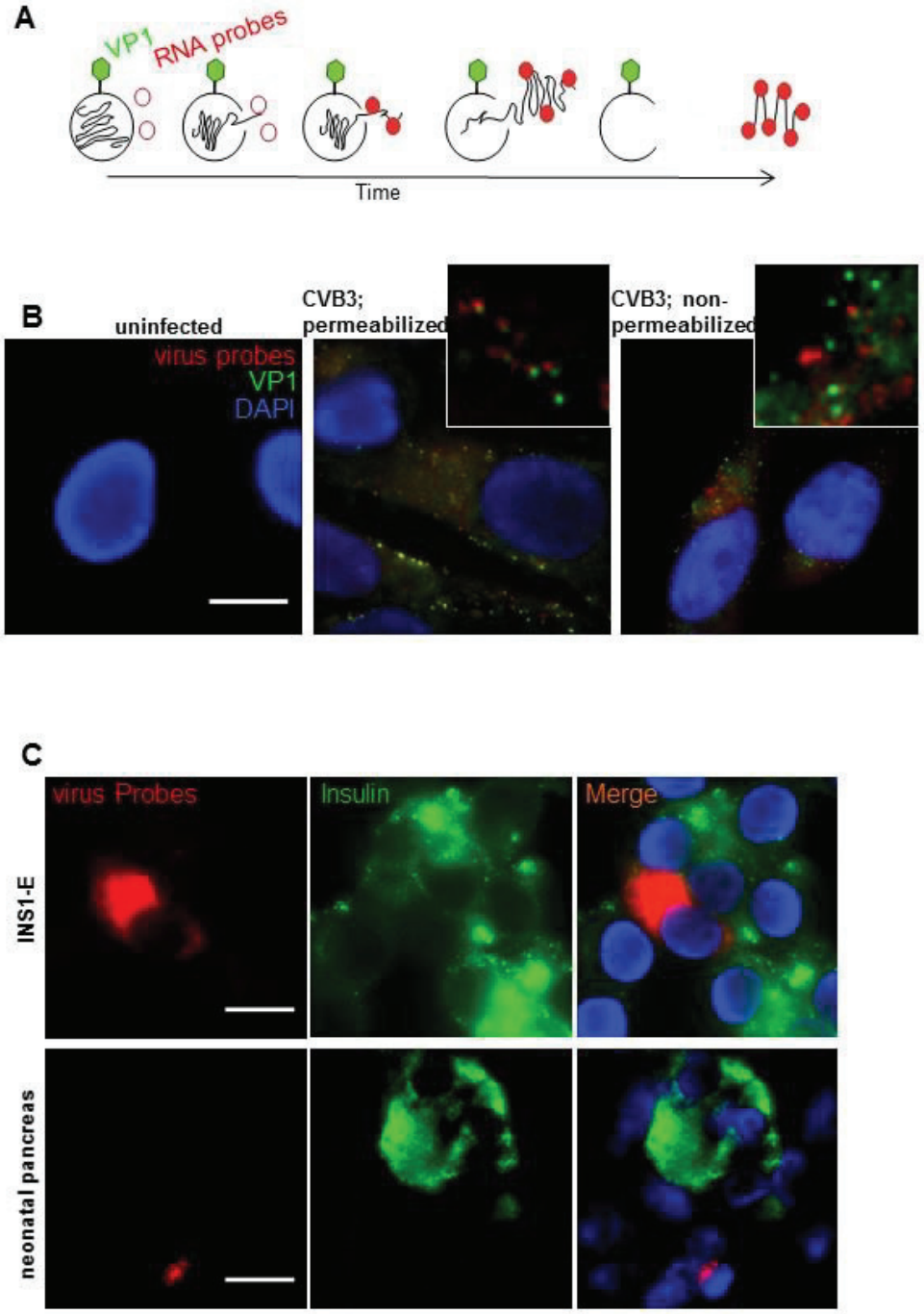
A
VP1
RNA probes
Time
B
uninfected
virus probes
VP1
DAPI
CVB3;
permeabilized
CVB3; non-
permeabilized
C
virus Probes
Insulin
Merge
INS1-E
neonatal pancreas

Figure 4

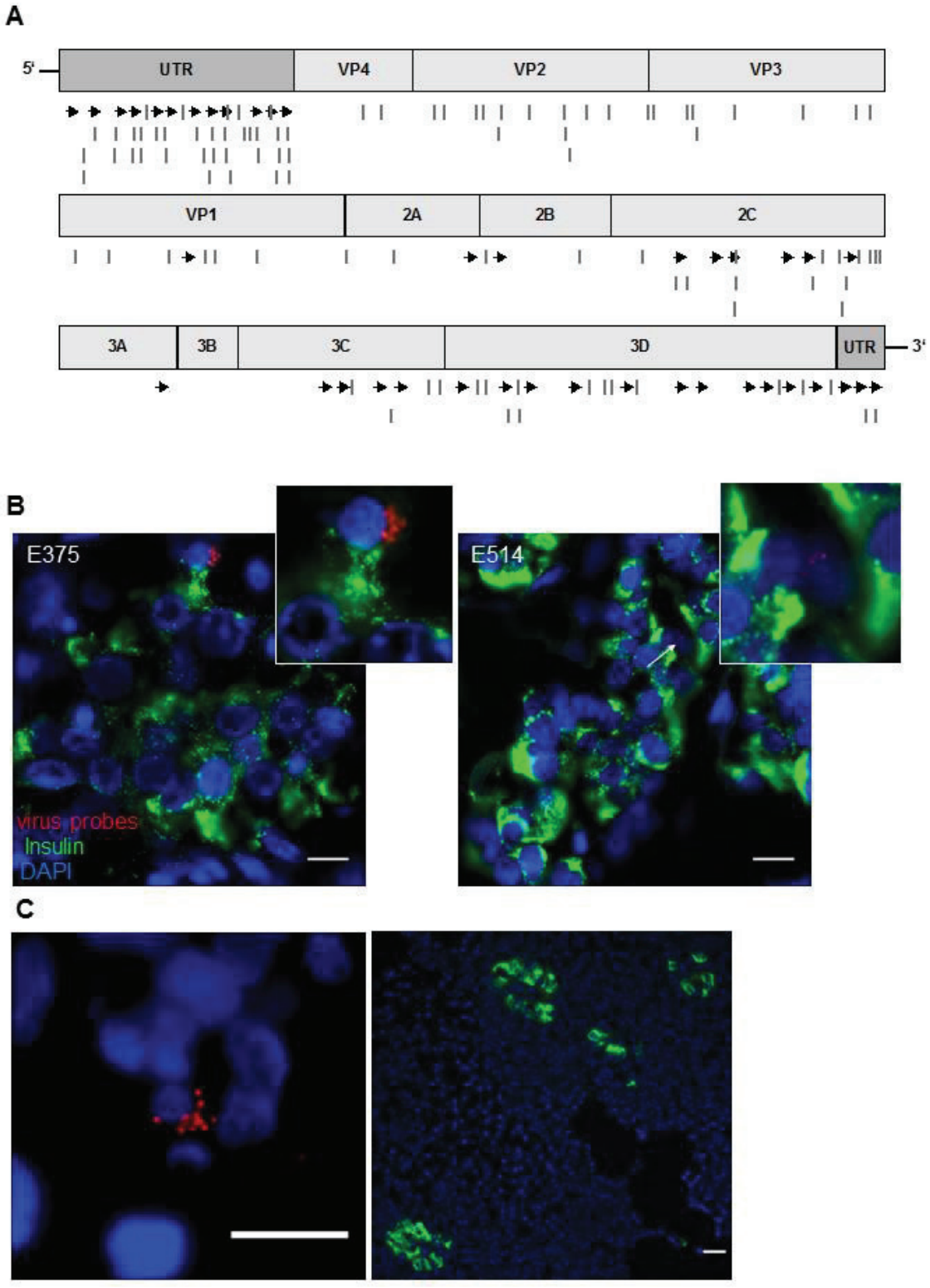
A
5'
UTR
VP4
VP2
VP3
VP1
2A
2B
2C
3A
3B
3C
3D
UTR
3'
B
E375
E514
virus probes
Insulin
DAPI
C

Figure 5

Table 1: RNA oligonucleotide staining of different picornaviridae and control viruses

Virus	Strain	Result	Virus	Strain	Result
EV71	PB-EV71Hus	**++**	**Echo3**	PB-E3DiT23	**++**
CVB1	ATCC	**++**	**Echo4**	ATCC	**++**
CVB2	ATCC	**++**	**Echo6**	ATCC	**+**
CVB3	ATCC	**++**	**Echo9**	ATCC	**+**
CVB4	ATCC	**++**	**Echo11**	ATCC	**+**
CVB5	ATCC	**++**	**Echo30**	ATCC	**++**
CVB6	ATCC	**++**	**PV3**	Sabin	**+**
CVA2	PB-CVA2V38	**++**	**HPeV1**	ATCC	**-**
CVA4	PB-CVA4V36	**++**	**Adenovirus C**	VR846	**-**
CVA5	PB-CVA5V43	**-**	**A549 cells**	-	**-**
CVA6	PB-CVA6V303V	**+**	**RD cells**	-	**-**
CVA9	ATCC	**++**	**Vero cells**	-	**-**
CVA10	PB-CVA10V2530	**++**	**HeLa cells**	-	**-**
CVA16	PB-CVA16V55	**++**	**GMK cells**	-	**-**

Probe specificity was tested on a cell array (FFPE); different cell lines were spotted either as uninfected controls or infected with different viruses. The results obtained with RNA probes set CVB_1 are displayed. Representative images are shown in Fig. S2.

Table 2: RNA oligonucleotide staining of human pancreases

Sample Group	ID	Age	Sex	Fixation	Viral RNA +*	Islet viral RNA +
VP1+ T1D	**E560**	42	F	BF	**++++**	**+**
VP1+ T1D	**11746**	6	M	$HgCl_2$	**++**	**+**
VP1+ T1D	**E375**	11	F	FS	**+**	**+**
VP1+ T1D	**E554A**	7	M	Bouin	**- §**	**+**
VP1 – T1D	**E428**	5	M	BF	**++**	**+**
VP1 – T1D	**E514**	23	M	BF	**-**	**+**
VP1 – T1D	**E235**	6	M	$HgCl_2$	**-**	**- §**
VP1 – T1D	**8869**	8	M	$HgCl_2$	**+**	**- §**
Non-diabetic control	**8579**	7	-	$HgCl_2$	**-**	**-**
Non-diabetic control	**12054**	7	-	$HgCl_2$	**-**	**-**
Non-diabetic control	**330/71**	47	M	BF	**-**	**-**
Non-diabetic control	**21/89**	4	F	BF	**++**	**-**
Non-diabetic control	**274/91**	6	M	BF	**-**	**-**
Non-diabetic control	**191/67**	25	M	BF	**-**	**-**
Non-diabetic control	**315/89**	9	M	BF	**+**	**+**
Non-diabetic control	**540/91**	11	M	BF	**-**	**-**

Summary of the comparative study of pancreata from T1D and non-diabetic control patients. Sections were first stained for viral RNA, with a combination RNA probe sets CVB_1, CVB_2 and CVB_3, followed by insulin staining. - = less than 10 fully-infected cells, + = 10 to 30 full-infected cells, ++ = 30 to 100 fully-infected cells, +++ = 100 to 200 fully-infected cells, ++++ = more than 200 fully-infected cells in the exocrine. §E554A showed ten fully-infected cells, E235 contained just 5 islets on the section and 8869 just 2 full and 1 fragmented islets (very small sections).

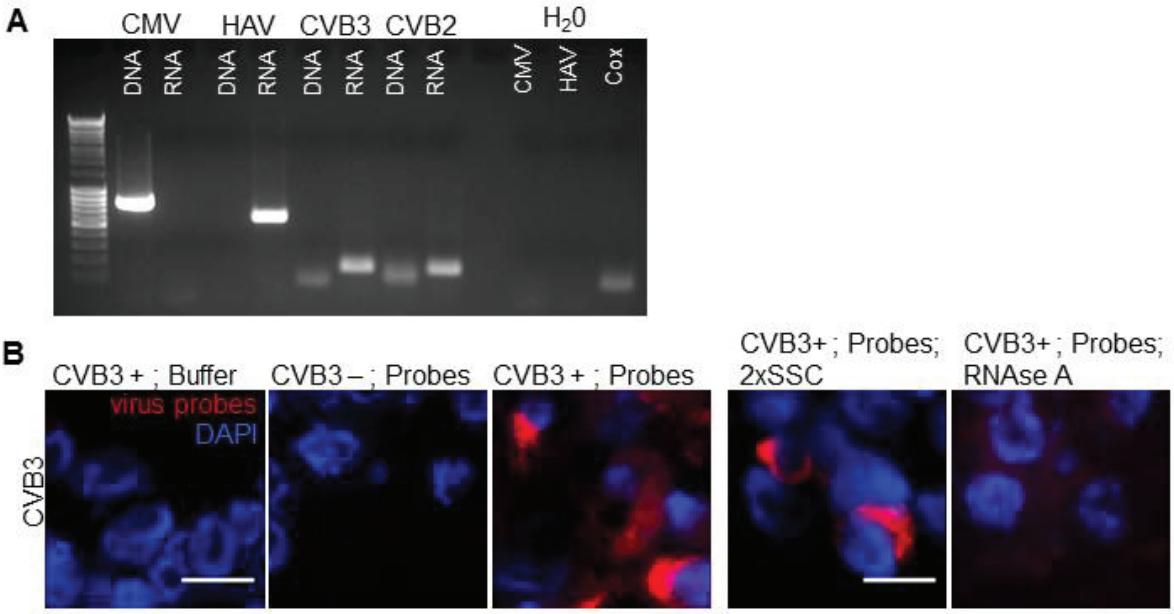

Supplementary Figure 1

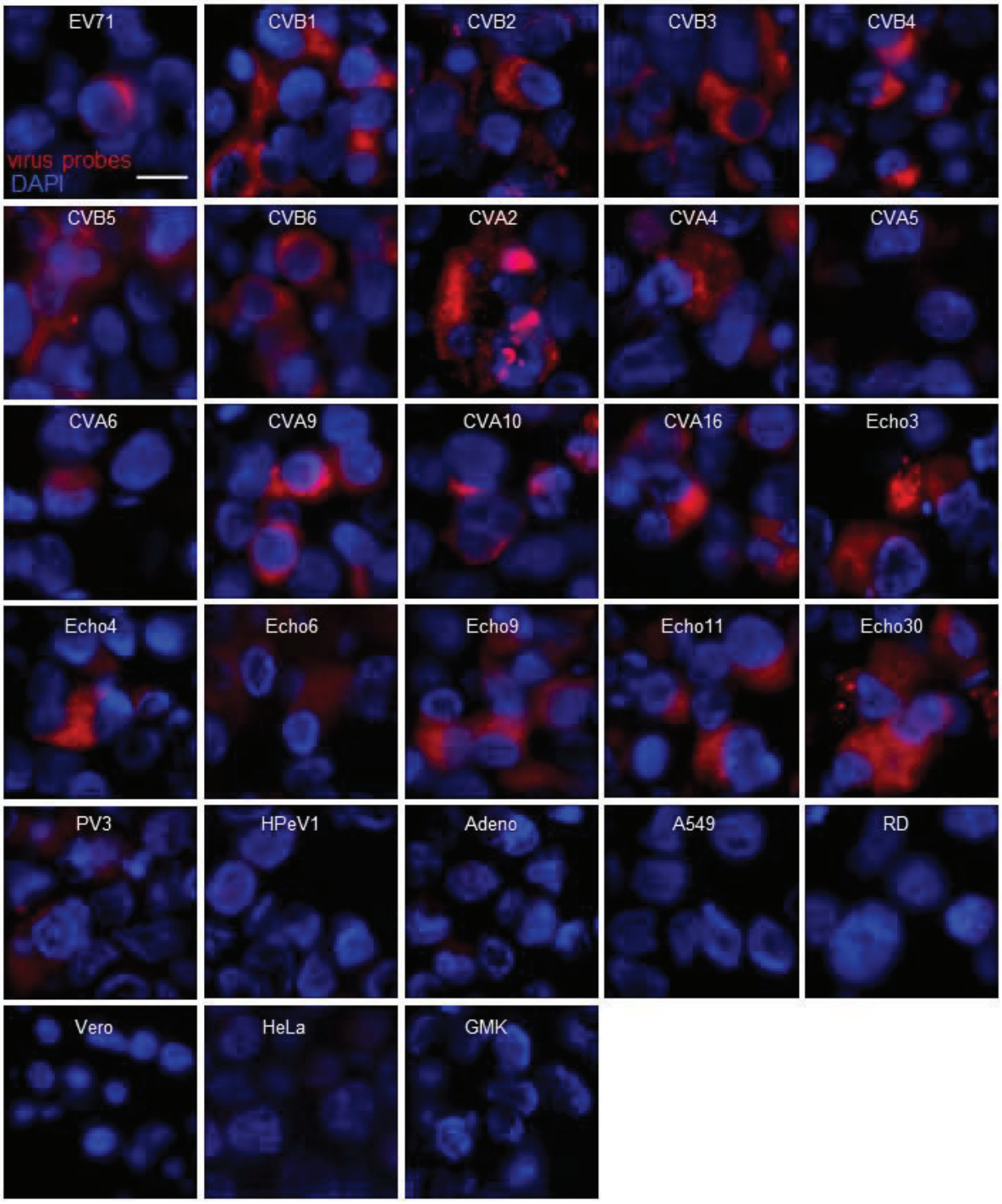

Supplementary Figure 2

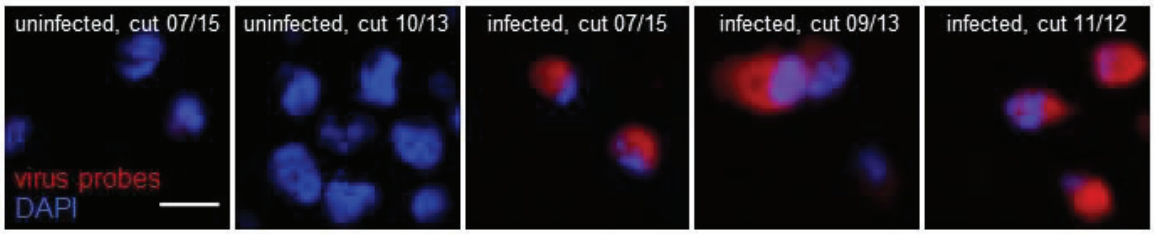

Supplementary Figure 3

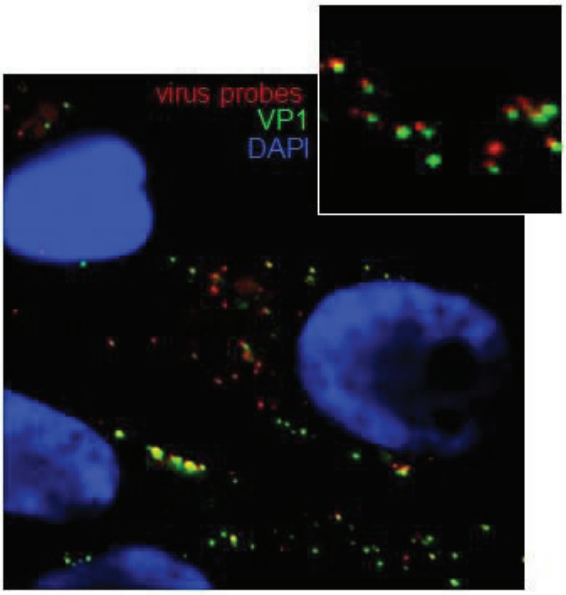

Supplementary Figure 4

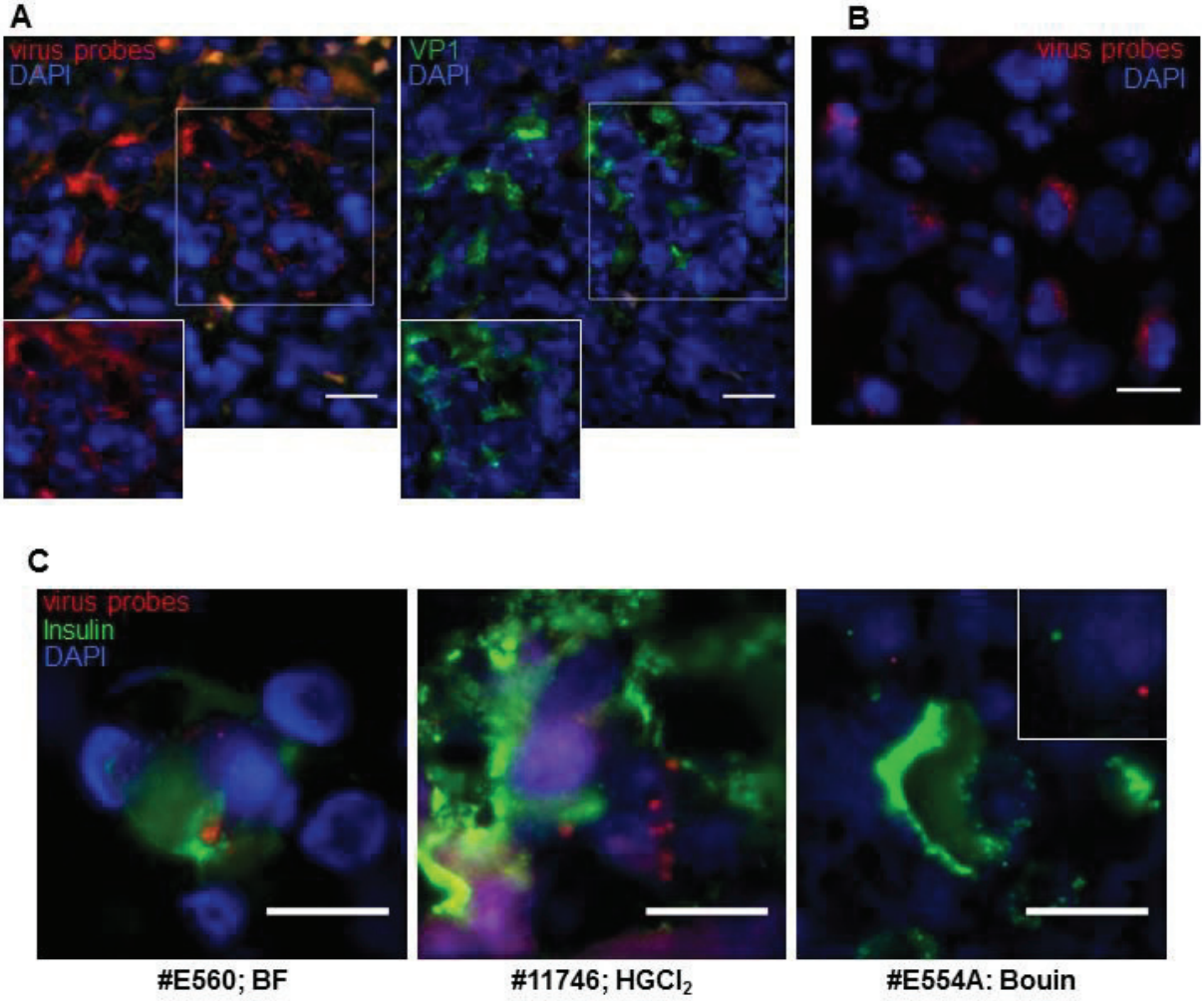

Supplementary Figure 5

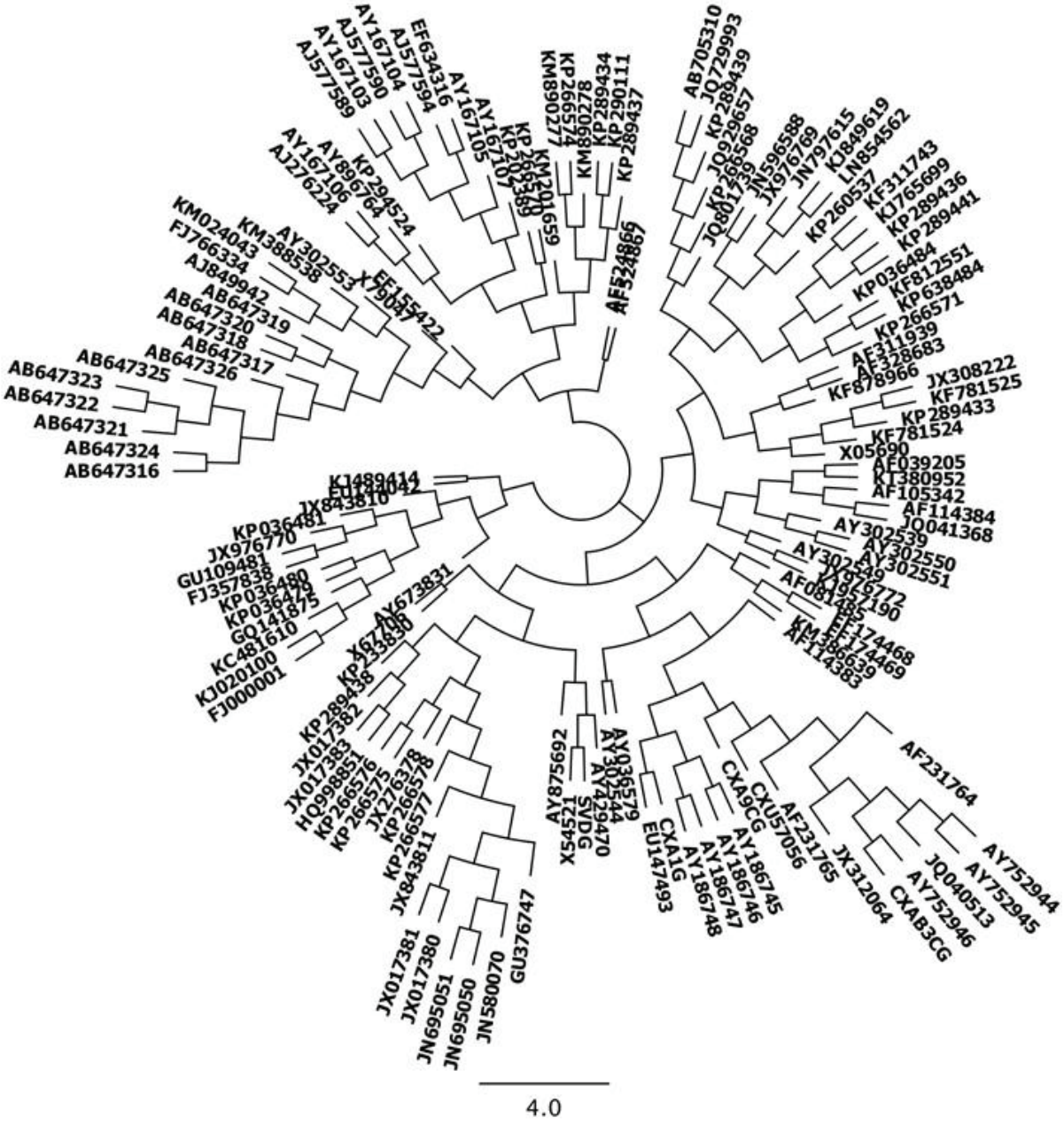

Supplementary Figure 6

Table S1: Counted fluorescent spots of RNA-FISH sensitivity test

Dilution	HEK293 (total spots)	CM9 (total spots)	HEK293 (dots/cell)	CM9 (dots/cell)
10^2	7378	387	19,80656173	0,525101759
10^1	1025	161	2,282483251	0,259821157
10^0	98	103	0,289588584	0,130535155
10^{-1}	51	39	0,112774084	0,058245893
10^{-2}	39	20	0,096695942	0,025043732
10^{-3}	18	33	0,033731891	0,048228387
10^{-4}	8	16	0,02117113	0,022302297
10^{-5}	8	10	0,017853038	0,014837777
10^{-6}	14	23	0,036317252	0,029477528
10^{-7}	6	20	0,018873785	0,028428992
10^{-8}	9	19	0,022544999	0,026538136

CM 9 and HEK 293 were infected with a dilution series (MOI 10^2–10^{-8}) of CVB3 and stained with custom-designed FISH probes (Fig.3). Ten single images were acquired for each dilution and single fluorescent spots as well as number of cells were manually counted (ImageJ).

Table S2: CT values of CVB and housekeeping genes

	CM CVB		CM HK		HEK 293 CVB		HEK 293 HK	
MOI	**C_T Mean**	**C_T SD**	**C_T Mean**	**C_T SD**	**C_T Mean**	**C_T SD**	**C_T Mean**	**C_T SD**
10^2	19,1	± 0.2	23.2	± 0.1	18.8	± 0.1	20.4	± 0.1
10^1	22,2	± 0.0	23.4	± 0.0	22.9	± 0.0	21.1	± 0.0
10^0	26,3	± 0.5	23.2	± 0.1	25.7	± 0.2	21.2	± 0.0
10^{-1}	29,7	± 2.0	22.9	± 0.0	27.8	± 0.2	21.4	± 0.0
10^{-2}	35,0	± 1.9	23.8	± 0.0	30.7	± 0.5	22.5	± 0.0
10^{-3}	33,9	± 0.7	23.7	± 0.1	29.0	± 0.2	21.0	± 0.0
10^{-4}	34,9	± 2.1	23.1	± 0.0	30.4	± 0.5	21.7	± 0.0
10^{-5}	33,4	± 1.7	22.6	± 0.0	31.1	± 0.6	21.4	± 0.0
10^{-6}	31,5	± 2.0	23.3	± 0.0	31.9	± 0.5	21.6	± 0.9
10^{-7}	28,5	± 1.9	22.6	± 0.1	37.2	± 1.8	23.2	± 0.1
10^{-8}	37,5	± 0.6	23.8	± 0.1	32.9	± 1.5	20.7	± 0.0

CM9 and HEK 293 were infected with a dilution series (MOI 10^2–10^{-8}) of CVB3. Viral RNA was extracted and analyzed with PCR (Fig.3). Shown are the CT and SD (standard derivation) values for the respective viral RNA (CVB) and housekeeping gene (HK, β2-Microglobulin).

Table S3: CVB_1 set sequences

#	Probe 5'→ 3'	Sequence 5' → 3'
1	caacccacaggctgttttaa	ttaaaacagcctgtgggttg
2	aacaggcgcacaaaggtacc	ggtacctttgtgcgcctgtt
3	ctattgatactcagtccggg	cccggactgagtatcaatag
4	taacgaacgctttctccttc	gaaggagaaagcgttcgtta
5	gtagtgctgagcgaaacact	agtgtttcgctcagcactac
6	tgactcatcgacctgatcta	tagatcaggtcgatgagtca
7	caccatgtctgtattagagc	gctctaatacagacatggtg
8	aggactaccaactagctcaa	ttgagctagttggtagtcct
9	ttaggattagccgcattcag	ctgaatgcggctaatcctaa

10	gaaacacggacacccaaagt	actttgggtgtccgtgtttc
11	caattgtcaccataagcagc	gctgcttatggtgacaattg
12	ggccaatccaatagctatat	atatagctattggattggcc
13	gtagatgtttgccacacgta	tacgtgtggcaaacatctac
14	tgttccattgcatcatcttc	gaagatgatgcaatggaaca
15	agtgattctttcaggaggtt	aacctcctgaaagaatcact
16	gcgtactttctgcaatagtg	cactattgcagaaagtacgc
17	ctgtatgtaattgctcatct	agatgagcaattacatacag
18	ggttcaatacggcatttgga	tccaaatgccgtattgaacc
19	ggcatagatcgtccataatc	gattatggacgatctatgcc
20	gaaaccatttggcagaacaa	ttgttctgccaaatggtttc
21	gacatgggcatgtttatctt	aagataaacatgcccatgtc
22	gacatgtttctcaatttgga	tccaaattgagaaacatgtc
23	ctgaacttctcattccggtt	aaccggaatgagaagttcag
24	tcattaacctccacttcctc	gaggaagtggaggttaatga
25	tgccacctaggtttaggaag	cttcctaaacctaggtggca
26	gttgtacataagcattctct	agagaatgcttatgtacaac
27	cttggtgtgttgatgactgg	ccagtcatcaacacaccaag
28	tgtgtgttgacatttcctat	ataggaaatgtcaacacaca
29	tccagtttcattggttcagt	actgaaccaatgaaactgga
30	catacttgtccatacattcc	ggaatgtatggacaagtatg
31	gtcaatgtagtttgtctctt	aagagacaaactacattgac
32	caagtcaatccctttgtaca	tgtacaaagggattgacttg
33	catcaccatatgcgatcatc	gatgatcgcatatggtgatg
34	gtactgttcatctgctctaa	ttagagcagatgaacagtac
35	tcgtgtatgtctttcatggg	cccatgaaagacatacacga
36	atcttgggtgttctttggat	atccaaagaacacccaagat
37	tgaactcctcatattcgtgc	gcacgaatatgaggagttca
38	agtagggttaagccaatcta	tagattggcttaaccctact
39	ccgttatctggttcggttag	ctaaccgaaccagataacgg
40	cgaatgcggagaatttaccc	gggtaaattctccgcattcg

Sequences of probes and respective viral target regions of set CVB_1. Designed with Stellaris® RNA FISH Probe Designer (Biosearch Technologies, Inc., Petaluma, CA).

Table S4: CVB_2 set sequences

#	Probe 5'→ 3'	Sequence 5' → 3'
1	aggtttctcgaagtaattgg	ccaattacttcgagaaacct
2	tgatctacactggggttgtg	cacaaccccagtgtagatca
3	ttacgacagactgcccactg	cagtgggcagtctgtcgtaa
4	caaagtagtcggttccgctg	cagcggaaccgactactttg
5	tgcttaccattgtcactgtt	aacagtgacaatggtaagca
6	ccaacatcccatatgacgtg	cacgtcatatgggatgttgg
7	acatgagctttgcacatcag	ctgatgtgcaaagctcatgt
8	acggcatttggacttgaact	agttcaagtccaaatgccgt
9	tcagtccggggtaacagaag	cttctgttaccccggactga
10	gtttctcgaagtaattggcc	ggccaattacttcgagaaac
11	tagctcaatagactcttcgc	gcgaagagtctattgagcta
12	ctgctccgcagttaggatta	taatcctaactgcggagcag
13	agcagccagttcaagaataa	ttattcttgaactggctgct
14	ggccaatccaatagctatat	atatagctattggattggcc
15	tgtgtggttattgtggagtt	aactccacaataaccacaca
16	gttgaagggaatgcctgacc	ggtcaggcattcccttcaac
17	gggttgtgctagtaaactca	tgagtttactagcacaaccc
18	tgtatggcatcactatggtg	caccatagtgatgccataca
19	tgtgaagttgtagtgcctaa	ttaggcactacaacttcaca
20	aaattgcgtactccctggtg	caccagggagtacgcaattt
21	cctggtatattcatactagg	cctagtatgaatataccagg
22	cacaacggagtccacttctg	cagaagtggactccgttgtg
23	aacatttccatttggtcggt	accgaccaaatggaaatgtt
24	ggcattaatggtcactggaa	ttccagtgaccattaatgcc
25	acagaaaagtcgttgcaagc	gcttgcaacgacttttctgt
26	tttctgagttgctaggtcca	tggacctagcaactcagaaa
27	ggactcagaacgagtatggt	accatactcgttctgagtcc
28	ctacgcatttgcaccatttg	caaatggtgcaaatgcgtag
29	cactggcatgtcttgtgcta	tagcacaagacatgccagtg

30	cctcacatatatgtgaccta	taggtcacatatatgtgagg
31	gtggttacagtgttaatgtc	gacattaacactgtaaccac
32	tggtccctcgaagctaactg	cagttagcttcgagggacca
33	gggtagtattcactctcctg	caggagagtgaatactaccc
34	aatcccgagccaaaagcgtt	aacgcttttggctcgggatt
35	tcatcatggtttctcaccac	gtggtgagaaaccatgatga

Sequences of probes and respective viral target regions of set CVB_2. Designed with Stellaris® RNA FISH Probe Designer (Biosearch Technologies, Inc., Petaluma, CA).

Table S5: CVB_3 probe set sequences

#	Probe 5'→ 3'	Sequence 5' → 3'
1	ggtaccgtgataccagagtg	cactctggtatcacggtacc
2	gggtaacagaagtgcttgat	atcaagcacttctgttaccc
3	tagactcttcgcaccatgtc	gacatggtgcgaagagtcta
4	tgaattcttcatccactgca	tgcagtggatgaagaattca
5	gagccattctataaatttct	agaaatttatagaatggctc
6	acaaaatgcctttctcttct	agaagagaaaggcattttgt
7	acctcgatgttcatatcaaa	tttgatatgaacatcgaggt
8	caacactcttcatcacacgt	acgtgtgatgaagagtgttg
9	tcaagggagtatctgacttg	caagtcagatactcccttga
10	tgaacatctcagttaccagc	gctggtaactgagatgttca
11	ctggtgttaattgctagcac	gtgctagcaattaacaccag
12	cattctcttggtgggtgtac	gtacacccaccaagagaatg
13	gagaagccttgatgaccatt	aatggtcatcaaggcttctc
14	aactcgatttctccttgttc	gaacaaggagaaatcgagtt
15	aggactgctggctctttatt	aataaagagccagcagtcct
16	gccaattgaccagcataatg	cattatgctggtcaattggc
17	tctgcagatctgagttcatc	gatgaactcagatctgcaga
18	aacatcactggtatcttgct	agcaagataccagtgatgtt
19	gctagcgtcatatccagaat	attctggatatgacgctagc
20	ttggtccatctgattgattc	gaatcaatcagatggaccaa
21	cgttgtgccaggccaataag	cttattggcctggcacaacg
22	aaaagagtccaaccacttcc	ggaagtggttggactctttt
23	ccctggatcttgagtgaaat	atttcactcaagatccaggg
24	gagctctgttgccacattac	gtaatgtggcaacagagctc
25	tcgggaaatttccaccacca	tggtggtggaaatttcccga
26	aggtaatggtattgcatgtt	aacatgcaataccattacct
27	cctgtggagttttgggattc	gaatcccaaaactccacagg
28	atggtcagattgccaactc	gagttggcaatctgaccata
29	gacaatcgtcgcactattgt	acaatagtgcgacgattgtc
30	ctgcgatttccatcaagttg	caacttgatggaaatcgcag
31	tcactttgagtgtctgcagg	cctgcagacactcaaagtga

32	tggtttgcatagtgtctgct	agcagacactatgcaaacca
33	aagttgtcaccatcagtacc	ggtactgatggtgacaactt
34	tattgacatacggggtggtg	caccaccccgtatgtcaata
35	gcattgcctatgctgatgaa	ttcatcagcataggcaatgc
36	acggcatttggacttgaact	agttcaagtccaaatgccgt

Sequences of probes and respective viral target regions of set CVB_3. Designed with Stellaris® RNA FISH Probe Designer (Biosearch Technologies, Inc., Petaluma, CA).

4 Discussion

The incidence of T1D increases worldwide and most insulin-containing islets (ICIs) are irreversible extinct at time of diagnosis. While patients manage a life with the disease nowadays with advanced insulin injections, but the direct cause of onset remains undiscovered and so the cure. More and more evidence point towards an environmental factor that triggers an autoimmune attack in genetically predisposed individuals, although the time of a first encounter and diagnosis might vary **(1)**. Epidemiological and *in vitro* studies strongly point toward viral pathogens, especially coxsackieviruses, as possible trigger for T1D onset **(2-5)**. Infections can occur unnoticed **(6)** and have the potential to directly or indirectly kill pancreatic β-cells **(7)**. However, causality has not been fully proven so far and the response of infected β-cells is not entirely understood. This doctoral thesis includes two studies addressing (1) the presence and (2) the effect of coxsackieviruses in human pancreatic islets in the context of T1D. The first study shows how CVB induced β-cell death and the series of events within the infected β-cell. The second study shows a novel method for viral genome detection at a level of single RNA molecules in FFPE sections from autopsy and established a smFISH protocol.

Both studies in this thesis demonstrate via different technical approaches that islets are permissive to CVB infection. Viral protein and RNA were detected in insulin-containing cells of cultured human islets and of rodent and human β-cell lines after *in vitro* infection as well as in autopsy recovered islet sections of patients with T1D. Long-term infection studies showed that CVB3 and 4 infect β-cells with the same trend, whereas the ratio of both serotypes changed in α-cells. Significantly more α-cells were VP1 positive when infected with CVB4 than CVB3. Perhaps the recently reported "clearance" mechanism of α-cells **(8)** does not affect all infiltrating pathogens to the same extend or varies in between donors. In line with this study, there was no induction of apoptosis observed in infected human α-cells. This suggests that α-cells could serve as an unaffected viral reservoir for a persistent infection **(9, 10)**. An external factor or a change in metabolic conditions might reactivate the persistent virus in α-cells and induce a viral attack of neighboring β-cells. This could occur at a much later time point than the initial infection. In another speculative scenario, persistently infected α-cells might serve as bystander **(11)** that initiate the recruitment of anti-islet T-cells to the endocrine pancreas of genetically predisposed individuals and finally induce β-cell death. Otherwise, an additional, independent, viral infection could activate this pool of preexisting autoreactive T-cells and induce an attack of insulin-containing cells. **(12)**. The Picornaviridae HAV and T1D-associated CMV successfully infected human islets, but just CVBs impaired β-cell function and induced

apoptosis. Apoptosis is a common defense mechanism of infected cells to prevent viral spreading and safe their environment **(13, 14)**. Virus evolutionary adapted to such events and utilize host proteins to facilitate their own life cycle and prevent premature demise of the required host **(15)**. In confirmation with previous studies **(16-18)**, the two survival pathways AKT and ERK are activated by replicating CVBs but also by dsRNA analogues in human β-cell lines. We observed that a reduction of one kinase results in an elevated activation level of the remaining and vice versa. It is possible that this effect is based on a repealed cross-inhibition of the two signaling pathways **(19, 20)** or rather a counter-balance to facilitate cellular survival during infection. ERK could be required to attenuate ER-stress during CVB replication in infected cells **(21)**. In line with this theory, inhibition of ERK affected the virus more than AKT, and overexpression of ERK1/2 promoted viral replication. When we tested this theory *in vitro*, we observed that ERK1/2 overexpression rescued cells from ER-stress induced apoptosis, but did not benefit viral replication under these conditions. This indicates that cellular survival pathways can be utilized by pathogens, however, host survival appears to be prioritized under difficult settings. The same pathways, AKT and ERK, seem also to be involved in the later JNK activation, which is induced after viral replication. But how survival AKT/ERK pathways are switched towards death (JNK), remains elusive. The MAP kinase JNK is required for the viral lifecycle and β-cell demise, but JNK inhibition elevates cellular apoptosis in the presence as well as in the absence of viral agents. Thus, also the balance JNK kinase is important for cell survival.

Infiltrating pathogens are detected by cellular pattern recognition receptors (PRRs) that are generally expressed by immune cells. Viral specific PRRs are also expressed by non-professional cell such as β-cells, which suggests that islets have encountered viral attacks in their evolutionary past **(8, 22-24)**. CVB replication and the dsRNA analogue poly(I:C) triggered an upregulation of cytokines and viral related PRRs in cultured human islets. In line with previous reports **(25, 26)** cytosolic MDA5 and RIG-I bind viral RNA in long-term infection studies. However, we show that during the early phase of pathogen infiltration, TLR3/7 and PKR are the initial receptors that recognize the invader and represent the first line of cellular protection. In confirmation with earlier results of this study, CVB3 and 4 was bound by β-cell resident TLR3, whereas CVB4 was also recognized by TLR7, located only in α-cells. The activated receptors seem to have a dual role during infection; they are involved in the pathogen lifecycle and activate the innate immune response. Both PRRs regulate viral replication by promoting the previously described pro-survival pathways. TLR3 activates AKT via TBK1 and

PKR triggers ERK phosphorylation as shown in TLR3-deficient CM9 cells and as previously described **(27)**. In addition, viral infection induced cytokine upregulation is mediated by endosomal TLR3 in concert with the cytosolic dsRNA sensor PKR. PKR activation further triggers phosphorylation of eIF2α and subsequently inhibits host protein synthesis **(28)**. As expected, downregulation of PKR improves viral replication, while inhibition of TLR3 reduced cytokine expression, viral replication and cell death upon infection. TLR3 might recognize early dsRNA replication complexes in endosomes or rather secondary structures in the 5'-terminus of the genome **(29)** directly after viral endocytosis **(30)**. Whereas PKR binds cytosolic intermediate dsRNA structures shortly after release from the endocytic pathway. Strikingly, this hypothesis is supported by an experiment using short oligonucleotide viral RNA probes designed to recognize several coxsackieviruses (including CVB3) consensus sequences. The human β-cell line CM9 was infected with CVB3 and shortly after infection fixed and stained. We did not detect annealing of labeled oligonucleotides to their densely-packed targets within virions, but observed the signal at the time when viral RNA was released (colocalization of VP1 and FISH probes). These single RNAs where predominantly located around the cellular membrane, an area where we would expect TLR3 **(26)**.

For the design of viral RNA probes, several coxsackievirus genomes were aligned and suitable **(31)** conserved regions were chosen. In total 40 small oligonucleotides that align throughout the viral genome were generated by the manufacture. Specificity of our custom probe set was tested in infected cells from our lab as well as on a provided cell array, which was spotted with divers cell lines and viruses. We detected all viruses showing at least 60% homology to the consensus sequence and cover the same range of serotypes as Quantigene ViewRNA FISH and VP1 immunostaining **(32)**, except for CVA5 (11/40 oligos anneal and subsequently, did not result in a signal).

This smFISH probe set was originally designed to screen for enteroviral genomes in FFPE tissue sections. Several pathogens have been linked to virus-induced T1D onset in the past **(3, 33-36)**, but causality has not been fully proven so far. The first part of this thesis demonstrated that coxsackieviruses but former T1D-associated viruses, e.g. CMV and other picornaviruses, e.g. HAV trigger cytokine release *in vitro* (which would result in an immune response *in vivo*) and induce β-cell-death. Further strong support is provided by one recent study of pancreatic biopsies samples from living patients with T1D **(5)**. Viral protein 1 (VP1) was found in all and enteroviral RNA in four out of six diabetic donors. However, access to tissue samples from living patients is generally limited and forces researchers to use FFPE pancreatic sections from

autopsy **(5)**. Unfortunately, data obtained via the standard techniques IHC and PCR remain elusive. The use and consistency of antibodies is generally under debate **(37, 38)**, especially the widely used VP1 antibody clone5-D8/1 for enteroviral screening **(39)**. It recognizes the viral capsid protein 1 but cross-reacts with mitochondrial proteins at low dilutions as recommended by the manufacture and used by some laboratories. This could explain why VP1 was predominantly found in islet β-cells **(24, 39, 40)** and not in α-cells as shown in the first part of this thesis. Variations in antibody dilution might further explain inconsistent results among different studies. For example, viral protein was found in the gut mucosa of patients with T1D in a Finnish study (dilution 1:300, clone 5-D8/1) **(41)** but not in an Italian study (dilution 1:1000, clone 5-D8/1) **(42)**. Finally, T1D organ donors rather have a persistent than an acute infection at the time of death **(9, 10).** In line with this theory poly(I:C) and CVB infection show the same effect in cultured human islets. Both trigger upregulation of PRRs and cytokine secretion in a concentration dependent manner. As the virus gradually proliferates, the amount of PRRs and cytokines increases, whereas it decreases during the course of the decline of the artificial dsRNA analogue in culture. This observation strongly points towards a receptor-driven initial immune response, since low amounts of RNA alone are enough to slowly trigger this cascade. Persistent infection may be sufficient to induce an autoimmune response; this is suggested by the temporally separated initial viral hit and the final T1D onset **(7)**. Further, these low amounts of viral RNAs, with little to no protein production, would be missed by any protein-dependent detection method **(10)**. PCR, the second general technique of choice, shows high sensitivity and specificity and is a valid tool to confirm IHC results **(43)**. However, RNA can be modified by the embedding procedure **(44)**, restraining the amount of extracted RNA and hinder PCR reactions. Additionally, donor tissue architecture needs to be disrupted, which abolishes evidence for any possible islet infection. Serum samples of living donors can be analyzed via PCR and seem to be an effective indicator for T1D **(4)**. However, results can neither be correlated to certain organ infiltration nor would any persistent infection be detected **(45)**. In a recent analysis of pancreatic biopsies, even less donors were tested positive for viral RNA than for protein **(5)**; a circumstance probably due to the low sensitivity of the technical approaches. A protein cannot be present without the pathogens' genome. Not a single patient was tested positive with all used techniques, and just one case was positive by three out of five methods.

To overcome such difficulties and limitations, we adapted a single molecule (sm) FISH assay **(31)** in a way that combines the advantages of both PCR and IHC techniques for viral RNA

screening in FFPE tissue sections and provide a protocol for detection of viral RNA up to a single molecule level. With this assay, I was able to detect and identify viral genomes within its cellular localization with high sensitivity and specificity. Viral RNA was found in 7 out of 8 patients with T1D at autopsy from a UK cohort.

Formalin fixation and paraffin embedding is generally used for donor tissues and allows long-term storage without affecting morphology **(32, 46)**. However, one of the general drawbacks of FFPE pancreatic sections is its high-auto-fluorescence caused by endogenous tissue-related molecules as well as from paraffin wax **(47, 48)**. High background noise can interfere with weak fluorescence signals as expected for low persistent infections and causes a false-negative result. Additionally, auto-fluorescence emission is in the range of 450 and 650nm **(47)** and can cause a false-positive result due to fluorescence bleed-through from one microscope filter to another **(49)**. These obstacles were major challenges at the time when we started with viral RNA detection by smFISH in FFPE tissues. In the first step, we used a premade probe set that recognizes the human housekeeping gene GAPDH as control, since it should be abundant and equally expressed. Following manufactures' protocol, we received a very good signal in cell culture, but poor signal quality and quantity in FFPE human islet sections. Pre- and post-hybridization procedures were gradually modified, which reduced auto-fluorescence and consequently enhanced signal intensity. Step-by-step, we improved the deparaffinization protocol to remove remaining wax crystals, used Sudan Black B to quench any tissue related auto-fluorescence **(48)** and altered post-hybridization procedures to eliminate unspecific probe binding. These modifications enhanced the outcome significantly, enabling distinction of single fluorescently labeled RNA molecules without disturbing tissue morphology. The provided protocol in this thesis can now be generally used for smFISH in FFPE tissue sections for future studies.

Despite this established protocol, chances to detect acute infected cells in pancreases of deceased patients with diabetes remain low. Custom-designed probes are required to stain single viral genomes with a high sensitivity comparable to standard PCR techniques. This prerequisite for reliable enterovirus screening in autopsy tissues was tested in two different experimental approaches. HEK 293 and CM9 cells were infected with a serial dilution of CVB3. The number of viral RNA decreases logarithmically with each dilution step. The cells were used for PCR and microscopically smFISH analysis, respectively and showed comparable results. In another experiment the sensitivity of labeled oligonucleotides was compared to standard IHC staining on a dilution array **(50)**. Acutely infected cells were diluted with

uninfected cells before fixation. Hence, the number of fully infected cells among non-infected cells must decrease with higher dilutions. Clone 5-D8/1 (VP1) was used for IHC staining on an additional section at a dilution that should exclude cross-reactivity (1-2000). Labeled-RNA probes recognized single viral genomes even in the highest dilution whereas VP1 was undetectable starting from 10^{-2}. Fully infected cells were observed with FISH probes till 10^{-3}, followed by single spots that gradually decreased in numbers with higher dilutions. This rapid drop of acutely infected cells was surprising to us. A possible reason could lay in the array preparation. Membranes of highly infected cells are extreme fragile **(51)** and could easily break during the process of dilution and harsh pipetting. Released viral material could cross-contaminate non-infected cells in the following steps. Furthermore, the low-infected cells might simply represent an early infection state without protein production, undetectable by immunostaining and hardly by PCR or FISH. In a former study **(50)** this array was stained for VP1 (clone 5-D8/1) in three independent laboratories and, interestingly, shows positive signals at three different dilution maxima (10^{-4}-10^{-6}). Although all of them are higher than in our study (detection limit of viruses by VP1 staining was at a dilution of 10^{-1}), this demonstrates the problem of inconsistency with antibody staining **(37, 38)**, possibly caused by specificity, dilution, inappropriate antibody pre-evaluation or batch differences. Another possible explanation could be a different distribution of infected cells among the arrays, as our undiluted control already showed a low number of infected cells. Viral RNA in frozen cells was found by PCR analysis at the highest dilution (10^{-8}) by semi-nested PCR and till a dilution of 10^{-7} (C_t 40,6) by RT-PCR **(50)**. In the same study this array stained positive for viral RNA till a dilution of 10^{-4} by commercial FISH assays RNAscope and Quantigene ViewRNA. Our smFISH probes require less nucleotides (17-22) on complementary annealing sites than branched-tree based assays (combined 50 nts) and are in total smaller due to their direct 3' fluorescent labeling **(31, 52, 53)**. The size and independence of signal amplification makes this assay very suitable for tight RNA-protein complexes as well as degraded RNAs in FFPE tissues **(44, 54, 55)**. Obstacles that are even more problematic in pancreatic tissues from autopsy **(54)**. Furthermore, just a small pool of added probes are required to generate distinguishable signals (17 out of 40 in our tested conditions) without producing background noise. These advantages make smFISH the method of choice for viral RNA screening in FFPE sections and its high sensitivity was successfully demonstrated by us.

Although PCR and smFISH show similar sensitivity in *in vitro* infection studies, RNA needs to be extracted for PCR assays and therefore cannot provide any information about virus

localization. Since the morphological characteristics are important for pancreas evaluation and screens for islet resident enteroviruses we used co-staining of VP1 and insulin by classical IHC and smFISH. In the initial staining procedure, labeled oligonucleotides were applied and analyzed, followed by an additional round of IHC staining under optimized conditions for antibodies and probes. Combination of IHC and smFISH was successfully performed in all tested cell lines as well as in diverse types of tissues. Colocalization of probes and VP1 was observed in CM9 cells and of insulin in INS1-E cells **(56)**. Apparently, RNA-RNA-hybrids were not disrupted by additional antibody staining. In pancreases of infected neonatal mice, viral RNA was found in proximity to immunostained insulin-containing islets as expected **(57-59)**. The pancreas was fixed with $HgCl_2$ and required iodine pre-treatment before applying our deparaffinization protocol. We cannot say whether it was the fixation technique or whether it was the poor quality of this section itself, which affected tissue morphology and made granular insulin staining invisible on this slide. However, I can say, that the poor quality was not caused by our pre-hybridization procedure, since also single classical IHC did not show granular insulin at this section and other slides, in which we combined IHC and smFISH, showed the usual granular insulin staining (Fig.5). Still, this experiment represents an important step in our assay development and additionally shows that it works fixation-independent.

In summary, I adapted smFISH successfully for FFPE tissue sections and confirmed high specificity and sensitivity of the designed probe set in several infected cells *in vitro*. To complete the test series, I analyzed 16 donor sections from a UK cohort **(60, 61)** within a blinded concordance study. Half of the pancreatic sections were from T1D patients, from which four were previously tested positive for VP1 within the islets ("T1D VP1+"), and the other half from non-diabetic controls, which were negative for VP1. To avoid false-negative results by not recognizing any resident enteroviral serotypes, we extended our CVB_1 set by two additional sets (CVB_2 and 3) and used all three in combination. Seven out of eight pancreata from patients with T1D were positive for enteroviral RNA throughout the pancreatic tissue. Previously positive VP1 staining was confirmed, but also in two previously negative VP1 pancreases, we found viral RNA. Thereof six contained viral genomes within islets and surprisingly **(22)** one exclusively in the exocrine. Of note, the two sections without positive endocrine signal contained just 5 and 3 islets, respectively. It is imaginable that we just missed viral positive islets due to their low numbers. In agreement with previous studies **(5)** we just found few infected islets, and most viral RNAs were in the exocrine. Unexpectedly, we found resident enteroviral genomes in pancreases of two young non-diabetic control patients. Chances

are, that these individuals would have had developed diabetes in their future live, but such hypothesis cannot not be tested. Otherwise, this could be an indicator that viruses per se would not induce T1D onset, but rather its potentiation and how the respective immune system responses to a pathogen infiltration. Finally, our analysis results show that a correlation of viral infection in the pancreas in T1D should not be solely defined by islet infection, since also exocrine infection could have future deleterious effects for the endocrine cells.

4.1 Outlook

The relevance of enteroviruses in the context of T1D was highlighted in two parts of this doctoral thesis. Both studies support the hypothesis of viral triggered T1D. Nevertheless, several questions remain open that require future attention.

Data from the *in vitro* study and the smFISH assay point towards viral RNA detection by TLR3 at the cellular membrane and an early endosomal pathway. To support this hypothesis, colocalization studies using classical IHC to label PRRs and/ or endosomal marker proteins in combination with smFISH for viral genomes in a time dependent study would answer the question, what receptors primarily induce virus entry and replication. With the combination of both techniques, a time-dependent analysis could exactly determine where, when and how long such interaction occurs. Further, it must be tested, if any mutation in the N-terminal PAMP binding domain would abolish or delay a pathogen-driven immune-response. AKT and ERK pathways are part of cellular survival machinery and are upregulated in infected cells. However, their exact role remains elusive. The kinases should be individually inhibited before, as well as at different times during and post viral infection. This approach could help to clearly understand which phase of activation is most important for viral replication or if it would just delay the infectious cycle. In the same line, future smFISH experiments could examine, if any reduction in AKT or ERK levels would impede viral entering. My experiments showed that ERK affects viral replication more than AKT. To gain a better understanding whether one of the kinases alone is sufficient to ensure viral replication, ERK1/2 could be overexpressed in AKT-deficient cells and vice versa.

The establishment of smFISH in FFPE pancreatic sections from autopsy represents a crucial milestone for future work in the virus recognition and causative correlation with diabetes. CVBs can induce a persistent infection **(9, 10)** and we showed that human α-cells can serve as an unaffected reservoir for CVB4. However, no one has demonstrated persistent viral infection in human pancreata so far. Labeled oligonucleotides aligning to the negative or positive strand of

viral RNA, respectively, will show which type is predominantly expressed in infected cells and will shed light on the specific type of the present infection. In addition, probes targeting host genes such as HLA-1 **(62)** could be used for co-staining and confirmation of inflammation. Surprisingly, we mostly stained exocrine tissue positive for viral genomes in the cohort study. This would be in line with murine studies **(57-59)**, but immunostaining of human pancreata generally found VP1 within islets. Future smFISH studies need to clearly identify viral containing cells in human pancreatic donor tissues, and show whether the infected cells are of immune **(63)** or other cell origin. The wide field of potential viral candidates needs to be narrowed down to gain a future therapeutic benefit. All three probe sets (CVB_1-3) can be used individually on consecutive sections, analyzed and re-evaluated with remaining sets to see if any difference in quantity of viral genome can be observed. To ease this task each set could be labeled with different fluorophores and used sequentially or multiple labeled probes are used simultaneously. In this case, it would be possible to allocate barcodes to different serotypes **(64)**. If different viruses are identified, it would be exciting to see if they also infect different islet cells or different cell types and confirm the first part of the thesis. Further future studies should correlate the respective viral agents to the origin of organ donors to gain a better perspective on the regional differences of T1D incidences. Finally, different pathogens, if present, infecting patients with T1D and non-diabetic control patients need to be categorized. Overall, with this established method, we hope to find more specific virus strains affecting the disease, but do not expect that a single virus serotype will cause type 1 diabetes.

4.2 Conclusion

In my thesis I show that viral serotypes can infect human islet cells with different ratios and are directly recognized by toll-like receptors at the time of infiltration. The first presented study used an *in vitro* setting of human islets and β-cell lines to explore the early response upon viral infections in human β-cells and identified a series of initial events that lead to cellular death. The involved PRRs mediate cytokine upregulation, as well as AKT and ERK activation to cushion cellular stress during viral replication. The second study focused on technical obstacles of smFISH in FFPE tissue sections and provides a protocol for future use. The advantages for enteroviral screening were successfully demonstrated in a blinded concordance study on pancreata from autopsy from a UK cohort. Former VP1 immunostaining was confirmed and even more T1D donors were tested positive for enteroviral RNA, than for VP1. Both studies independently support the hypothesis that enterovirus are the environmental trigger that induces

a disease state. However, we also showed that pancreata of few non-diabetic controls were positive for viral genomes. This opens the question if viruses are a direct cause of T1D onset. Although we confirmed that CVBs induce β-cell death in cultured human islets, we have no information about living individuals. Perhaps the key to T1D onset upon viral infection is how the immune system responds to the infiltrating aggressor, rather than the viral agent itself: any mutation in PRRs of the first defense line or 5' deletions that disturb secondary structures within the viral genome would change the cellular response. Modifications in the host survival pathway such as AKT or ERK could induce premature apoptosis, abolish viral replication and protect neighboring cells. Independent of the direct or indirect destructive effect of viral agents, smFISH could be used as a diagnostic tool for future pancreatic biopsy samples and would allow an early detection and treatment of infection, although, such experiments would need to be performed under highest ethical standards and restrictions. Finally, at the time when the T1D related enterovirus is clearly identified, vaccination programs can be developed to immunize diabetic-risk individuals. This approach eventually would reduce the currently escalating number of T1D incidence in the future **(65)**.

References

1. Atkinson MA. The pathogenesis and natural history of type 1 diabetes. Cold Spring Harb Perspect Med. 2012;2(11).
2. Gamble DR, Taylor KW. Seasonal incidence of diabetes mellitus. Br Med J. 1969;3(5671):631-3.
3. Yoon JW, Austin M, Onodera T, Notkins AL. Isolation of a virus from the pancreas of a child with diabetic ketoacidosis. N Engl J Med. 1979;300(21):1173-9.
4. Yeung WC, Rawlinson WD, Craig ME. Enterovirus infection and type 1 diabetes mellitus: systematic review and meta-analysis of observational molecular studies. BMJ. 2011;342:d35.
5. Krogvold L, Edwin B, Buanes T, Frisk G, Skog O, Anagandula M, et al. Detection of a low-grade enteroviral infection in the islets of langerhans of living patients newly diagnosed with type 1 diabetes. Diabetes. 2015;64(5):1682-7.
6. Whitton JL. Immunopathology during coxsackievirus infection. Springer Semin Immunopathol. 2002;24(2):201-13.
7. Coppieters KT, Boettler T, von Herrath M. Virus infections in type 1 diabetes. Cold Spring Harb Perspect Med. 2012;2(1):a007682.
8. Marroqui L, Lopes M, dos Santos RS, Grieco FA, Roivainen M, Richardson SJ, et al. Differential cell autonomous responses determine the outcome of coxsackievirus infections in murine pancreatic alpha and beta cells. Elife. 2015;4:e06990.
9. Tracy S, Smithee S, Alhazmi A, Chapman N. Coxsackievirus can persist in murine pancreas by deletion of 5' terminal genomic sequences. J Med Virol. 2015;87(2):240-7.
10. Klingel K, Hohenadl C, Canu A, Albrecht M, Seemann M, Mall G, et al. Ongoing enterovirus-induced myocarditis is associated with persistent heart muscle infection: quantitative analysis of virus replication, tissue damage, and inflammation. Proc Natl Acad Sci U S A. 1992;89(1):314-8.
11. Horwitz MS, Bradley LM, Harbertson J, Krahl T, Lee J, Sarvetnick N. Diabetes induced by Coxsackie virus: initiation by bystander damage and not molecular mimicry. Nat Med. 1998;4(7):781-5.
12. von Herrath MG, Fujinami RS, Whitton JL. Microorganisms and autoimmunity: making the barren field fertile? Nat Rev Microbiol. 2003;1(2):151-7.
13. Colli ML, Nogueira TC, Allagnat F, Cunha DA, Gurzov EN, Cardozo AK, et al. Exposure to the viral by-product dsRNA or Coxsackievirus B5 triggers pancreatic beta cell apoptosis via a Bim / Mcl-1 imbalance. PLoS Pathog. 2011;7(9):e1002267.
14. Clarke P, Tyler KL. Apoptosis in animal models of virus-induced disease. Nat Rev Microbiol. 2009;7(2):144-55.
15. Diehl N, Schaal H. Make yourself at home: viral hijacking of the PI3K/Akt signaling pathway. Viruses. 2013;5(12):3192-212.
16. Wang B, Zhang H, Zhu M, Luo Z, Peng Y. MEK1-ERKs signal cascade is required for the replication of Enterovirus 71 (EV71). Antiviral Res. 2012;93(1):110-7.
17. Zhu M, Duan H, Gao M, Zhang H, Peng Y. Both ERK1 and ERK2 are required for enterovirus 71 (EV71) efficient replication. Viruses. 2015;7(3):1344-56.
18. Wong WR, Chen YY, Yang SM, Chen YL, Horng JT. Phosphorylation of PI3K/Akt and MAPK/ERK in an early entry step of enterovirus 71. Life Sci. 2005;78(1):82-90.
19. Mendoza MC, Er EE, Blenis J. The Ras-ERK and PI3K-mTOR pathways: cross-talk and compensation. Trends Biochem Sci. 2011;36(6):320-8.
20. Zimmermann S, Moelling K. Phosphorylation and regulation of Raf by Akt (protein kinase B). Science. 1999;286(5445):1741-4.
21. Zhang HM, Ye X, Su Y, Yuan J, Liu Z, Stein DA, et al. Coxsackievirus B3 infection activates the unfolded protein response and induces apoptosis through downregulation of p58IPK and activation of CHOP and SREBP1. J Virol. 2010;84(17):8446-59.

22. Ylipaasto P, Klingel K, Lindberg AM, Otonkoski T, Kandolf R, Hovi T, et al. Enterovirus infection in human pancreatic islet cells, islet tropism in vivo and receptor involvement in cultured islet beta cells. Diabetologia. 2004;47(2):225-39.
23. Garcia M, Dogusan Z, Moore F, Sato S, Hartmann G, Eizirik DL, et al. Regulation and function of the cytosolic viral RNA sensor RIG-I in pancreatic beta cells. Biochim Biophys Acta. 2009;1793(11):1768-75.
24. Richardson SJ, Willcox A, Bone AJ, Foulis AK, Morgan NG. The prevalence of enteroviral capsid protein vp1 immunostaining in pancreatic islets in human type 1 diabetes. Diabetologia. 2009;52(6):1143-51.
25. Aida K, Nishida Y, Tanaka S, Maruyama T, Shimada A, Awata T, et al. RIG-I- and MDA5-initiated innate immunity linked with adaptive immunity accelerates beta-cell death in fulminant type 1 diabetes. Diabetes. 2011;60(3):884-9.
26. Takeuchi O, Akira S. Pattern recognition receptors and inflammation. Cell. 2010;140(6):805-20.
27. Deb A, Zamanian-Daryoush M, Xu Z, Kadereit S, Williams BR. Protein kinase PKR is required for platelet-derived growth factor signaling of c-fos gene expression via Erks and Stat3. EMBO J. 2001;20(10):2487-96.
28. Dabo S, Meurs EF. dsRNA-dependent protein kinase PKR and its role in stress, signaling and HCV infection. Viruses. 2012;4(11):2598-635.
29. Tatematsu M, Nishikawa F, Seya T, Matsumoto M. Toll-like receptor 3 recognizes incomplete stem structures in single-stranded viral RNA. Nat Commun. 2013;4:1833.
30. Chung SK, Kim JY, Kim IB, Park SI, Paek KH, Nam JH. Internalization and trafficking mechanisms of coxsackievirus B3 in HeLa cells. Virology. 2005;333(1):31-40.
31. Raj A, van den Bogaard P, Rifkin SA, van Oudenaarden A, Tyagi S. Imaging individual mRNA molecules using multiple singly labeled probes. Nat Methods. 2008;5(10):877-9.
32. Laiho JE, Oikarinen S, Oikarinen M, Larsson PG, Stone VM, Hober D, et al. Application of bioinformatics in probe design enables detection of enteroviruses on different taxonomic levels by advanced in situ hybridization technology. J Clin Virol. 2015;69:165-71.
33. Helmke K, Otten A, Willems W. Islet cell antibodies in children with mumps infection. Lancet. 1980;2(8187):211-2.
34. Ramondetti F, Sacco S, Comelli M, Bruno G, Falorni A, Iannilli A, et al. Type 1 diabetes and measles, mumps and rubella childhood infections within the Italian Insulin-dependent Diabetes Registry. Diabet Med. 2012;29(6):761-6.
35. Pak CY, Eun HM, McArthur RG, Yoon JW. Association of cytomegalovirus infection with autoimmune type 1 diabetes. Lancet. 1988;2(8601):1-4.
36. Menser MA, Forrest JM, Bransby RD. Rubella infection and diabetes mellitus. Lancet. 1978;1(8055):57-60.
37. Baker M. Antibody anarchy: A call to order. Nature. 2015;527(7579):545-51.
38. Baker M. Reproducibility crisis: Blame it on the antibodies. Nature. 2015;521(7552):274-6.
39. Hansson SF, Korsgren S, Ponten F, Korsgren O. Enteroviruses and the pathogenesis of type 1 diabetes revisited: cross-reactivity of enterovirus capsid protein (VP1) antibodies with human mitochondrial proteins. J Pathol. 2013;229(5):719-28.
40. Dotta F, Censini S, van Halteren AG, Marselli L, Masini M, Dionisi S, et al. Coxsackie B4 virus infection of beta cells and natural killer cell insulitis in recent-onset type 1 diabetic patients. Proc Natl Acad Sci U S A. 2007;104(12):5115-20.
41. Oikarinen M, Tauriainen S, Oikarinen S, Honkanen T, Collin P, Rantala I, et al. Type 1 diabetes is associated with enterovirus infection in gut mucosa. Diabetes. 2012;61(3):687-91.
42. Mercalli A, Lampasona V, Klingel K, Albarello L, Lombardoni C, Ekstrom J, et al. No evidence of enteroviruses in the intestine of patients with type 1 diabetes. Diabetologia. 2012;55(9):2479-88.

43. Skog O, Ingvast S, Korsgren O. Evaluation of RT-PCR and immunohistochemistry as tools for detection of enterovirus in the human pancreas and islets of Langerhans. J Clin Virol. 2014;61(2):242-7.
44. Masuda N, Ohnishi T, Kawamoto S, Monden M, Okubo K. Analysis of chemical modification of RNA from formalin-fixed samples and optimization of molecular biology applications for such samples. Nucleic Acids Res. 1999;27(22):4436-43.
45. Oikarinen S, Martiskainen M, Tauriainen S, Huhtala H, Ilonen J, Veijola R, et al. Enterovirus RNA in blood is linked to the development of type 1 diabetes. Diabetes. 2011;60(1):276-9.
46. Blum F. Notiz uber die Anwendung des Formaldehyds (Formol) als Hartungs-und Konservierungsmittel. Anat Anz. 1894;9:229.
47. Viegas MS, Martins TC, Seco F, do Carmo A. An improved and cost-effective methodology for the reduction of autofluorescence in direct immunofluorescence studies on formalin-fixed paraffin-embedded tissues. Eur J Histochem. 2007;51(1):59-66.
48. Erben T, Ossig R, Naim HY, Schnekenburger J. What to do with high autofluorescence background in pancreatic tissues - an efficient Sudan black B quenching method for specific immunofluorescence labelling. Histopathology. 2016;69(3):406-22.
49. Waters JC. Accuracy and precision in quantitative fluorescence microscopy. J Cell Biol. 2009;185(7):1135-48.
50. Laiho JE, Oikarinen M, Richardson SJ, Frisk G, Nyalwidhe J, Burch TC, et al. Relative sensitivity of immunohistochemistry, multiple reaction monitoring mass spectrometry, in situ hybridization and PCR to detect Coxsackievirus B1 in A549 cells. J Clin Virol. 2016;77:21-8.
51. Tran TT, Dietmair S, Chan LC, Huynh HT, Nielsen LK, Reid S. Development of quenching and washing protocols for quantitative intracellular metabolite analysis of uninfected and baculovirus-infected insect cells. Methods. 2012;56(3):396-407.
52. Raj A, Tyagi S. Detection of individual endogenous RNA transcripts in situ using multiple singly labeled probes. Methods Enzymol. 2010;472:365-86.
53. Wang F, Flanagan J, Su N, Wang LC, Bui S, Nielson A, et al. RNAscope: a novel in situ RNA analysis platform for formalin-fixed, paraffin-embedded tissues. J Mol Diagn. 2012;14(1):22-9.
54. Griffin M, Abu-El-Haija M, Abu-El-Haija M, Rokhlina T, Uc A. Simplified and versatile method for isolation of high-quality RNA from pancreas. Biotechniques. 2012;52(5):332-4.
55. von Ahlfen S, Missel A, Bendrat K, Schlumpberger M. Determinants of RNA quality from FFPE samples. PLoS One. 2007;2(12):e1261.
56. Asfari M, Janjic D, Meda P, Li G, Halban PA, Wollheim CB. Establishment of 2-mercaptoethanol-dependent differentiated insulin-secreting cell lines. Endocrinology. 1992;130(1):167-78.
57. Hilton DA, Day C, Pringle JH, Fletcher A, Chambers S. Demonstration of the distribution of coxsackie virus RNA in neonatal mice by non-isotopic in situ hybridization. J Virol Methods. 1992;40(2):155-62.
58. Alirezaei M, Flynn CT, Wood MR, Whitton JL. Pancreatic acinar cell-specific autophagy disruption reduces coxsackievirus replication and pathogenesis in vivo. Cell Host Microbe. 2012;11(3):298-305.
59. Moon MS, Joo CH, Hwang IS, Ye JS, Jun EJ, Lee HS, et al. Distribution of viral RNA in mouse tissues during acute phase of coxsackievirus B5 infection. Intervirology. 2005;48(2-3):153-60.
60. Foulis AK, Liddle CN, Farquharson MA, Richmond JA, Weir RS. The histopathology of the pancreas in type 1 (insulin-dependent) diabetes mellitus: a 25-year review of deaths in patients under 20 years of age in the United Kingdom. Diabetologia. 1986;29(5):267-74.
61. Willcox A, Richardson SJ, Bone AJ, Foulis AK, Morgan NG. Analysis of islet inflammation in human type 1 diabetes. Clin Exp Immunol. 2009;155(2):173-81.
62. Richardson SJ, Rodriguez-Calvo T, Gerling IC, Mathews CE, Kaddis JS, Russell MA, et al. Islet cell hyperexpression of HLA class I antigens: a defining feature in type 1 diabetes. Diabetologia. 2016;59(11):2448-58.

63. Mena I, Perry CM, Harkins S, Rodriguez F, Gebhard J, Whitton JL. The role of B lymphocytes in coxsackievirus B3 infection. Am J Pathol. 1999;155(4):1205-15.
64. Lubeck E, Cai L. Single-cell systems biology by super-resolution imaging and combinatorial labeling. Nat Methods. 2012;9(7):743-8.
65. Larsson PG, Lakshmikanth T, Laitinen OH, Utorova R, Jacobson S, Oikarinen M, et al. A preclinical study on the efficacy and safety of a new vaccine against Coxsackievirus B1 reveals no risk for accelerated diabetes development in mouse models. Diabetologia. 2015;58(2):346-54.

Acknowledgement

Time has passed so fast and I learned so much in these last four years, now I am sitting here writing this acknowledgement section of my thesis, incredible. None of this would have been possible without the people who I got to know during this exciting time.

Firstly, I would like to express my gratitude to Prof. Dr. Kathrin Mädler, who gave me the opportunity to perform my PhD thesis in her lab and for her support throughout my work. We had so much fun at 5K at EASD in Vienna and Munich, I hope to see you at a future race.

I would like to thank Prof. Dr. Urs Christen for taking time to review my thesis.

My special thanks go to Fede, who taught me plenty and worked with me on this project during the last years. Without his support and guidance, this thesis would not have been possible and my time in the lab time less fun. I always enjoyed to come up with new ideas for the project, but also to talk about non-scientific topics. Although we never manage to start a “lab band”, I promise to pick up my bass again, when I am done with my PhD.

I would like to express my gratitude to all the current lab members: Katrischa, who is not only helping with any lab concerning questions, but also listened to all my student problems. Durga and Ting for all the fun and help during the countless hours spend at the “western-blot shaker”. Kathi and Wei, who I really got to know far too late, as well as Sahar and Amin.

I would also like to thank some former members of this lab: Jenny and Katharina who were a huge help and assistance during the first half of my PhD and Payal and Michael.

At last, I want to express my gratitude to my greatest supporter, Ulrike, who always encouraged and helped me through all the up and downs of my PhD, thank you.